



D2.3 – Report on the climate impact of the first set of operational improvements

F. Linke (DLR), Z. Zengerling (DLR), C. Weder (DLR), S. Matthes (DLR), S. Dal Gesso (Amigo), C. Abate (DBL), N. Valderrabano (DBL), A. Tedeschi (DBL), S. Gottofredi (DBL), E. Branchini (SEA), L. Bissossero (SEA), M. Grampella (SEA), D. Canuti (SEA), B. Baspinar (ITU), I. Ozkol (ITU), P. Rao (TUD), F. Yin (TUD), B. Santos (TUD), M. Noorafza (TUD), P. Roling (TUD), K. Sutopo (NLR), Jan Middel (NLR), A. Rivera Gil (IATA)

Document Number	D2.3
Document Title	Report on the climate impact of the first set of operational improvements
Version	1.0
Status	Final
Work Package	WP 2
Deliverable Type	Report
Contractual Date of Delivery	31.12.2021
Actual Date of Delivery	31.12.2021
Responsible Unit	DLR
Contributors	DBL, NLR, TUD, DLR, AMIGO, ITU, IATA, SEA
Keyword List	Climate Impact, Operational Improvements, Non-CO ₂ effects
Dissemination level	PU



CLIMOP Consortium

CLIMOP Consortium consists of a well-balanced set of partners that cover all the needed competencies and the whole value chain from research to operations. ClimOp Consortium includes representatives from aviation industry (IATA, SEA), academic and research institutes (NLR, DLR, TU-Delft, ITU) and SMEs (DBL, AMIGO).

1		DEEP BLUE Srl (DBL) 00193 Roma, Italy www.dblue.it	Contact: Alessandra TEDESCHI alessandra.tedeschi@dblue.it
2		KONINKLIJK NEDERLANDS LUCHT- EN RUIMTEVAARTCENTRUM (NLR) Anthony Fokkerweg 2 1059CM , Amsterdam, Netherlands	Contact: Kinanthi Sutopo Kinanthi.Sutopo@nlr.nl
3		TECHNISCHE UNIVERSITEIT DELFT (TU Delft) Stevinweg 1 2628 CN , Delft, Netherlands	Contact: Bruno F. Santos b.f.santos@tudelft.nl
4	 Deutsches Zentrum für Luft- und Raumfahrt German Aerospace Center	DEUTSCHES ZENTRUM FUER LUFT - UND RAUMFAHRT EV (DLR) Linder Hoehe 51147 , Koeln, Germany	Contact: Florian Linke Florian.Linke@dlr.de
5		AMIGO SRL (AMIGO) via Flaminia 48 00196 , ROMA Italy	Contact: Sara Dal Gesso sara.dalgesso@amigoclimate.com
6		ISTANBUL TEKNIK UNIVERSITESI (ITU) Ayazaga Kampusu 34469 , Maslak Istanbul Turkey	Contact: Ibrahim Ozkol ozkol@itu.edu.tr
7		IATA ESPANA SL SOCIEDAD UNIPERSONAL (IATA) Paseo de la Castellana 95, 5 28046 , Madrid, Spain	Contact: Thomas Roetger roetgert@iata.org
8	 Milan Airports	SOCIETA PER AZIONI ESERCIZI AEROPORTUALI SEA SPA (SEA) Aeroporto Linate 20090 , Segrate Italy	Contact: Elena Branchini elena.branchini@seamilano.eu

Document change record

Version	Date	Status	Author (Unit)	Description
0.1	26/10/2020	Draft	Z. Zengerling (DLR)	Draft structure
0.2	07/12/2020	Draft	ClimOP consortium (all partners)	Preparation of integrated document for review: <ul style="list-style-type: none"> - Chapter 1 - Chapter 2 - Chapter 3
0.3	13/12/2020	Draft	F. Yin, P. Rao, M. Noorafza (TUD) C. Weder, Z. Zengerling (DLR)	Review of current draft Executive Summary and Chapter 4 added Chapters 1 and 3 adjusted
0.4	17/12/2020	Draft	ClimOP consortium (all partners) C. Weder, Z. Zengerling (DLR)	Adjustments Abbreviations section, References
0.5.	20/12/2020	Final draft	C. Weder, Z. Zengerling (DLR)	Preparation of final document, quality checks, cross references, figures, tables
1.0		Final document	C. Abate, A. Tedeschi (DBL)	Final quality check

Index

Executive summary.....	7
Abbreviations.....	8
1. Introduction.....	12
1.1 ClimOP project.....	12
1.2 Overview of Work package 2.....	12
1.3 Deliverable 2.3 in the Project's context.....	13
2. Result of the case studies for the initial set of operational improvements.....	14
2.1 Flying low and slow.....	14
2.1.1 Executive Summary.....	14
2.1.2 Methodology.....	14
2.1.2.1. Basic study: Flying low & slow.....	15
2.1.2.2. Weather impact on flying low and slow.....	19
2.1.2.3. Climate impact on flying low and slow.....	19
2.1.3 Results.....	19
2.1.3.1. Individual case studies.....	19
2.1.3.2. Results for full flight plan.....	23
2.1.4 Open issues.....	24
2.2 Free routing in high-complexity environment/flexible waypoints.....	25
2.2.1 Executive Summary.....	25
2.2.2 Methodology.....	25
2.2.2.1Traffic Scenario and Focused Airspace.....	26
2.2.2.2Trajectory Simulator/Trajectory Generation Tool (TGT).....	27
2.2.2.3Emission Model.....	28
2.2.3 Results.....	29
2.2.4 Open issues.....	29
2.3 Climate-optimised flight planning.....	31
2.3.1 Executive Summary.....	31
2.3.2 Methodology.....	31
2.3.3 Results.....	32
2.3.4 Open issues.....	34
2.4 Wind/weather-optimal dynamical flight planning.....	35
2.4.1 Executive Summary.....	35

2.4.2	Methodology	35
2.4.2.1	Previously Described Models and Traffic Scenario.....	35
2.4.2.2	Trajectory Optimization Tool (TOT).....	36
2.4.2.3	Wind Model.....	37
2.4.1	Results.....	38
2.4.2	Open issues.....	38
2.5	Strategic planning: merge/separate flights; optimal network operations.....	39
2.5.1	Executive Summary	39
2.5.2	Methodology	39
2.5.2.1	Representative airlines.....	40
2.5.2.2	Demand preparation.....	42
2.5.2.3	Climate-related parameters	43
2.5.2.4	AOMAS	45
2.5.3	Results.....	47
2.5.3.1	Conclusion	53
2.5.4	Open issues.....	53
2.6	Climate-optimised intermediate stop-over	54
2.6.1	Executive Summary	54
2.6.2	Methodology	54
2.6.3	Results.....	58
2.6.4	Open issues.....	64
2.7	Single engine taxiing / E-taxi and hybrid	65
2.7.1	Executive Summary	65
2.7.2	Methodology	65
2.7.3	Results.....	68
2.7.4	Open issues.....	69
2.8	Electrification of ground vehicles and operations.....	70
2.8.1	Executive Summary	70
2.8.2	Methodology	70
2.8.3	Results.....	71
2.8.4	Open issues.....	76
2.9	Upgrade of the airport infrastructure according to energy efficient criteria.....	76
2.9.1	Executive Summary	76

2.9.2	Methodology	76
2.9.3	Results	81
2.9.4	Open issues.....	85
3.	Overview over climate impact of operational improvements.....	86
3.1	Trajectory-related OIs.....	86
3.2	Network-related OIs	87
3.3	Ground-related OIs	88
4.	Conclusion and future work.....	89
	References.....	91
	Annex A	95

Executive summary

This deliverable presents the documentation of the results of the first simulation iteration performed with regards to the selected operational improvements (OI) in ClimOP. The context to the overall ClimOP project is given followed by a detailed description of the current status of modelling the different OIs. Every OI is separately presented in a subsection structured in executive summary, methodology description, presentation of results and an outlook to future work and open issues. Necessary adjustments of the experiments are explained with regards to the previous deliverables. The methodology sections thus present the selected reference traffic scenario (e.g. the investigated days in 2018, restrictions to a certain geographic area, limitations to specific aircraft types or airports) as well as how the implementation of the OIs is modelled. Among others, further details on climate impact simulations are provided and selection of required atmospheric data is described. The focus of work package 2 is a calculation of the climate metrics associated with an implementation of the OIs in terms of CO₂ and non-CO₂ effects. Therefore, the result sections of the different OIs present changes in climate-related KPIs, such as fuel flow, emission quantities, energy consumption and average temperature response. Due to a wide diversification of the OIs in terms of their application area as well as their simulation approach, a large variability along the results can be observed. However, this deliverable also provides a first summary of the OIs' impact on climate-related KPIs, where different assumptions and limitations have to be considered. A description of open issues per OI study gives further details on planned adjustments to the modelling workflows in a second iteration as well as additional questions that have been raised in the first iteration and will be answered in the following work. Furthermore, limitations and uncertainties of the individual studies are discussed. The results presented in this deliverable build the basis for evaluating the OIs effectiveness with regards to climate mitigation measures as well as for quantifying their impact on the different Stakeholders. Consequently, the following project work is based on the presented outcomes: Deliverable 1.5 will describe the focus of the second iteration of modelling the OIs and also recommend combinations of individual OIs into several scenarios. Deliverable 2.4. will not only present the results of this second iteration, but also include further adjustments that are derived from the current results and present comprehensive assessments of non-climate KPIs such as cost or safety related figures.

Abbreviations

#	number of
3D	three dimensional
AC	aircraft
ACACIA	Advancing the Science for Aviation and Climate
aCCF	algorithmic climate change function
AEDT	Aviation Environmental Design Tool
ALTERNATE	Assessment on alternative aviation fuels development
AJF	Al-Jawf Domestic Airport
ANSP	air navigation service providers
AOMAS	multi-agent airline operation planning model
ASHRAE	American Society of Heating, Refrigerating, and Air Conditioning Engineers
ASK	available seat kilometres
ATAG	Air Transport Action Group
ATC	air traffic control
ATCo	air traffic controller
ATM	air traffic management
ATR	Average Temperature Response
ATS	air traffic service
BADA	base of aircraft data
BC	black carbon
BES	building energy simulation
BOS	Boston (Massachusetts) Airport
BXR	Bam Airport
CAS	calibrated air speed
CASK	cost per available seat kilometre
CCF	climate change functions
CFL	cruise flight level
CLIM	Climate-optimised flight planning
CMIP 5	Coupled-Model Intercomparison Project 5
CND	Mihail Kogalniceanu International Airport
CO	carbon monoxide
CO2	carbon dioxide
CYL	Coyoles Airport
CYU	Cuyo Airport
DBL	Deep Blue

DDR2	Demand data repository 2
DLR	German Aerospace Centre (Deutsches Zentrum für Luft- und Raumfahrt)
DOH	Doha Airport
DP	dynamic programming
DUB	Dublin Airport
DWD	German Weather Service (Deutscher Wetterdienst)
ECAC	European Civil Aviation Conference
ECMWF	European Centre for Medium-Range Forecast
EDUU	Karlsruhe upper area control centre
EE	Electrical energy
ECHAM	ECMWF Hamburg
EI	emission index
ELEC	electrification of ground equipment of an Airport
EMAC	ECHAM5/MESSy Atmospheric Chemistry Climate Model
EPS	expanded polystyrene
EU	European Union
FESG	Forecast and Economic Analysis Support Group
FL	flight level
FREE	free routing
FSP	St Pierre Airport
ft	feet
GFS	Global Forecast System
GHG	greenhouse gas
GRIDLAB	Global air traffic emission distribution laboratory
GreAT	Greener Air-Traffic Operations
HAM	Hamburg Airport
H2O	water vapour
IATA	International Air Transport Association
ICAO	International Civil Aviation Organization
ILS	instrument landing system
INEA	Innovation and Networks Executive Agency
INFR	Upgrade of the Airport infrastructure according to energy efficient criteria
IPCC	Intergovernmental Panel on Climate Change
ISO	intermediate stop operations
ISOC	climate-optimised intermediate stop operations
ITU	Istanbul Technical University
JFK	New York Airport John F. Kennedy

JNN	Nanortalik Airport
KLM	Royal Dutch Airlines (Koninklijke Luchtvaart Maatschappij)
KPI	key performance indicator
LED	light-emitting diode
LIN	Milano Linate Airport
LOSL	Flying low and slow
LTO	Landing and Take-off
MAD	Madrid Airport
MPX	Milano Malpensa Airport
NAFC	North-Atlantic flight corridor
NETW	strategic network planning
NCEP	National Centers for Environmental Prediction
NLR	National Aerospace Laboratory (Nationaal Lucht- en Ruimtevaartlaboratorium)
NM	nautical miles
NOx	nitrogen oxides
OD	origin/destination
OI	operational improvement
ppm	parts per million
RCP	Representative Concentration Pathway
R&D	research and development
SEA	Societa per azioni esercizi aeroportuali
SETX	Single engine taxiing/ electric taxiing/ hybrid taxiing
SOx	sulphur oxides
SO2	sulphur dioxide
SPC	La Palma Airport
SRES	Special Report on Emissions Scenarios
T	temperature
TAP	TAP Air Portugal (Transportes Aéreos Portugueses)
TCM	Trajectory Calculation Module
TGT	Trajectory Generation Tool
TMY	typical meteorological year
TOE	tons of oil equivalent
TOF	Bogashevo Airport
TOM	Trajectory Optimization Model
TOT	Trajectory Optimization Tool
TUD	Delft University of Technology
UTC	coordinated universal time

VEY	Vestmannaeyjar Airport
VIE	Vienna-Schwechat Airport
VOC (HC)	Volatile organic compounds (hydrocarbons)
WIND	Wind/weather optimal flight planning
WP	work package
YDF	Deer Lake Airport
YJT	Stephenville Airport
YLC	Kimmirut Airport
YMN	Makkovik Airport
YQX	Gander International Airport
YYR	Goose Bay Airport
YYT	St. John's International Airport
ZRH	Zurich Airport

1. Introduction

1.1 ClimOP project

The aviation industry contributes to human-made emissions primarily by releasing carbon dioxide (CO₂), water vapour (H₂O), nitrogen oxides (NO_x), sulphur oxides (SO_x), soot, and sulphate aerosols. In terms of the influence human activities as a whole have in altering the balance of incoming and outgoing energy in the earth-atmosphere system, that is, the anthropogenic radiative forcing, the contribution from aviation has been estimated at slightly less than 5% [1]. At present, the Covid-19 crisis has caused an abrupt contraction of the activities in the aviation sector, which is still far from recovery and is not likely to return to 2019 levels before 2024 at the earliest [2]. However, once the current pandemic is overcome, air traffic is expected to resume its growth by 3 – 4% per year. This suggests that the aviation impact on climate will significantly increase over the next decades unless effective counteractions are planned and implemented.

Under the coordination of the Air Transport Action Group (ATAG), the aviation sector has long committed to cut its emissions and implement mitigation strategies to reduce its impact on the environment and climate [3]. This commitment has been recently restated despite the current crisis [4]. At the institutional level, the European Commission is supporting these efforts by promoting the research of innovative methods and technologies aimed at reducing the impact of aviation on climate. ClimOP is one of the four projects selected by the Innovation and Networks Executive Agency (INEA) within the action “Aviation operations impact on climate change” that pursues this purpose. These four projects, namely GreAT (Greener Air-Traffic Operations), ACACIA (Advancing the Science for Aviation and Climate), ALTERNATE (Assessment on alternative aviation fuels development), and ClimOP, focus on complementary aspects, respectively: innovative methods for a more climate-friendly air traffic management; a scientifically sound understanding of the aviation contribution to climate change; new fuels less dependent on fossil sources; and the identification and assessment of the most promising operational improvements to reduce the aviation climate impact and the evaluation of their impact on all the aviation stakeholders.

In the first year of the project, ClimOP made an inventory of the currently known operational improvements (OIs) and the available key performance indicators (KPIs) to quantify the effect of these OIs. Alternative sets of compatible OIs will subsequently be determined, and their impact on climate change will be assessed, taking CO₂ and non-CO₂ effects, such as, from NO_x, H₂O, and contrails, into account. In addition, in collaboration with the stakeholders in the consortium and the Advisory Board, ClimOP will evaluate the impact of these OIs on airports, airlines, air navigation service providers (ANSP), manufacturers, and passengers. As a result, ClimOP will develop a body of harmonised, most-promising mitigation strategies based on the alternative sets of OIs and will provide recommendations for target stakeholders on policy actions and supporting measures to implement the alternative sets of OIs.

1.2 Overview of Work package 2

The overall objective of work package 2 is the iterative quantification of the implications the OIs, which have been selected in the course of work package 1, have on climate change.

For this purpose, an air traffic simulation environment is required, in which the OIs are modelled such that changes in the amount, and the location (including the geographic position and altitude) of the different engine emissions species and effects due to the altered operations become visible with respect to a baseline scenario. Some OIs, such as climate-optimised routing, require the inclusion of weather data and climate change functions (CCFs) in order to assess their climate impact since the OI is directly linked to a weather phenomenon, such as contrail formation regions. For other OIs, such as Intermediate Stop Operations (ISO), where the focus is not on specific

weather phenomena, their climate impact is adequately estimated using a climate-chemistry response model AirClim. Hence, these selected tools and air traffic data are adapted to capture the specific characteristics of the defined OIs appropriately and to capture the climate performance metrics selected in WP1. CO₂ emissions and non-CO₂ effects, such as ozone and methane changes from NO_x-emissions, H₂O changes, contrail-cirrus coverage, and possible impacts from particulates, will be addressed in terms of changes in the concentrations and the resulting average temperature response.

1.3 Deliverable 2.3 in the Project's context

The deliverable D2.3 “Report on the climate impact of the first set of operational improvements” describes the first set of results on the climate impact assessment of the selected operational improvements.

In the course of work package 1, the OIs have been shortlisted according to a multi-step multi-criteria assessment procedure described in detail in deliverable D1.3 [5]. From the original 25 OIs, 11 OIs were selected with priority, covering four different categories of OIs: Climate-optimized operation of the airline network (five OIs), Climate-optimized trajectories (two OIs), Operational and infrastructural measures on the ground (three OIs), Operational measures at regulatory level (one OI). The selected OIs were then further outlined in deliverable D1.4 with respect to their impact on climate and on the involved stakeholders. The expected advantages/disadvantages of those 11 OIs were also discussed in D1.4. Moreover, a preliminary description of the necessary methodology to study those OI's impact on climate and the KPIs/methods to evaluate its impact on stakeholders also in terms of feasibility were given in D1.4 [6].

Work package 2 focuses on the “Climate impact assessment including non-CO₂-effects”. The previously submitted deliverables from this work package focused the definition of the reference scenario including its technological and operational boundary conditions and the selected air traffic sample (D2.1, [7]) as well as a description of the modelling workflow for the climate impact simulation of all selected operational improvements and the corresponding adaptation of the combined air traffic scenario (D2.2, [8]). This work on the simulation of the different OIs represents the basis for the work conducted in the course of this deliverable. The following sections of this document summarize the results that have already been achieved in the respective working groups modelling the operational improvements. Results on climate-related KPIs such as fuel-flow, emissions or average temperature response are analysed and given per study of operational improvements. Furthermore, recommendations for the next simulation iteration are derived. An outlook to non-climate KPIs is given. Chapter 3 of this document provides a first comparison of the climate-impact KPIs of the different OIs, before Chapter 4 concludes this deliverable and describes the following work.

The next modelling iteration will not only include adjustments to the modelling workflow but also calculate non-climate and stakeholder related indicators. Furthermore, several OIs could be combined and their impact could be analysed in summary. The findings from work package 2 are essential inputs for WP3, where climate impact indicators and stakeholder impact indicators are analysed to select and provide recommendation for the implementation strategies.

2. Result of the case studies for the initial set of operational improvements

This chapter documents the results of the nine working groups with regards to the climate impact of implementing the selected OIs. It focuses on the results that have been achieved in the first iteration of OIs. The outcomes on climate-related KPIs represent the required basis for comparing the OIs as well as an evaluation of non-climate KPIs.

The presentation of results is structured as follows. One section is dedicated to every OI and is divided into four subsections, starting with an executive summary, where the goal of the study and its current status is presented. The second section provides further details on the methodology based on deliverable 2.2 [8] including further aspects that appeared during the modelling process. The third subsection of every study presents the current status of the results achieved so far before the final part describes remaining open issues and addresses uncertainties and limits of the respective study.

2.1 Flying low and slow

2.1.1 Executive Summary

Higher flight altitudes come along with lower fuel burn and thus lower CO₂ emissions. Due to their independence of altitude, CO₂-induced climate effects are reduced. Nevertheless, the climate impact of contrails, water vapour, and NO_x varies with the altitude of their emission and can potentially be reduced by lowering flight altitudes. As this is associated with higher fuel consumption, an additional reduction in flight speeds could diminish those effects. This will be analysed in the following study.

Based on an air traffic scenario with detailed point profile data, flight trajectories including their different altitudes are reconstructed and the corresponding fuel flows and emissions as well as the flight times are calculated. Real atmospheric conditions are applied. On this basis, average temperature responses over 20 and 100 years are calculated. Cruise altitudes and speeds are lowered systematically, and results are compared to the reference case. A second aspect of the study investigates atmospheric effects from different weather situations as well as climatological changes over decades and compares effects from flying low and slow.

A first analysis of the results shows an improvement in ATR20 by approx. 4 - 7 % for North Atlantic long-haul flights. Case studies on specific missions even show potential reductions up to 55%. Summarizing results cannot confirm these by results on an aggregated level, where further research is possible especially in terms of considering different weather situations. Impact on Stakeholders and non-climate KPIs will also be analysed in the following deliverables.

2.1.2 Methodology

The modelling workflow and the utilized data base have already been described in Deliverables D2.1 and D2.2 [7][8]. A summary of the workflow is shown in Figure 1.

As discussed previously, the study is carried out in different parts. First of all, the impacts of flying low and slow are calculated for one representative day. In a second step, the influence of different seasonal weather situations and impact of long-term climatological changes are included. On the one side, a weather-based analysis is performed, i.e. the effect of flying low and slow is modelled for specific weather conditions on four days of the different seasons throughout the year 2018. On the other side, a climate-based study is conducted, where the effect of long-term climatological changes over the years are examined.

Flying Low and Slow

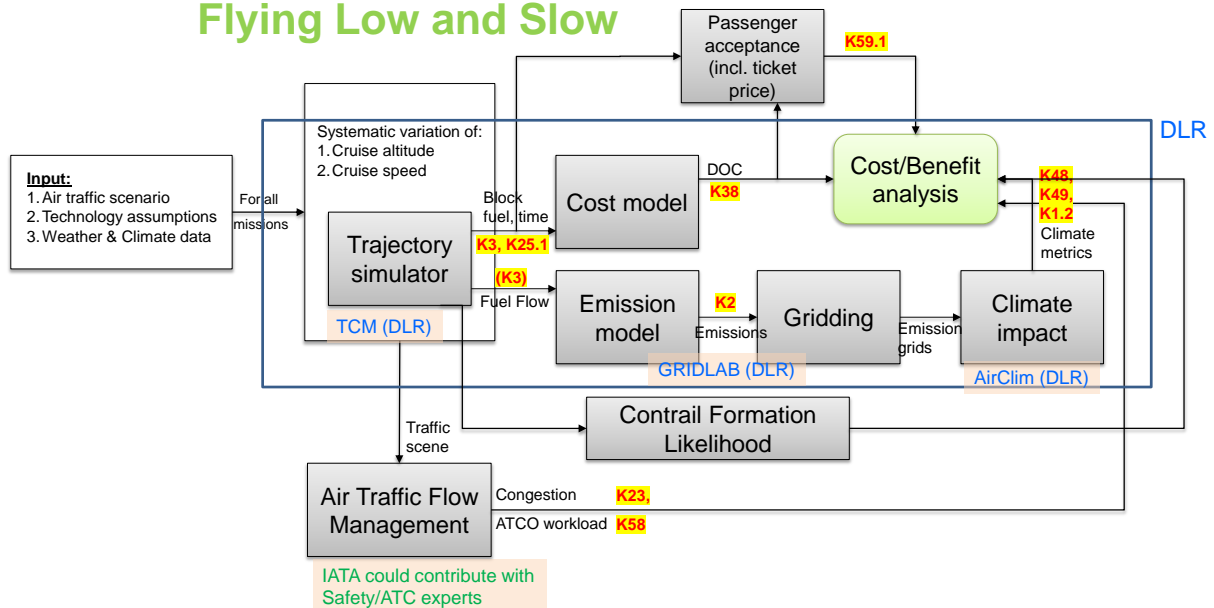


Figure 1. Modelling workflow for OI of 'Flying Low & Slow'

2.1.2.1. Basic study: Flying low & slow

The basic study investigates the effect of flying low and slow for the traffic scenario of a full day from 2018. It represents the basis for the following studies that analyse the impact of different atmospheric conditions (different weather conditions due to seasonal variability in 2.1.2.2. or climatological changes in 2.1.2.3.).

Reference scenario

Modelling the reference case consists of two major parts. Firstly, the days to examine have to be identified and the atmospheric data for those selected days is prepared. Secondly, the air traffic scenario is prepared for the selected days. The basis for this air traffic scenario is Eurocontrol's R&D archive, where detailed point profiles for every mission of the selected days are provided. Since this data is only available for the months March, June, September, and December, this restricts the selection of representative days for the air traffic scenario.

Day selection & atmospheric data

To find days with representative weather patterns, the objective weather type classification provided by German meteorological service (DWD) was utilised [9]. In this context, every day of the year is classified into one out of forty significant weather types regarding wind direction, cyclonality, and humidity over Germany. To find representative days, the frequencies of every weather type in 2018 is calculated and the most frequent weather types are identified for the seasons spring, summer, autumn and winter individually. For each of the four months, where traffic data is available, one day is selected as representative, when the weather circulation pattern over Europe is stable regarding the adjacent days. The temporal progress of weather patterns and its persistence around the selected days has been analysed qualitatively with the Global Forecast system (GFS) model output [10]. That ensures a high level of representation also over the ECAC area and finalizes the selection. The selected days and their characteristics are summarized in Table 1.

Table 1. Selection of days with characteristic weather

Selected day	Weather type	Wind direction	Cyclonality in 950 hPa	Cyclonality in 500 hPa	Humidity in Troposphere
March, 28 th	29 – SWZAF	Southwest	Cyclonic	Anticyclonic	Wet
June, 16 th	9 – SWAAF	Southwest	Anticyclonic	Anticyclonic	Wet
September, 27 th	5 – NWAAT	Northwest	Anticyclonic	Anticyclonic	Dry
December, 11 th	15 – NWZAT	Northwest	Cyclonic	Anticyclonic	Dry

Based on the preselected days, the covered ASKs can be analysed with an analysis of the respective days in the Sabre Market Intelligence data base. This analysis shows that the aircraft types B777-300ER and A330-243 (as selected BADA4 equivalents) cover a major share of ASK for all long-haul flights. B737-800 and A320 represent the largest share of short-range missions. Therefore, the analysis is limited to those aircraft types to reduce computational efforts.

With the defined filter criteria, June 16th is selected as the day to be analysed. The selected fleet covers 36% of all ECAC ASK and 13% of all worldwide ASK of this day. The required atmospheric data is derived from ECMWF ERA-5 reanalysis data. The data is provided every three hours of the day, i.e. 00UTC, 03UTC, 06UTC etc. The time that is closest to the average between start and landing time is selected as representative for the weather situation of the respective flight. Due to the limited spatial resolution of 0.25° x 0.25°, a linear interpolation is performed for every trajectory reference point.

Preparation of air traffic scenario

The air traffic scenario is derived from Eurocontrol’s R&D archive in form of point profile data. It consists of every flight, that crosses the European airspace and starts on the selected day. The following information available is utilised in the progress of the study:

- Origin and destination airport,
- Take-off and landing time,
- Aircraft type,
- The flights point profile per flight consisting of Latitude, Longitude, Altitude and Time elapsed.

In a pre-processing step, it was ensured, that only flights with reliable input data are considered. That means, only missions with a flight level above 20.000 ft, a minimum of four waypoints, and a minimum duration of 15 minutes are further considered.

Further assumptions are made with regards to the available waypoints: To reconstruct the trajectory horizontally, all waypoints with a flight level above 10.000 ft are considered (except Origin and Destination point), to exclude holding cycles or comparable. Furthermore, waypoints have to be at least 5km away from each other to ensure stable modelling. For a vertical reconstruction of the trajectory, the reference case is divided in two subcases: Firstly, the way points are analysed regarding possible step climbs or descents. These are identified, if there are at least two points on that CFL. Furthermore, the mission should remain for at least ten minutes and ten kilometres on that flight level to be identified as a new flight level. Climb and descent sections are then inserted accordingly. A second reference scenario ignores step climbs and descents and assumes a constant flight level at the defined main CFL (cruise flight level, altitude which is flown at for the longest period of time during cruise). This scenario also represents the baseline for the implementation of reduced CFLs. Figure 2 shows an example of the available point profiles (in

orange) and how they are utilised to reconstruct the actual mission (in blue) of this day. The second adjusted reference scenario with one constant FL is represented by the dashed line.

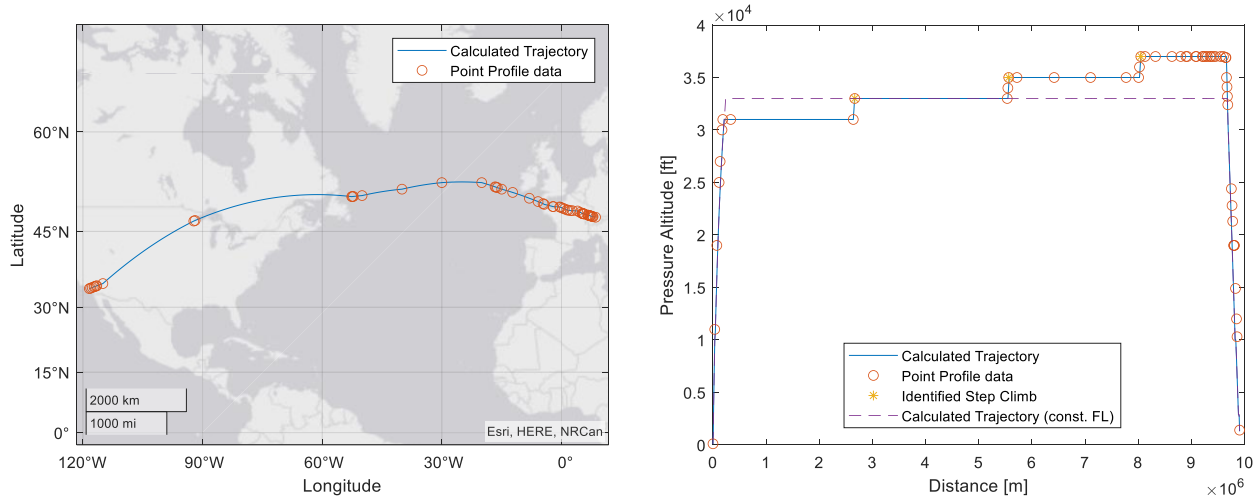


Figure 2. Horizontal (left) and vertical (right) flight profile for a flight from LAX to ZRH with B777 on June 16th, 2018

Scenario of implemented OI

Modelling the OIs implementation is performed on the same basis as the reference scenario in order to ensure comparability of results. Atmospheric data and vertical point profile data are applied identically. However, cruise speeds and cruise flight level are varied in this part. Thus, the elevation information of the point profiles is ignored in this context and replaced with a constant flight level for the respective mission. The constant flight level is derived from the main flight level (i.e. the altitude where the aircraft spend most of the time during cruise). Reduction is performed in 2000 ft steps, so that three scenarios as displayed in Table 2 are analysed.

The additional cruise speed variation is conducted as follows: The first scenario does not include any explicit changes in cruise speed. Nevertheless, cruise speed can be reduced in some cases if cruise flight level is reduced below Crossover-Altitude. The second and third scenario include an explicit speed reduction of 5% and 10% (see Table 2).

Table 2. Variation of cruise flight level and speed

		Cruise speed reduction		
		No explicit speed change	- 5%	- 10%
Cruise flight level reduction	- 2000 ft	Scenario 1.1	Scenario 1.2	Scenario 1.3
	- 4000 ft	Scenario 2.1	Scenario 2.2	Scenario 2.3
	- 6000 ft	Scenario 3.1	Scenario 3.2	Scenario 3.3

Modelling the climate impact

Based on the available input data (atmospheric data and air traffic scenario), the individual trajectories are calculated with DLR's Trajectory Calculation Module¹ (TCM). The different way

¹ For more details on the tools used, please refer to D2.1 and D2.2.

points along the route are included with their respective horizontal location (latitude, longitude) and additional FL information during cruise for the reference case. The OI implementation scenario replaces the different CFL with one constant altitude. A European average load factor of 0.84 is assumed [11] and BADA4 aircraft speed and performance data base are utilised.

Figure 3 and Figure 4 visualize the resulting vertical flight profile as well as the speed over flight distance. The results include the aircraft's state at the simulation point (every 20s), as well as time, distance, fuel consumed and atmospheric conditions at that point. The figures illustrate, how the cruise flight level can already be reduced by assuming a constant flight level and avoiding step climbs. Furthermore, speed changes are not only caused by explicitly reducing the speed in the respective scenarios, but also implicitly by lowering the flight level for constant Mach numbers above the cross-over altitude (speed increase) and below it (speed decrease). Additionally, the wind situation influences the flight speeds.

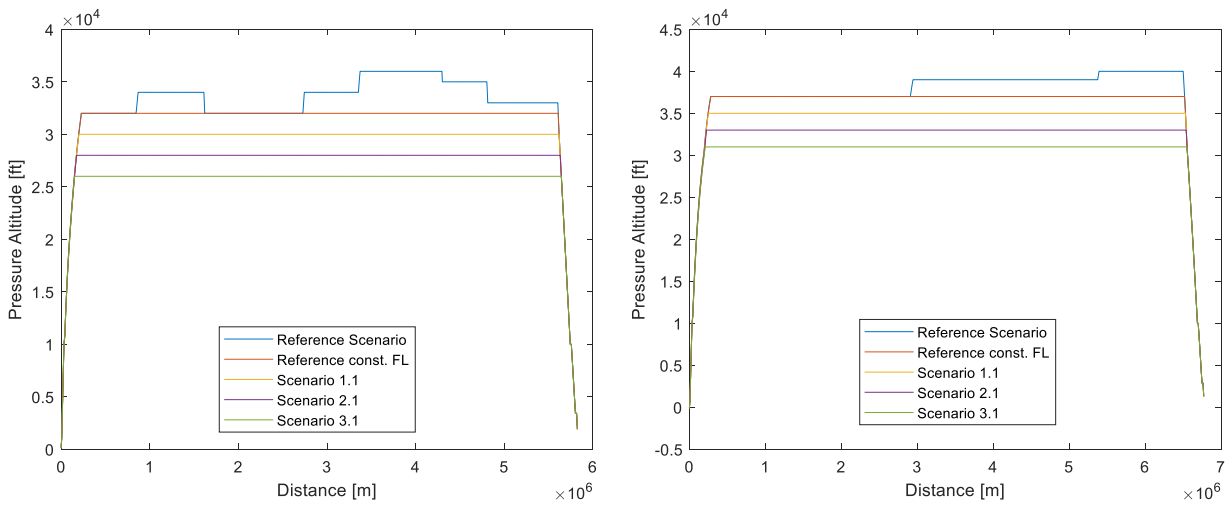


Figure 3. Vertical flight profiles for reference case and different OI scenarios for a flight from DOH to MAD with B777 (left) and a flight from JFK to ZRH with A330 (right) on June 16th, 2018

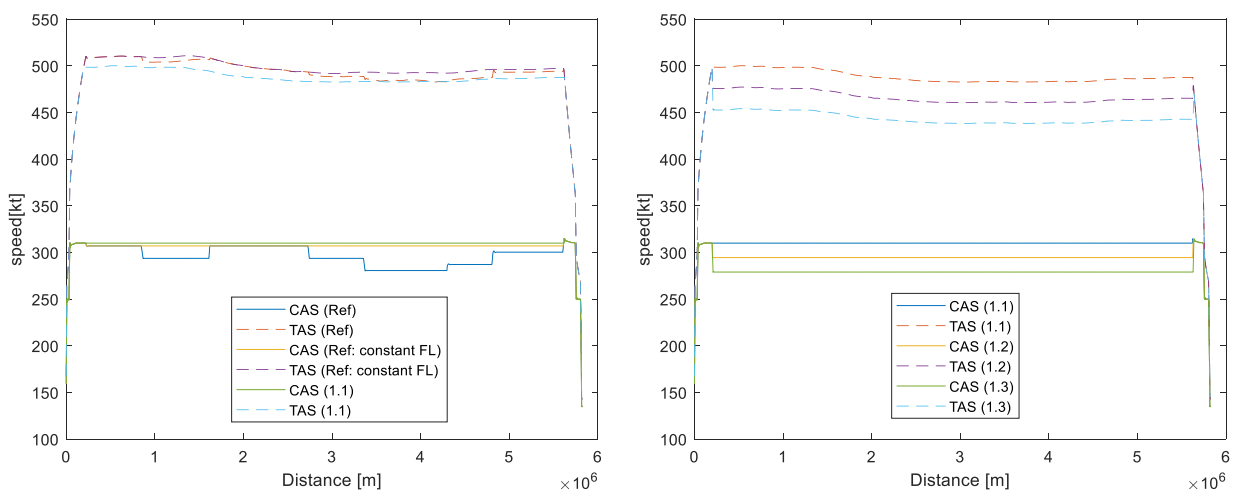


Figure 4. Flight speeds for reference case and different OI scenarios for a flight from DOH to MAD with B777 on June 16th, 2018

The trajectory output of position, altitude, time increment, atmospheric background conditions and fuel flow is used to calculate the emission flows for each time step individually. CO₂ and water

vapour emissions are linear to fuel burn, nitroxides (NO_x) are modelled with the fuel flow correlation method by DLR [12].

With the algorithmic climate change functions (aCCFs) for CO₂, ozone, methane, water vapour and contrail induced cirrus clouds we can calculate the instantaneous climate impact for each species individually. Daily and seasonal variation and the effects of latitude on solar irradiance are regarded by the aCCF as well as atmospheric conditions of temperature, humidity and potential vorticity. The timestep specific climate impact will be aggregated along the entire trajectory to obtain the total climate impact. For further details please refer to the description of aCCFs in [13].

2.1.2.2. Weather impact on flying low and slow

Based on the results from 2.1.2.1 the impact of different weather situations during the year will be analysed. The procedure is according to the basic study. However, the flight plan will be replaced by a subset of missions, that occur on all four preselected days. Instead of detailed point profile missions great circle connections will be assumed, since the point profiles are day and time specific and cannot be used for a comparable flight scenario. Furthermore, flight times are defined as averages from the varying starting times. The main CFLs are derived from the point profile connections, represented by the median of the different seasons' flight altitudes per mission to avoid synthetic CFL. The atmospheric conditions are prepared for all four days according to the methodology described in 2.1.2.1. Modelling the reference case and scenarios of implemented OI are performed as described in the previous section.

This representative flight plan is used to calculate all the trajectories for the four seasons. Thus, results can be analysed on a comparable basis. Calculation of emissions and climate metrics are performed accordingly. An analysis of the results for the climate-related study will be part of the next deliverable D2.4.

2.1.2.3. Climate impact on flying low and slow

The main difference between the climate-based and the weather-based study is the way atmospheric information is included. For a climate-based analysis, climatological mean values are assumed that represent a 30-year multi model mean for the Representative Concentration Pathway (RCP4.5) for the periods from 1991 – 2020, 2021 – 2050, and 2051 – 2081. This data is retrieved from CMIP5 database. Input data (flight missions for long-haul and short-range segments as well as aircraft types) are equivalent to section 2.1.2.2 and the modelling workflow is also equal, i.e. Trajectory calculation with TCM, emission calculations and climate-impact simulation with aCCFs.

An analysis of the results for the climate-related study will be part of the next deliverable D2.4.

2.1.3 Results

At first, the study results are explained by three flight-specific case studies, that represent one mission each. On this basis, the second sub-section analyses effects for a full flight plan.

2.1.3.1. Individual case studies

The impact of flying low and slow will be investigated for several specific routes, covering different mission specifications. The following analysis focuses on three flights, consisting of one transatlantic flight, one long-range flight from Europe to Middle East and one intra-European flight on June 16th, 2018, i.e.:

- Flight from JFK (New York, USA) to ZRH (Zurich, Switzerland) with an A330
- Flight from DOH (Doha, Qatar) to MAD (Madrid, Spain) with a B777

- Flight from VIE (Vienna, Austria) to HAM (Hamburg, Germany) with an A320

JFK - ZRH (A330)

To illustrate, how results are achieved based on the individual flights, a mission representing a transatlantic mission is analysed. The selected flight is from New York (JFK) to Zurich (ZRH) with an A330-234. The mission distance along the point profile is approx. 6,800 km. The flight starts at 00:55 UTC (i.e. 07:55 pm local time) and takes approx. 7:17 hours. Thus, the meteorological situation from 06:00 UTC is selected as representative for this flight. The point profiles additionally show an initial CFL of 37,000 ft, followed by two step climbs to 39,000 and 41,000 ft. Thus, this reference flight requires 38.9 tons of fuel and leads to an ATR20 of $3.2 \cdot 10^{-9}$ K. The speed is derived from BADA4 database (Cruise Mach for A330-234 is 0.82). The second reference scenario assumes a constant CFL and since the point profile shows that most of time CFL370 is used, this is set to the main flight level. The different scenarios representing the OI implementation are derived accordingly.

Table 3 illustrates the changes in major KPIs of fuel flow, flight time and average temperature response. The reference scenario including the identified step climbs leads to a fuel consumption of approx. 39 tons. The second reference scenario requires a slightly higher amount of fuel (1.2% more) and all other scenarios also require more fuel. Especially scenarios 1.2, 1.3, and 2.2 keep additional fuel consumption below 3%. With regards to flight time, it appears that Reference case 2 and Scenarios 1.1, 2.1 and 3.1 lead to shorter flight times, what can be explained by the reduced flight level above cross-over altitude on the one side and possibly changed wind-conditions on the other side, while no explicit reduction of cruise speeds is enforced. It is noticeable that especially average temperature response varies a lot with flight level and at first sight, no systematic correlation can be identified. The reference case at constant flight level shows a large reduction potential of ATR (38%), where as a reduction of the flight level by 2000ft leads to smaller reductions in ATR. Further altitude reductions by 4,000ft and 6,000ft show increasing potentials on ATR reduction.

Table 3. Changes in major KPIs compared to reference scenario for selected flight JFK - ZRH

	CFL [100 ft]	Cruise Mach [-]	Fuel Flow [t]	Flight Time [h]	ATR20
Reference case 1	370 (Step climbs/descents)	0.82	38.89 t	07:17h	3.37e-09 K
Reference case 2	370 (const. FL)	0.82	+ 1.17 %	- 0.34 %	- 38.3 %
Scenario 1.1	350	0.82	+ 4.32 %	- 1.02 %	- 7.72 %
Scenario 1.2	350	0.82	+ 0.99 %	+ 3.26 %	- 8.47 %
Scenario 1.3	350	0.82	+ 0.28 %	+ 7.99 %	- 7.20 %
Scenario 2.1	330	0.78	+ 9.10 %	- 1.69 %	- 29.6 %
Scenario 2.2	330	0.78	+ 4.75 %	+ 2.59 %	- 29.3 %
Scenario 2.3	330	0.78	+ 2.81 %	+ 7.33 %	- 29.0 %
Scenario 3.1	310	0.74	+ 15.1 %	- 2.38 %	- 52.2 %
Scenario 3.2	310	0.74	+ 9.51 %	+ 1.90 %	- 55.8 %
Scenario 3.3	310	0.74	+ 6.46 %	+ 6.62%	- 56.2 %

A deeper analysis shows of the ATR of different emission species, that these differences mainly arise from contrail effects (Figure 5, detailed numbers can be found in Table 28 in Annex A). While impacts of CO₂ and H₂O emissions do not vary significantly across the three flight levels, NO_x

effects increase with decreasing flight altitudes. Additionally, contrail effects vary widely and not systematically across the different flight levels. Figure 6 illustrates this issue, as different warming and cooling contrail areas appear on the different flight levels according to aCCFs.

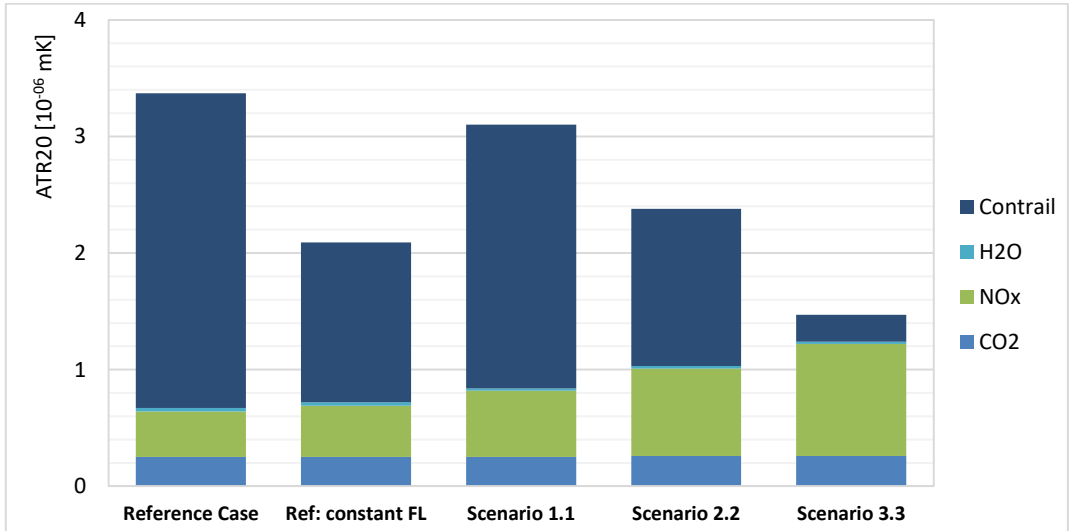


Figure 5. Comparison of ATR across different scenarios for flight JFK – ZRH

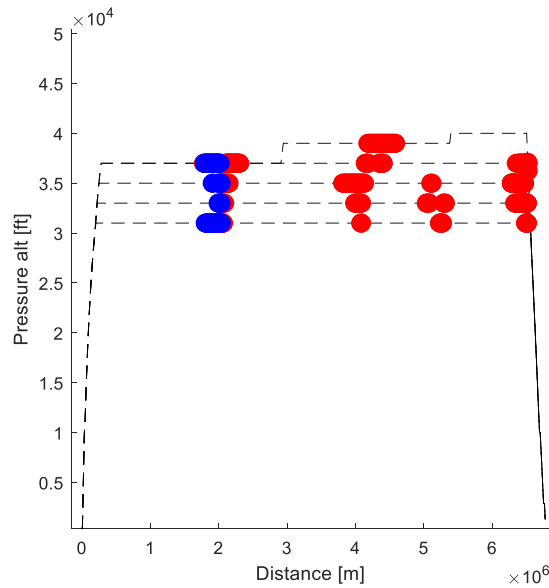


Figure 6. Regions with contrail effects on climate along the trajectory (red: warming effect, blue: cooling effect)

DOH - MAD (B777)

A second mission that is investigated is from Doha (DOH) to Madrid (MAD) with an B777-300ER. The mission distance along the point profile is approx. 6,300 km. The flight starts at 09:12 UTC (i.e. 12:12 pm local time) and takes approx. 6:41 hours. Thus, the meteorological situation from 12:00 UTC is selected as representative for this flight. The point profiles additionally show an initial CFL of 32,000 ft, followed six different step climbs and descents up to 36,000 ft and back to 33,000 ft (see Figure 3). The main flight level, i.e. the flight level where aircraft is most of the time is 32,000ft. The reference flight requires 52.25 tons of fuel and leads to an ATR20 of $2.61 \cdot 10^{-9}$ K. The speed is derived from BADA4 database (Cruise Mach for A330-234 is 0.84). The second reference

scenario assumes a constant CFL at 32,000ft and the different scenarios representing the OI implementation are derived accordingly.

Table 29 (annex) shows the results on major KPIs Fuel Flow, Flight Time and ATR20. Higher fuel consumption is systematically correlated with lower flight levels and a reduction of cruise speeds by 5% leads to the best fuel efficiency per flight level. Flight times increase with lower cruise speeds and also with lower cruise altitudes. ATR20 increases with decreasing flight level and decreases with decreasing speeds. Hence, flying low and slow for this reference case does not lead to benefits in terms of climate impact.

A possible reason can be identified by looking into ATR20 for different emission species, as displayed in Table 4. While H₂O and CO₂ effects do not vary significantly, NO_x effects appear to rise with lower altitudes. Since no warming effects from contrails come into place, the approach to avoid contrail regions by flying lower does not work in this example.

Table 4. ATR from different emission species for flight DOH - MAD

	ATR20 _{CO2}	ATR20 _{NOx_O3}	ATR20 _{NOx_CH4}	ATR20 _{H2O}	ATR20 _{Contrail}
Reference case 1	0.33e-09 K	3.59e-09 K	-1.36e-09 K	0.04e-09 K	0
Reference case 2	0.34e-09 K	3.90e-09 K	-1.40e-09 K	0.04e-09 K	0.09e-09 K
Scenario 1.1	0.34e-09 K	4.36e-09 K	-1.43e-09 K	0.03e-09 K	0
Scenario 2.2	0.35e-09 K	4.76e-09 K	-1.40e-09 K	0.03e-09 K	0
Scenario 3.3	0.36e-09 K	5.18e-09 K	-1.38e-09 K	0.03e-09 K	0

VIE – HAM (A320)

The flight Vienna (VIE) to Hamburg (HAM) with an A320 is selected as a representative flight for intra-European flights. The mission is approx. 800 km long and takes 1:05 h. The flight starts at 07:17 UTC (i.e. 08:17 pm local time), hence the meteorological situation from 09:00 UTC is selected as representative for this flight. No step climbs can be detected for this short mission, thus a constant flight level of 36,000 feet is used. In this case, there is no difference between reference case 1 and 2. This reference flight requires 2.7 tons of fuel and leads to an ATR20 of $1.2 \cdot 10^{-10}$ K. The speed is derived from BADA4 database (Cruise Mach for A320-214 is 0.78).

Table 5 shows the results for the different scenarios. Variation of fuel flow across the different scenarios is moderate and flight times vary as expected from cruise speeds reduction. ATR20 varies up to 33% compared to the reference case, which can be explained by contrail effects, that make up more than a third of the total ATR in this case. Lowering the cruise flight level by 4,000ft or even 6,000ft can potentially avoid formation of contrails at all, leading to significant reduction of total ATR. For this flight, moderate changes in fuel consumption and flight time (e.g. scenarios 2.2 and 3.2) can lead to significant benefits with regards to climate impact.

Table 5. Changes in major KPIs compared to reference scenario for selected flight VIE – HAM (A320)

	CFL [100 ft]	Cruise Mach [-]	Fuel Flow [t]	Flight Time [h]	ATR20 _{Total}	ATR20 _{Contrails}
Reference case 1/2	360 (const.)	0.78	2.725	1:05 h	3.38e-10	1.21e-10
Scenario 1.1	340	0.78	+ 0.95 %	- 0.50 %	+ 1.18 %	- 0.10 %
Scenario 1.2	340	0.78	- 0.36 %	+ 1.86 %	- 6.47 %	- 21.7 %
Scenario 1.3	340	0.78	- 0.49 %	+ 4.51 %	- 3.20 %	- 12.9 %
Scenario 2.1	320	0.74	+ 2.48 %	- 1.23 %	- 32.0 %	- 98.4 %

Scenario 2.2	320	0.74	+ 0.71 %	+ 1.23 %	- 32.5 %	- 99.3 %
Scenario 2.3	320	0.74	+ 0.10 %	+ 4.01 %	- 32.8 %	- 100 %
Scenario 3.1	300	0.70	+ 4.63 %	- 2.02 %	- 29.4 %	- 100 %
Scenario 3.2	300	0.70	+ 2.40 %	+ 0.54 %	- 30.0 %	- 100 %
Scenario 3.3	300	0.70	+ 1.29 %	+ 3.39 %	- 29.7%	- 98.3 %

2.1.3.2. Results for full flight plan

Modelling the different scenarios shows that not all flight level and speed combinations can be performed. In those cases, where a certain flight level is not possible, the next higher flight level is considered., a flight level reduction of 6000ft for the full scenario means, that all flights possible are reduced by 6000ft. For those where this was not possible, a reduction of 4000 or even 2000ft is considered. If no flight level changes are possible, the basic scenario with a constant flight level is used. For an interpretation of the results, that means the scenario ‘-6000 ft’ corresponds to a flight level reduction of up to 6000ft. For the long-haul flights, this only has to be applied for 1% of the -4000ft reduction cases and 2% of the -6000ft reduction cases.

Table 6 shows a summary for all examined long-haul flights as an addition of Fuel Flow, Flight Time and ATR20 of all single missions. Emission quantities for the full flight plan can be found in Table 30 (annex). It appears that the expected effect of lowering climate impact by flying lower and slower cannot be confirmed for the aggregated flight plan. Thus, reducing flight level for every flight does not lead to a positive climate impact for all long-haul flights from or to the ECAC area. However, avoiding step climbs and descents show a reduction in average temperature response while in parallel flight time does not change and fuel flow increases by approx. 0.9% for the entire flight plan. When limiting the analysis to North Atlantic flights (connecting the ECAC area with Canada, United States, or Mexico), the results for a summarized flight plan change: Table 7 illustrates this. For the considered 213 flights, several scenarios lead to a significantly positive climate effect. For example, a reduction of cruise altitudes by 2000ft and lowering cruise speeds by 5% at the same time, leads to an overall reduction in ATR20 by 5.8%. Fuel consumption is increased by 2.2% and flight time is extended by 4.6% on average. Scenarios 1.1, 2.1 and 2.2 also show positive climate impact while keeping additional fuel below 3 % and additional time needed below 5.3 %.

Table 6. Changes in major KPIs compared to reference scenario long-range flights (June 16th, 828 flights)

		Fuel Flow [t]	Flight Time [h]	ATR20 [K]
Reference case A	Step climbs/descents No speed change	39,596	5,704	1,70e-06
Reference case B	Constant FL, no speed change	+ 0.85 %	- 0.00 %	- 1.15 %
Scenario 1.1	- 2000ft CFL, No speed change	+ 0.87 %	- 0.60 %	+ 5.64 %
Scenario 1.2	- 2000ft CFL, - 5 % speed	+ 0.29 %	+ 4.48 %	+ 4.88 %
Scenario 1.3	- 2000ft CFL, - 5 % speed	+ 1.40 %	+ 8.87 %	+ 4.59 %
Scenario 2.1	- 4000ft CFL, No speed change	+ 2.96 %	- 0.50 %	+ 16.7 %
Scenario 2.2	- 4000ft CFL, - 5 % speed	+ 1.67 %	+ 4.58 %	+ 13.5 %
Scenario 2.3	- 4000ft CFL, - 10 % speed	+ 3.21 %	+ 10.1 %	+ 13.5 %

Scenario 3.1	- 6000ft CFL, No speed change	+ 2.91 %	- 2.0 %	+ 28.5 %
Scenario 3.2	- 6000ft CFL, - 5 % speed	+ 2.82 %	+ 3.97 %	+ 25.1 %
Scenario 3.3	- 6000ft CFL, - 10 % speed	+ 3.99 %	+ 10.12 %	+ 23.5 %

Table 7. Changes in major KPIs compared to reference scenario for flight from Europe to North-America and vice-versa (June 16th, 213 flights)

		Fuel Flow [t]	Flight Time [h]	ATR20 [K]
Reference case A	Step climbs/descents No speed change	11,379	2,414	4.696e-07
Reference case B	Constant FL, no speed change	+ 0.59 %	- 0.14 %	+ 1.39 %
Scenario 1.1	- 2000ft CFL, no speed change	+ 1.87 %	- 0.12 %	- 5.37 %
Scenario 1.2	- 2000ft CFL, - 5 % speed	+ 0.22 %	+ 4.56 %	- 5.77 %
Scenario 1.3	- 2000ft CFL, - 5 % speed	+ 1.70 %	+ 9.76 %	- 5.21 %
Scenario 2.1	- 4000ft CFL, no speed change	+ 4.30 %	- 0.02 %	- 4.41 %
Scenario 2.2	- 4000ft CFL, - 5 % speed	+ 2.81 %	+ 5.25 %	- 6.26 %
Scenario 2.3	- 4000ft CFL, - 10 % speed	+ 3.12 %	+ 10.5 %	- 6.40 %
Scenario 3.1	- 6000ft CFL, no speed change	+ 5.35 %	- 1.28 %	+ 4.25 %
Scenario 3.2	- 6000ft CFL, - 5 % speed	+ 4.64 %	+ 4.86 %	+ 1.66 %
Scenario 3.3	- 6000ft CFL, - 10 % speed	+ 5.62 %	+ 11.6 %	+ 1.73 %

An analysis of the intra-European flights does not show climate benefits from flying low and slow. Possible reasons could be the limited verification of aCCFs for missions outside North Atlantic, the specific weather situation of the selected days and the distribution of original flight levels. Further investigations will be required on this issue in the next iterations (D2.4).

2.1.4 Open issues

The assumptions made lead to limitations of the study's results:

- To model the trajectories, speed data from BADA4 data base is considered. Although these are good estimations on speeds during the different flight phases, modelling could be improved by considering real speeds. Median of time deviations from point profile data and modelled missions is 2.17%. This cannot only be explained by differences in actual speeds compared to speeds provided by BADA, but also by inaccuracies following the linear interpolation of atmospheric variables.
- To avoid synthetic thus unrealistic atmospheric conditions, only one weather situation is considered per flight and no temporal interpolation is performed. A higher resolution of weather data and advanced interpolation models would be able to describe atmospheric conditions during the flights more precise.
- All the flights assume a constant load factor that is derived from the European average load factor. A more precise modelling could be achieved, if actual load factor data per flight was

available. Individual load factors lead to more detailed weights and thus more realistic modelling of fuel consumption and KPIs derived therefrom.

- Limiting the study to several aircraft types and regions as well as specific days also limits the number of global flights covered. These uncertainties need to be considered if effects are scaled to a global level.

Further investigations are also required on the effects, that appear for the full flight plan. Especially the impact of reference flight level on climate effects will be considered and analysed in the next iteration. Furthermore, as described in Sections 2.1.2.2. and 2.1.2.3. the impact of different atmospheric conditions, caused by different weather situations during the seasons as well as long-term climatological changes, will be investigated in the following deliverable D2.4. Additionally, the non-climate KPIs with focus on cost and ATC impacts will be analysed in the following deliverable D2.4.

2.2 Free routing in high-complexity environment/flexible waypoints

2.2.1 Executive Summary

The free routing concept aims to remove the barriers originated from the fixed air traffic service (ATS) routes. In this way, the aircraft can fly more direct routes that results in better cost-efficiency and a reduction in fuel consumption and released emissions. This study mainly focuses on implementing the concept for a high-density airspace to figure out the impact of the concept from perspectives of different stakeholders in a high-complexity airspace.

The flight plans of the aircraft that operates in the focused airspace are obtained using the point profile data. Then, a base-case scenario is constructed in which the aircraft fly according to original flight plans to establish a baseline for comparison. The flown trajectories are calculated via simulations. As a second scenario, the free routing concept is implemented by considering the direct routes between the defined entry and exit points as the flight plans. The flown trajectories are also calculated for this scenario. Then, the simulation results are used to calculate the defined KPIs for different stakeholders to figure out the impact of the concept on climate and other stakeholders.

2.2.2 Methodology

The modelling workflow is presented in Figure 7. The study focuses on a specific enroute airspace in the ECAC area. Based on the given aircraft performance parameters and point profiles provided for a specific day, the trajectory simulator simulates the traffic for two scenarios. Then, the defined KPIs are calculated using the simulation results through the KPI-calculation/estimation modules. By comparing the KPIs, an assessment is performed to analyse the OI.

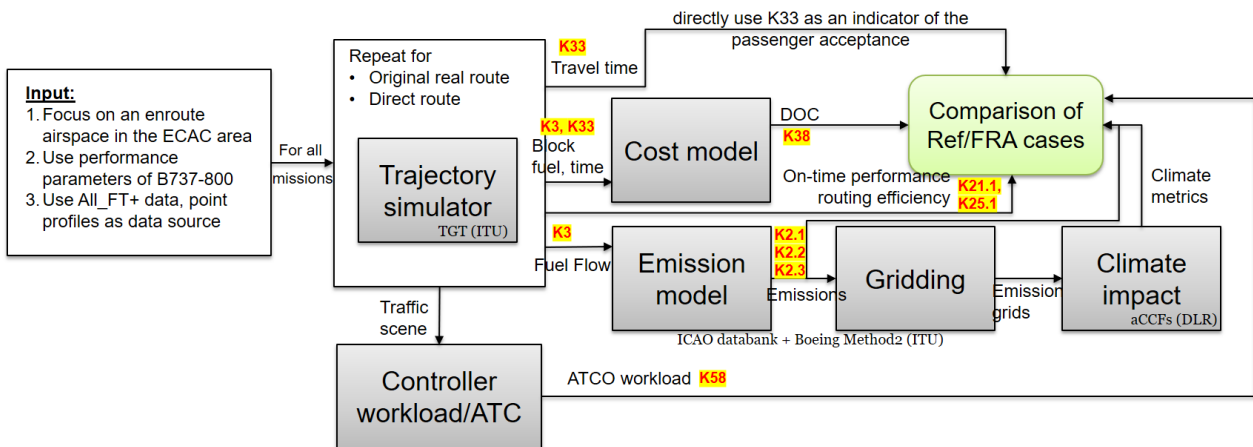


Figure 7. Modelling workflow for the OI of 'Free Routing in a High-Complexity Airspace'

2.2.2.1 Traffic Scenario and Focused Airspace

The study focuses on a high-density airspace in the ECAC area. The traffic scenario and the airspace density for the focused airspace (EDUU) are presented in Figure 8 and Figure 9 respectively. As illustrated in Figure 8, the focused airspace is an upper airspace in which the aircraft fly above 23500 ft. Figure 9 shows that there are around 120 aircraft in the airspace at rush hours and the average number of simultaneous movements is around 60. The focused airspace hosts considerable number of aircraft, and it is one of the high-density airspaces in the ECAC area. A more detailed analysis regarding the comparison of the airspace densities in the ECAC area can be found in the study [14].

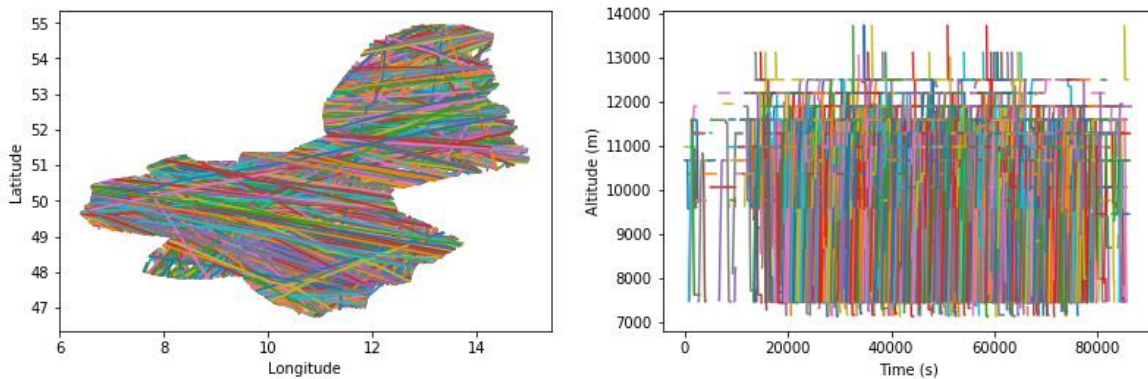


Figure 8. Flight Trajectories in the Focused Airspace (EDUU) on December 01, 2018

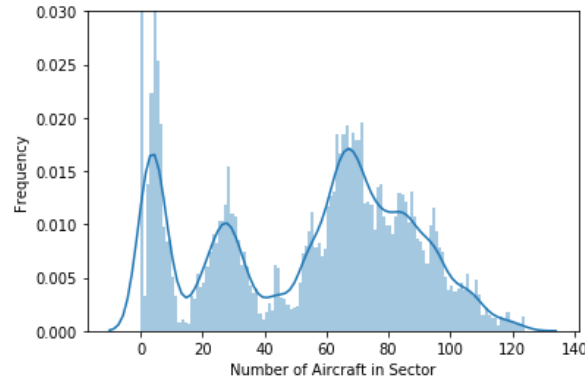


Figure 9. The Distribution of Airspace Density during the Analysed Day (December 01, 2018)

A day is chosen randomly in the available dataset. The flight plans for the aircraft that operate in the focused airspace during that day (December 01, 2018) are obtained using the point profile data in ALL_FT+ dataset [15]. After pre-processing the flight records to eliminate and fix the data anomalies, the point profile data is filtered to obtain the aircraft operating in the airspace with their flight plans inside the airspace. The redundant waypoints in the point profiles are also removed to present the flight plans with a minimum number of waypoints for a better trajectory tracking in the simulation environment. For each aircraft operating in the airspace, a set of waypoints defined in terms of longitude, latitude, and altitude are generated to present its flight plan.

2.2.2.2 Trajectory Simulator/Trajectory Generation Tool (TGT)

In the trajectory simulator, a point mass model is used to present the motion of the aircraft. The constructed model can use both BADA3 and BADA4. This model is represented by the following set of differential equations:

$$\begin{aligned}\dot{x} &= v \cos\chi \cos\gamma \\ \dot{y} &= v \sin\chi \cos\gamma \\ \dot{h} &= v \sin\gamma \\ \dot{v} &= \frac{Thr}{m} - g\sin\gamma - \frac{C_D S \rho v^2}{2m} \\ \dot{\chi}(t) &= \frac{C_L S \rho v \sin\mu}{2m \cos\gamma} \\ \dot{m}(t) &= -F\end{aligned}$$

where the state variables are defined as the position (x, y) , altitude h , velocity v , heading angle χ , and mass of the aircraft m . The control inputs are flight path angle γ , bank angle μ and thrust Thr . In this set of equations, aerodynamic lift and drag coefficients are denoted by C_L and C_D , total wing surface area is S , air density is indicated as ρ , and the fuel consumption is indicated as F . In this study, the coefficients and the required functions to calculate the performance parameters are obtained from the BADA4. When the required control inputs are provided, the motion of the aircraft can be simulated by integrating this set of differential equations.

The flight plan of an aircraft is defined as a set of waypoints in terms of longitude, latitude, and altitude. A path is produced as a combination of lines and arcs between the defined waypoints. During the flight, the aircraft follows this path. The required control inputs to follow the defined path are generated by a trajectory tracking layer. In trajectory tracking layer, two control functions are combined for lateral and longitudinal motions. In the longitudinal part, the desired velocity and

target altitude are reached by calculating the required flight path angle. The lateral control part includes the straight-line controller, turn controller, and heading controller. These controllers calculate the required bank angle to follow a horizontal path. In addition to them, a speed controller adjusts thrust of the aircraft to keep the speed at the desired level during cruise. The desired speed schedule is defined based on the airline procedure model presented in the BADA. More detailed information about the trajectory tracking algorithms and the traffic simulator can be found in [16][17].

2.2.2.3 Emission Model

The simulation module generates the flown trajectories that contain fuel burn, altitude, speed, and positions. The emission model uses these trajectories to calculate the released emissions for each aircraft in the traffic scenario. The emission model is constructed using the modelling approach in [18],[19]. The released emission is proportional with the fuel flow and the emission index of the pollutant such that:

$$\dot{m}_i = F \cdot EI_i \quad i \in \{NO_x, HC, CO, CO_2, H_2O, SO_x\}$$

while the emission indices for CO_2, H_2O, SO_x can be assumed as constants, the indices for NO_x, HC, CO should be presented as a function of flight condition [18]. The presented model uses the Boeing Method 2 [19] to estimate these emission indices at upper airspaces.

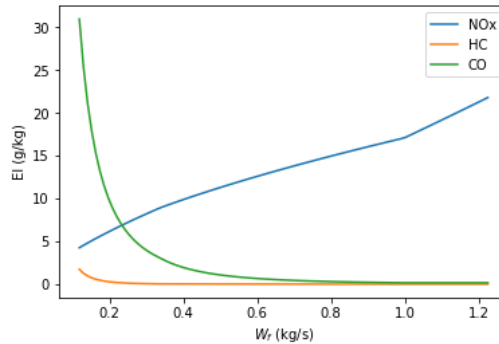


Figure 10. Cartesian Plot of Logarithmic Fit of ICAO datapoints (at sea level) with W_f (fuel consumption) for a B737-800

For different types of engines, the indices for NO_x, HC, CO are presented in the ICAO Emissions Data Bank [20] for the Landing and Take-Off Cycle (LTO). ICAO LTO covers four engine operation mode which are used to model Taxi-Out, Take-Off, Climb-Out, and Approach. Based on the Boeing Method 2, the presented emission factors are adapted to flight condition using the current speed, altitude, and fuel consumption of the aircraft. After adjusting the emission factors for LTO operation modes with small correction factors, the emission factors at sea level are presented as a function fuel consumption by fitting logarithmic bi-linear curves to ICAO datapoints as illustrated in Figure 10 for a B737-800.

Using the obtained curves, the emission indices at sea level can be estimated as a function of the fuel consumption. When operating in a higher altitude, firstly the correlated fuel flow rate at sea level is estimated via the following formula:

$$W_f^{SL} = W_f^{Alt} \frac{\theta_{amb}^{3.8}}{\delta_{amb}} e^{0.2M}$$

where the M is mach number, θ_{amb} and δ_{amb} are the temperature and pressure ratios at the operating altitude, and W_f^{Alt} is the fuel consumption for one engine at the operating altitude. Then,

using the W_f^{SL} , the corresponding emission indices at sea level can be estimated via the obtained curves. The emission indices are adapted to altitude using the formulas below:

$$EI_{CO}^{Alt} = EI_{CO}^{SL} \left(\frac{\theta_{amb}^{3.3}}{\delta_{amb}^{1.02}} \right)^x$$

$$EI_{HC}^{Alt} = EI_{HC}^{SL} \left(\frac{\theta_{amb}^{3.3}}{\delta_{amb}^{1.02}} \right)^x$$

$$EI_{NO_x}^{Alt} = EI_{NO_x}^{SL} \left(\frac{\delta_{amb}^{1.02}}{\theta_{amb}^{3.3}} \right)^y e^H$$

where x and y are constants, and H is the humidity correction factor. Using this model, the emission factors at cruising altitudes can be estimated based on the operation conditions. More detailed information about the Boeing Method 2 can be found in [19].

2.2.3 Results

The case study contains the implementation of the free routing concept in a high-density airspace, which is EDUU in the ECAC area. For a specific day in 2018, the flight plans for the traffic in this airspace are obtained from the ALL_FT+ data. Then, the base-case scenario and the free routing scenario are implemented in the presented simulation environment. As a preliminary result, the emissions (NO_x, CO_2, H_2O), travel duration, fuel consumption, and number of movements in the airspace are obtained and compared, which are presented in Table 8.

Table 8. Preliminary Results for the OI of 'Free Routing in a High-Complexity Airspace'

KPI	Base Case Scenario	Free Routing	Percentage Change
Travel Duration (avg. value per flight)	1073.31 sec	1071.71 sec	0.15% ↓
Fuel Consumption (avg. value per flight)	740.69 kg	724.33 kg	2.2% ↓
NO_x (avg. value per flight)	8.72 kg	7.77 kg	10.9% ↓
CO_2 (avg. value per flight)	2332.43 kg	2280.93 kg	2.2% ↓
H_2O (avg. value per flight)	911.05 kg	890.93 kg	2.2% ↓
# of movements (avg. value in airspace)	56.014	55.931	0.148% ↓

As presented in the preliminary results, there is a reduction in all the analysed KPIs. While the main improvement is on the NO_x , the travel duration and number of movements have a very small change.

2.2.4 Open issues

The obtained results are preliminary. Further assessments will be conducted to make sure that there is no modelling error and the results are reliable. Furthermore, the impact of the OI on ATR20/100 and ATC (Air Traffic Control) workload should be evaluated to draw a more general conclusion regarding the free routing concept in a high-complexity airspace.

In the next deliverable, the other KPIs such as ATR20/ATR100, ATC workload, safety (occurrence of conflicts), routing efficiency, ASK, direct operating cost, and CASK will be evaluated. The

climate-impact related KPIs will be calculated using the algorithmic climate change functions (aCCFs). For the rest of the KPIs, basic mathematical models will be developed to calculate them.

It is expected that the concept results in better cost-efficiency and reduces the impact on the environment by decreasing the fuel burn and greenhouse gas emissions. But, because all aspects of the non-CO₂ effects are not considered during the planning, the improved profiles could not lead to the optimal impact on climate. From an ATC perspective, the tasks may become more complicated or straightforward depending on the airspace and implementation. It can be argued that any negative effects may be counterbalanced by the reduction in the number of conflicts in a given sector by spreading the possible conflict points all over the sector areas. But, further assessments should be done to figure out the impact of the concept on the ATC. It should be also noted that the aircraft use direct routes in the implementation of the free routing. This assumption may also limit the efficiency of the operation. The efficiency can be improved by using a more advanced planning algorithm.

2.3 Climate-optimised flight planning

2.3.1 Executive Summary

Climate optimized flight planning (CLIM) aims to identify alternative aircraft trajectories which have a lower total effect on climate, by avoiding those regions of the atmosphere which are in particular sensitive to aviation emissions. In this deliverable, results for a winter day in the year 2015 are shown in order put results to be achieved with this OI in relation to earlier published studies and to exploit synergies. We provide mitigation gains for single trajectories in the European Airspace as well as mitigation gains for the Top 2000 routes in a 1-day European Traffic sample using re-analysis data.

2.3.2 Methodology

This OI aims to identify the mitigation potential of aviation overall climate impact (CO₂ and non-CO₂ effects) by identifying climate-optimized aircraft trajectories. This OI has been investigated in a series of earlier assessment studies, why it was decided to make sure in phase 1 that we put our modelling of this OI in context to earlier studies. Overall the modelling chain on climate optimized flight planning relies on the provision of spatially and temporally resolved information on the sensitivity of the atmosphere to aviation emissions in order to enable trajectory planning and optimisation under climate impact aspects. Considering this climate impact information in the overall objective function (mathematical cost function) of the trajectory optimisation allows us to evaluate and identify alternative trajectories which have a lower climate impact. The Trajectory Optimization Module (TOM) which uses optimal control techniques in order to determine climate optimized aircraft trajectories, has been used to identify fuel optimal trajectories as well as alternative trajectories. Relying on algorithmic climate change functions, which determine the climate effects of aviation emissions based on meteorological reanalysis data for a specific day and its meteorological situation, TOM uses fuel burn and climate effects measured as temperature change (average temperature response, F-ATR) in the objective function to optimize aircraft trajectories.

In Phase 1 we assess a 1-day case study which has been published in an earlier research article, in order to describe relation between our study and earlier studies in detail. The one-day case study published in [23] and [24] refers to a winter situation on 18th December 2015, which was characterized by a contrail forming region over the central European airspace on that specific day. Further details on the weather situation is given by DWD classification over Germany [9] and is displayed in Table 9.

Table 9. Characteristic weather pattern for selected day following DWD classification over Germany.

Selected day	Weather type	Wind direction	Cyclonality in 950 hPa	Cyclonality in 500 hPa	Humidity in Troposphere
Dec, 18 th (2015)	20 – NWAZF	Northwest	Anticyclonic	Cyclonic	Wet

The spatially and temporally resolved information on the climate effects of aviation emissions is derived by combining algorithmic climate change functions (aCCFs) to the reanalysis weather forecast for that specific day. Initially, aCCFs were developed [25] using climate change functions which have been calculated with Lagrangian comprehensive climate-chemistry simulations with EMAC/ATTILA/AirTraf for the North Atlantic Flight Corridor (NAFC). The resulting climate change functions for contrail cirrus, NO_x-induced and water vapour effects are described in [26]. These aCCFs are applied to the European Airspace. Comparing meteorological characteristics relevant for contrail formation, reveal both similarities as well as certain differences. Specifically, we briefly

discuss differences in characteristics in these two regions, comparing NAFC to the European Airspace. Previous studies [27] have shown that there are differences in the vertical distribution and seasonal variation of ice-supersaturated air masses in the northern mid-latitudes due to the variability of key atmospheric parameters such as temperature or humidity. These parameters directly affect contrail formation, so a more detailed study of the meteorological differences between the two regions is needed, which will be presented in Phase 2 (D2.4).

Meteorology between individual geographic regions differs, hence, as part of the ClimOP project, a comprehensive analysis of the climate effects in various regions is currently under preparation. For this purpose, the EMAC/ATTILA system will be applied. In order to expand the geographic scope also to other regions than the NAFC, we develop and analyse climate change functions for the Northern Hemispheric extra-tropics and lower latitudes with a comprehensive Lagrangian approach implemented in chemistry-climate modelling. Results will be available for the Phase 2 simulations in the project.

Reference case and OI implementation

In the first phase, reference case and OI implementation are modelled as follows:

- One day case studies are performed by identifying the fuel-optimal case (reference) and comparing alternative trajectories which have a lower climate impact.
- Traffic sample (1 day) comprises about 13,000 intra-European flights, while optimization is also provided for the Top 2000 routes.
- Current analysis is performed with aCCFs developed for the North Atlantic flight Corridor, applied to reanalysis data for 18 Dec 2018.
- The OI is implemented for on individual winter day, representing realistic characteristic weather pattern and ECAC traffic sample.
- We assume that reanalysis data represent the real atmospheric conditions. Additionally, our calculation of the climate effects of non-CO₂ emissions relies on the applicability of aCCFs, while we describe updates for phase 2 in section 2.3.4.

2.3.3 Results

When identifying alternative climate-optimized trajectories according to OI CLIM for this specific case study, we enable ATM for that specific day to propose alternative trajectories which have a lower climate impact measured in physical climate metrics, while other performance indicators might degrade. Results are presented for both individual trajectories (examples displayed are a flight from Luxemburg to Baku and a flight from Scandinavia to Spain) and the Top 2000 routes in Europe, resulting in higher mitigation gains (

Table 10). For non-climate KPIs the flight time was analysed. Missing values will be calculated in the following work.

Table 10 shows changes in the considered KPIs in comparison to the fuel-optimal reference case. Different fuel-penalties of 0.5%, 1%, and 2% or 5% allowed, lead to three cases per analysed flight plan or individual flight. The results can be interpreted as follows:

- Climate-optimized Top2000 routes: Allowing an additional fuel consumption of 0.5% in climate-optimized flight planning, could potentially reduce F-ATR20 by 45%. This is associated with an additional flight time of 0.8%.
- For a single flight from central Europe to South-East represented by a mission from Luxemburg to Baku, an increase in fuel burn by 0.5% enables climate-optimal flight planning with 9% decrease in F-ATR20 and F-ATR100. The flight will take 1.1% longer compared to the fuel-optimal reference case. Uncertainties quantify the results of ATR to be in a range between 8 and 10%.

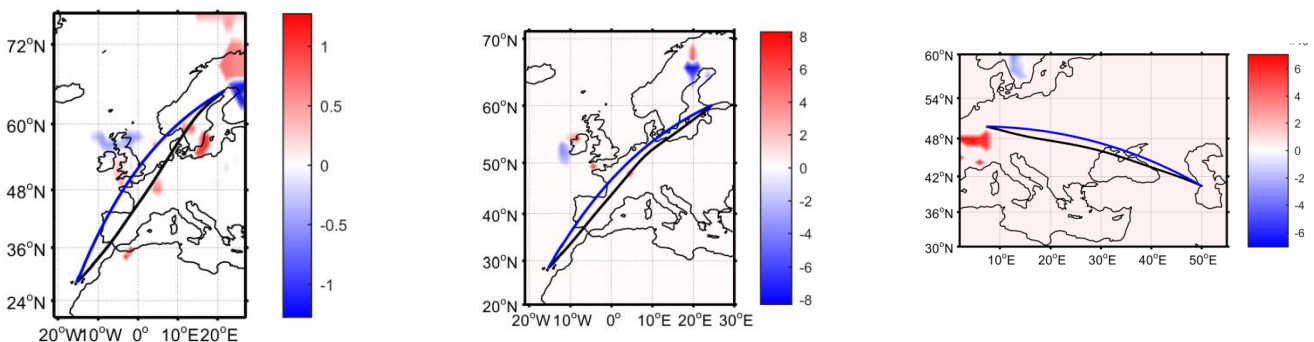
- For a single flight from North Europe to South-West Europe, i.e. from Scandinavia to Spain, climate-optimized flight panning with additional 0.5% of fuel burnt leads to reduction in ATR of 47% in 20 years and 50% in 100 years.

Table 10. Changes in major KPIs compared to reference scenario (fuel-optimal) for climate-optimized air traffic scenarios of Dez 18th, allowing different fuel penalties.

	Fuel Flow [%]	Flight Time [%]	F-ATR20 [%]	F-ATR100 [%]
Climate optimized Top 2000 routes	0.5 %	0.8%	-45%	-43%
	0.9 %	1.4 %	-53%	-50%
	5.0%	6.4%	-68%	-63%
Climate optimized Central to South-East Luxembourg-Baku (single flight)	0.5%	1.1%	-9%	-9%
	1.0 %	2.1%	-15%	-14%
	2.0 %	4.1%	-21%	-21%
Climate optimized North to South-West Scandinavia-Spain (single flight)	0.5%		-47%	-50%
	1.0%	N/A	-48%	-52%
	2.0%		-49%	-53%

As has been shown, the choice of metric influences the quantitative estimates on mitigation gains. However, the robustness analysis in [23] showed, that applying different metrics in the given situation resulted in alternative trajectories offering robust mitigation potentials.

By way of example, climate optimization of aircraft trajectories results in alternative trajectories which avoid contrail forming regions or regions where NO_x emissions have a large climate effect. In Figure 12 we illustrate how alternative trajectories compare to the great circle solution in terms of position (Latitude and Longitude). Fuel-optimal routing is displayed in black compared to shortest connection (great circle in blue) for the selected individual missions. Colour shading indicates warming (red) and cooling impacts (blue) along the trajectories as provided by the aCCFs in 10⁻¹³ K/s.



(a) Lulea-Gran Canaria (ESPA-GCLP) (b) Helsinki-Gran Canaria (EFHK-GCLP) (c) Baku-Luxembourg (UBBB-ELLX)
Figure 11. Aircraft trajectories (blue: great circle, black: fuel-optimized trajectory) for different missions [23]

Additionally, Figure 12 shows alternative flight altitudes of the trajectory profile aiming to avoid contrail forming regions (marked in red). The first row represents the fuel-optimal case where as the second row shows the climate-optimised case allowing 0.5% additional cost.

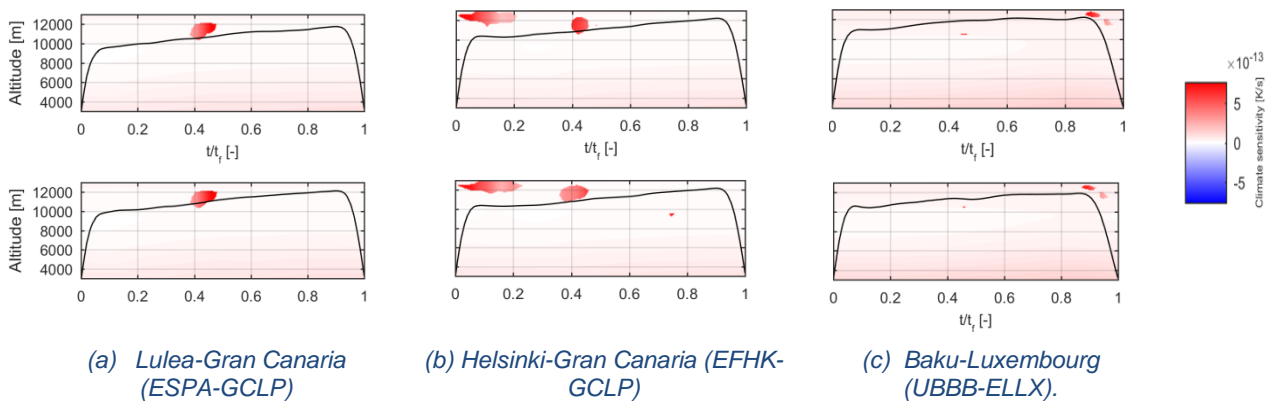


Figure 12. Altitude profile (top row: fuel-optimal case, bottom row: climate-optimised case with 0.5% additional costs) [23]

2.3.4 Open issues

For the provision of meteorological data in the simulation of the OI CLIM we use meteorological data provided by ECMWF. In the one-day case studies published earlier [23], ERA-5 reanalysis data was used, in order to estimate mitigation potentials, relying on a realistic representation of the real atmospheric conditions as they were prevailed on that specific (historic) day. Such reanalysis numerical model data also relies on the assimilation of observational data, in order to improve numerical weather forecast with observations.

Another option for an evaluation of the OI CLIM would be to apply historic forecasts, in order to simulate and identify alternative trajectory options with the knowledge which is available before departure. This means that no observational data would be included in the meteorological data. Such reanalysis data is also used when developing climate change functions, as the global chemistry climate model EMAC can be run in a nudged mode, using specified dynamics from real world situations as boundary conditions, in order to generate the meteorological situation that was prevailing on the specific day.

In Phase 2 this OI CLIM will be studied with dedicated traffic samples from reference year 2018 and scenarios which touch those geographic regions within ECAC area and which have been newly characterized with regards to their climate effects. Trajectory optimisations exploring this expanded geographic scope will be described in detail in D2.4. Applying these novel climate change functions in Phase 2, will allow to compare also to estimates relying to applying aCCFs (developed for the North Atlantic Flight corridor).

2.4 Wind/weather-optimal dynamical flight planning

2.4.1 Executive Summary

The wind/weather-optimized flight planning aims to minimize the defined flight operating costs by selecting the most appropriate and efficient route, altitude, and speed profiles, while considering the available wind/weather information. Optimizing the flight trajectories and minimizing the negative impact of wind/weather on the operation, the concept can reduce the impact on the environment. The implementation of the OI for an enroute airspace will be analysed to evaluate the concept from perspectives of different stakeholders.

Using the point profile data, the flight plans of the aircraft are obtained. These flight plans are used to simulate the operation in an airspace to create a base-case scenario for comparison. In the wind/weather-optimized flight planning, the planning problem is converted to a nonlinear optimization problem. And, this optimization problem is solved for each aircraft in the sector by defining its entry and exit points. Then, an optimized trajectory is obtained for each aircraft. By calculating the defined KPIs with both the nominal and optimized trajectories, the concept is analysed to figure out the impact of the operation on climate and other stakeholders.

2.4.2 Methodology

The modelling workflow of the OI is illustrated in Figure 13. The study focuses on a specific enroute airspace using the traffic records during a selected day. Using the trajectory simulator with the given aircraft performance parameters and the original flight plans, a base-case scenario is simulated to generate the baseline simulation results without implementing the concept. As the second scenario, the optimized trajectories are obtained. In the simulations, the performance parameters of the B737-800 are used to model the engine, fuel flow, and aerodynamic characteristics by assuming that all operating aircraft have similar characteristics. The wind/weather information obtained from the NCEP (National Centers for Environmental Prediction – Global Forecast System) data are used in the simulations and optimizations to support the system with the weather forecasts. The OI is analysed based on the calculated KPIs from the obtained trajectories in the defined scenarios.

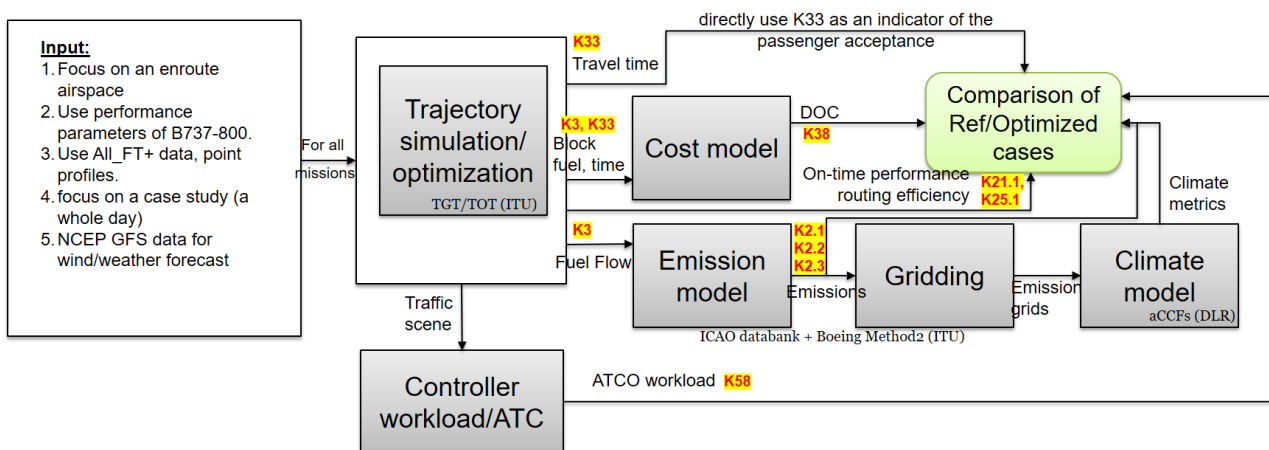


Figure 13. Modelling workflow for the OI of 'Wind/Weather Optimized Flight Planning'

2.4.2.1 Previously Described Models and Traffic Scenario

For the implementation of this OI, the same traffic scenario prepared in the free routing concept is used by focusing on the same airspace (EDUU). Also, the same day (December 1, 2018) is

analysed. Considering the wind fields in the corresponding airspace, trajectory simulator (TGT) presented in the free routing concept is utilized to simulate the traffic according to the reference flight plans. For the calculation of the released emissions, the emission model given in the free routing concept is also employed.

2.4.2.2 Trajectory Optimization Tool (TOT)

This tool transforms the trajectory planning problem into an optimization problem to generate an optimized trajectory based on a defined objective function while considering the wind/weather information. The general form of this optimization problem can be presented as follows:

$$J(t, \mathbf{x}(t), \mathbf{u}(t)) = c_Y \cdot Y(t_0, t_f, \mathbf{x}(t_0), \mathbf{x}(t_f)) + c_\Psi \cdot \int_{t_0}^{t_f} \Psi(\mathbf{x}(t), \mathbf{u}(t), t) dt$$

$$\min J(t, \mathbf{x}(t), \mathbf{u}(t))$$

$$\text{subject to } \dot{\mathbf{x}}(t) = f(\mathbf{x}(t), \mathbf{u}(t), t)$$

$$\mathbf{h}(\mathbf{x}(t), \mathbf{u}(t), t) \leq 0$$

$$\mathbf{x}(t) \in [x_{min}, x_{max}]$$

$$\mathbf{u}(t) \in [u_{min}, u_{max}]$$

where $J(t, \mathbf{x}(t), \mathbf{u}(t))$ is the objective function that is a combination of the performance quantities such as the travel duration, fuel consumption, and reaching the target waypoint. $\mathbf{x}(t)$ and $\mathbf{u}(t)$ are the state vector and the control vector at time t . The performance limits, path constraints and aircraft dynamics are presented as the constraints of the optimization problem. The following set of differential equations is used to present the dynamic constraints based on the aircraft dynamics and wind information:

$$\dot{x}(t) = v(t) \cos \chi(t) \cos \gamma(t) + W_x(x(t), y(t))$$

$$\dot{y}(t) = v(t) \sin \chi(t) \cos \gamma(t) + W_y(x(t), y(t))$$

$$\dot{h}(t) = v(t) \sin \gamma(t)$$

$$\dot{v}(t) = \frac{Thr_{max} \delta}{m(t)} - g \sin \gamma(t) - \frac{C_D S \rho v(t)^2}{2m(t)}$$

$$\dot{\chi}(t) = \frac{C_L S \rho v \sin \mu(t)}{2m(t) \cos \gamma(t)}$$

$$\dot{m}(t) = -F$$

where $W_x(x(t), y(t))$ and $W_y(x(t), y(t))$ are wind speeds (m/s) in east and north directions respectively. The control inputs or decision variables regarding the aircraft dynamics in the optimization problem are the throttle level ($\delta \in [0,1]$), bank angle (μ), and flight path angle (γ). The state variables are defined as the position (x, y), altitude h , velocity v , heading angle χ , and mass of the aircraft m . For the calculation of the performance parameters, a set of functions obtained from the BADA is also defined as constraints in the optimization problem such as:

$$\rho = f_1(h), \quad C_L, C_d = f_2(m, \rho, v, \mu), \quad Thr_{max} = f_3(h, v), \quad F = f_4(h, v, \delta)$$

where ρ is air density, C_L and C_d are aerodynamic coefficients. Thr_{max} and F refer to the maximum thrust and fuel consumption respectively. All of the mentioned parameters are expressed in terms

of the SI base units (International System of Units). The performance limits are also considered to bound the optimization variables.

2.4.2.3 Wind Model

The wind information can be obtained from the NCEP GFS data. An illustrative example is presented in Figure 14. The wind components in the x and y directions can be presented as a function of longitude and latitude. The altitude has also an impact on these components, so a realistic wind model can be presented as a function of longitude, latitude, and altitude.

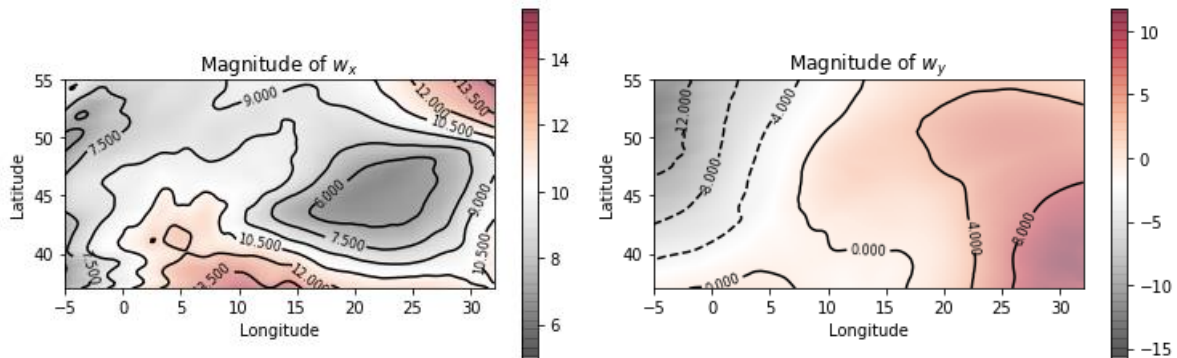


Figure 14. An example for Wind Fields (m/s) obtained from NCEP GFS

To create a case-study for the preliminary results, a simplified wind model in the following form is used in this deliverable.

$$W_x = b, \quad W_y = ax + c$$

where the wind component in x direction W_x is presented as a constant, and the wind in y direction W_y is defined as a function of longitude. Then, the wind field used in the case study is defined as presented in Figure 15.

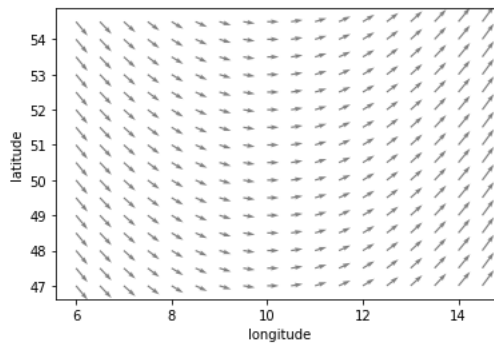


Figure 15. Simplified Wind Field for the Case Study

The simplified wind model is reasonable in the focused airspace for the wind fields presented in Figure 14. As seen in this figure, W_x is almost constant and W_y is approximately a linear function of longitude in the focused airspace whose borders are illustrated in Figure 15. However, the model is not generalizable, Therefore, in the next deliverable, it is planned to use high degree polynomials to present the wind components in x and y directions based on the NCEP GFS data to create a more generalizable and more realistic wind model.

2.4.1 Results

The preliminary results are obtained by focusing on a case study in the aforementioned high-density enroute airspace. For the selected day in 2018, the ALL_FT+ data [15] is used to generate the flight plans for the traffic in this airspace. Then, the base-case scenario is implemented in the trajectory simulation environment using the original flight plans of the aircraft. In the second scenario, the proposed optimal control method is utilized to produce the optimized trajectories for the aircraft operating in the sector. As a preliminary result, the emissions (NO_x , CO_2 and H_2O) travel duration, and fuel consumption are obtained using the generated trajectories. The averages for the traffic are presented in Table 11.

As presented in the Table, there is a reduction in all of the analysed KPIs. But, the improvement in the NO_x is relatively small compared to the other KPIs.

Table 11. Preliminary Results for the OI of 'Wind/weather optimised Flight Planning'

KPI	Base-Case Scenario*	Wind- Optimized Planning*	Percentage Change*
Travel Duration (avg. value per flight)	1097.56 sec	1068.41 sec	2.65% ↓
Fuel Consumption (avg. value per flight)	757.25 kg	737.34 kg	2.62% ↓
NO_x (avg. value per flight)	8.25 kg	8.16 kg	1.02% ↓
CO_2 (avg. value per flight)	2384.58 kg	2321.91 kg	2.62% ↓
H_2O (avg. value per flight)	931.42 kg	906.94 kg	2.62% ↓

* Results are based on BADA3 and a simplified wind field

2.4.2 Open issues

In this deliverable, only the preliminary results are obtained. Further assessments will be performed to make sure that the results are reliable. Moreover, a simplified wind model and BADA3 are used to create the optimization problem. More advanced models can improve the accuracy of the results.

The next deliverable will contain the assessments using the other KPIs such as ATR20/ATR100, ATC workload, safety (occurrence of conflicts), routing efficiency, number of movements in the airspace, ASK, direct operating cost, and CASK. The optimization problem will be improved using an advanced wind model and benefiting from the BADA4. Some estimation models will also be developed for the KPI-related calculations.

The concept leads to better cost-efficiency and mitigates the impact on the environment by reducing the fuel burn and greenhouse gas emissions. However, the improved profiles could not lead to the optimal impact on climate, because all aspects of the non- CO_2 effects are not considered during the trajectory optimization. Besides, the OI is limited to the enroute airspaces by assuming that there will be SID (Standard Instrument Departure) and STAR (Standard Terminal Arrival) procedures in the approach airspaces that define the routes and the main benefit of the dynamic flight planning can be obtained by focusing on the enroute airspaces. Focusing on a specific part of a trajectory without considering the rest of it that affect the arrival traffic can limit the implementation, but the changes in the travel durations will be kept small by arranging the objective function to mitigate any congestion and violation of the capacities in the approach and consecutive airspaces. Further assessments should be done to determine the impact of the

concept on different stakeholders. To draw a more general conclusion, an improved model for wind fields and BADA4 should be integrated into the model.

2.5 Strategic planning: merge/separate flights; optimal network operations

2.5.1 Executive Summary

Strategic network planning for airlines is a long-term problem influenced by allocating a fleet of aircraft to a set of routes composing the airline's network. Traditionally, the main objectives followed in the involved decisions are the monetary aspect of allocating each fleet type to a route and its network implication in terms of connecting passengers between flights at hub airports. However, climate considerations are arguably becoming or must become more relevant when planning airline operations. Considering the climate impacts of the flights while planning the airline's network can be a helpful step to mitigate the aviation climate footprint at the airline level.

This study aims to assess the impact of airlines considering climate footprint when optimizing their network and fleet allocation plans. An airline planning decision model using a multi-agent system was developed to do this. The model is used to assess the consequences of limiting the airline's total yearly climate impact on the profit, average temperature response (ATR20), and other KPIs listed in the previous deliverables. We assumed that flights in the ECAC area (including international flights with an origin or destination in this area) to tackle this problem. Three main airline types are considered to be modelled, namely, main hub-and-spoke, secondary hub-and-spoke, and low-cost carriers. In order to find the impact of this OI at the ECAC level, results from each representative airline will be scaled up based on the fleet number for all airlines with similar types and operating areas.

In this deliverable, we discuss the results for the KLM airline, the representative airline of the main hub-and-spoke airline type.

2.5.2 Methodology

The modelling workflow and required inputs for assessing the OI of strategic network planning are depicted in the Figure 16.

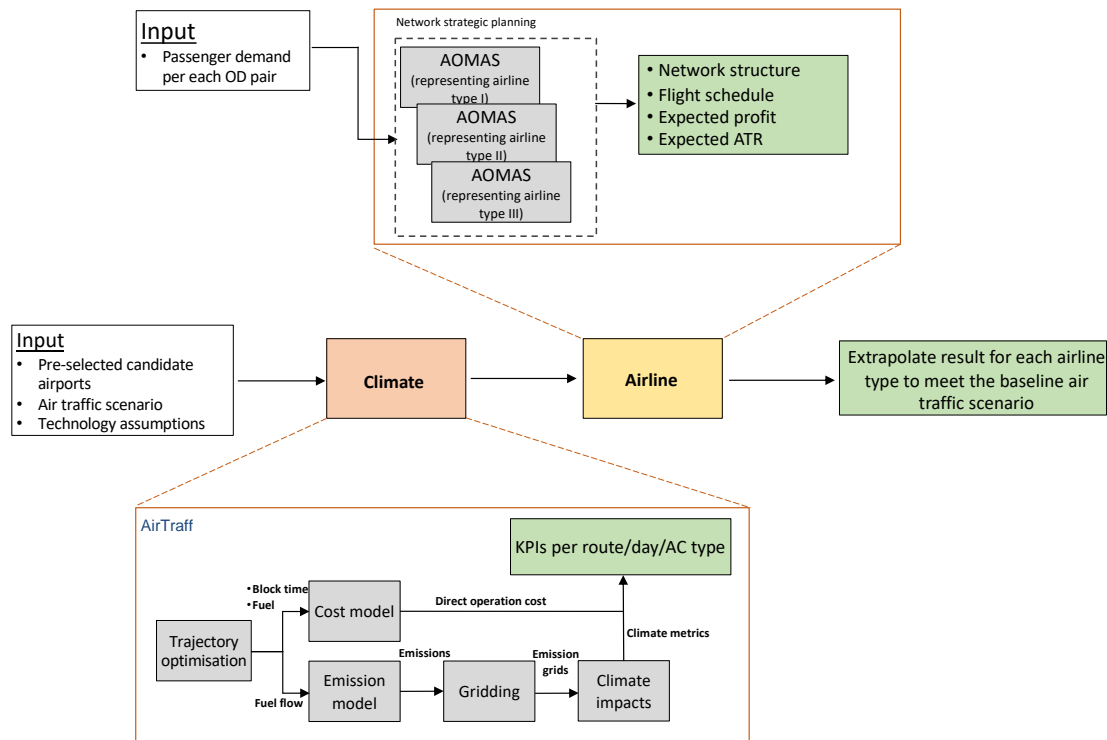


Figure 16. Modelling workflow for OI of 'Strategic Network Planning'

The passenger itinerary and flight schedule data for each representative airline are extracted based on the study's desired geographical and year assumptions. The EMAC/AirTraff 2.0 submodel [13] model was used to calculate climate and emission related KPIs for all OD pairs per AC type on four representative days of 2018. AOMAS model [8] will find the most profitable network for each airline type given the demand, ATR20, costs, and airfare per route separately in each quarter of 2018. Aggregated results of all quarters will indicate the OI effect in 2018.

The basic scenario is comparing KPIs while implementing vs. not implementing this OI in 2018. One fundamental assumption here is considering the change in the airline operation strategy as a result of implementing this OI. This assumption is limiting this OI to be used for future years because tracing the changes in airlines' operational strategies depends not only on the changes due to implementing OI but also changes in demand and market share of the airline. As modelling demand and market share evolution in future years are out of the scope of this study, we will focus on the modelling changes and measure their implications within 2018.

To achieve accurate climate-related KPIs, we planned to run the AOMAS for each quarter separately. One representative day in each quarter is set as a reference for weather conditions in that quarter. The following sections will provide more details on assumptions and descriptions of workflow stages.

2.5.2.1 Representative airlines

Measuring the changes in KPIs after implementing this OI for all airlines operating within the ECAC area would be highly time and resource demanding in practice. Most importantly, according to each airline's operations, fleet, airfares, etc., a vast amount of data is needed, which may not be available thoroughly. To tackle this, airlines are categorised into three main types, and one representative has been chosen for each category. The idea behind this is to do the calculations for the representative airlines and extrapolate the result based on the size of other airlines (fleet

size) within that category to estimate the total KPIs for the associated category. The airline types and their representatives are as follows:

- Main hub-and-spoke: KLM
- Secondary hub-and-spoke: TAP
- Low cost carrier: Ryanair

This categorisation was not meant to include all airline types. The airliners, such as charters, cargos, and regionals, are not considered in this study as either the required input data was not available for them, or the OI did not apply to them.

There is a very different business model in operating each of the mentioned types. For instance, in most cases, main hub-and-spoke airlines have very few direct flights between their spoke cities and manage to connect their passengers in several connecting banks at their hub airport(s). In contrast, secondary hub-and-spoke airlines operate from smaller hub airports. They do not only rely on connecting passengers and they may operate several direct flights between spoke cities. On the other hand, low-cost carriers mainly have their fleet operating direct flights between two or more airports.

The differences between these three airline types can be seen in the demand matrix of airlines. Figure 17 and Figure 18 show the demand matrixes for the three representative airlines in this study². In Figure 17, the two perpendicular lines of hot pixels indicate flights to and from the hub. Existing more bright pixels in OD pairs other than the hub (direct flights) distinguishes between main and secondary hub-and-spoke airlines. In contrast, point-to-point airlines have more spread hot pixels across the demand matrix. So categorising airlines have a twofold benefit in this study. First, each category's strategies and business models could be captured more precisely. Second, the problem size will be reduced significantly compared to incorporating all airlines in one model.

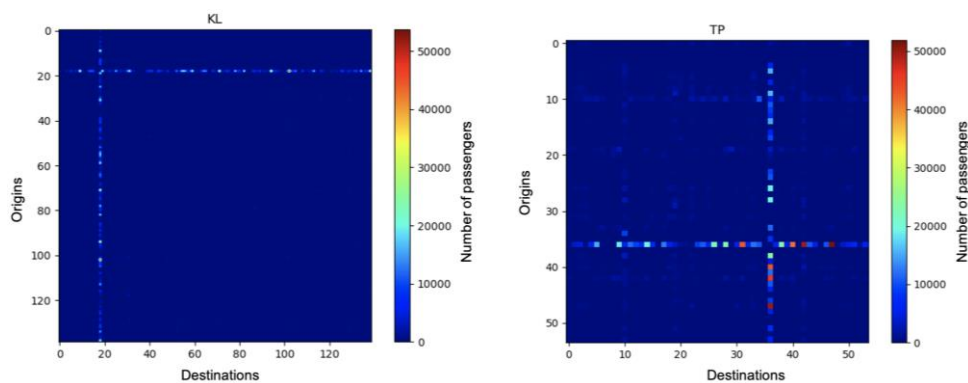


Figure 17. Passenger demand for all pairs of origin and destination for hub-and-spoke airlines (a) KLM (KL) and (b) TAP (TP)

² Data is derived from Sabre Market Intelligence Database.

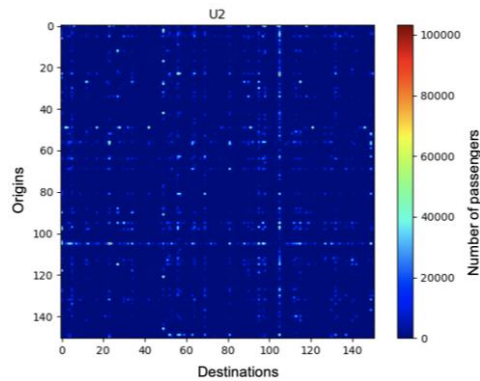


Figure 18. Passenger demand for all pairs of origin and destination for point-to-point airlines Ryanair (U2)

2.5.2.2 Demand preparation

Passenger itineraries and flight schedule databases were extracted for all ECAC flights for each quarter of 2018 from the SABRE Market Intelligence Data base. The quarter demand per itinerary was then spread over time based on the flight schedule, assuming that most of the demand is willing to fly at the moment they have flown in the database. The demand was modelled using a normal distribution with mean equals to the departure time and a standard deviation of 1 hour. In the case of itineraries with non-matching records, a uniform distribution of weekly demand was assumed. Both demand distribution is shown in Figure 19.

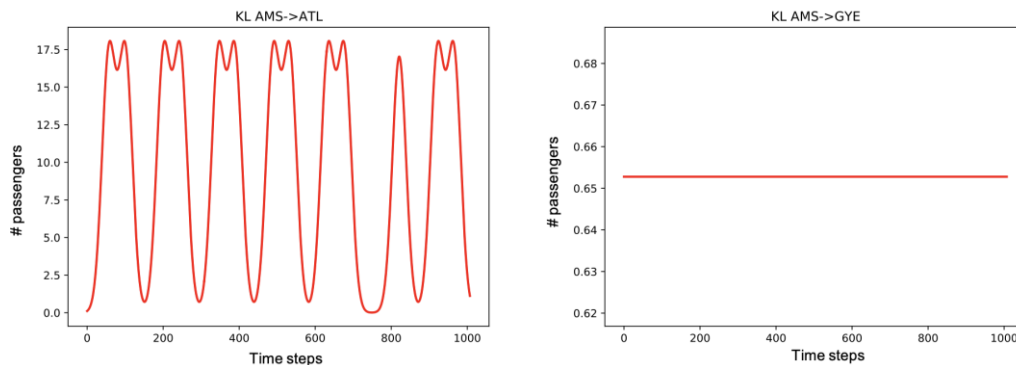


Figure 19. Average weekly demand distribution examples for a matching and non-matching case. The horizontal axis indicates time steps of 10 minutes in a week.

Using this method, the total quarterly demand per origin-destination was converted into a weekly demand-time diagram. Note that the most frequent flight departures during each quarter were assumed to be the airline's flights schedule in that quarter.

The result of matching records of the schedule and passenger itinerary database are summarized in Table 12. The number of itineraries database that matched records in the schedule database varies from 60 to 67% depending on the quarter. Still, these itineraries correspond to 90% to 96% of passengers served by KLM. On average, only 64.75% of the remaining itineraries cover 94% of the total demand served by KLM in 2018, which is a fair number to be assumed as the KLM passenger flow in the time scope of this study.

Table 12. Summary of matching itinerary demand and schedule databases

	Q1	Q2	Q3	Q4
Matching itineraries (% of itineraries)	67	60	61	67
Matching demands (%of passengers)	96	95	90	95

Pre-selected airports

Compiling all demand and schedules of representative airlines for 2018 will result in a list of airports visited during that year which is considered the airports served in the business-as-usual state of the airline. This list is the reference for pre-selected airports associated with each representative airline. Climate-related parameters will also be calculated for all OD pairs on this list. The rationale behind developing this list is that we assumed airlines are not willing to change their fleet, hub, or spoke airport due to implementing OIs. As a result, replanning an airline's network and flight schedule is done based on this list to keep the initial conditions similar in the entire modelling process. The number pre-selected airports for representative airlines are shown in Figure 17 and Figure 18 on both horizontal and vertical axis.

Table 13. Summary of pre-selected airports for each representative airline

	KLM	TAP	Ryanair
Number of pre-selected airports	126	56	144

2.5.2.3 Climate-related parameters

All the prerequisite climate-related parameters to run the AOMAS are calculated in the module "Climate" depicted in Figure 16. AirTraf is the primary model used in this part of workflow and requires the following input:

- Optimization objective**
 AirTraf uses a genetic algorithm (GA) to optimize the trajectories between each OD pairs and to calculate the output based on the GA result. The GA can run considering multiple objectives, including flight time, fuel consumption, simple operating cost (SOC, considering only flight time and fuel cost), climate impact calculated by average temperature response over a time horizon of 20 years (ATR20) due to CO₂, NO_x, H₂O and contrails, etc. the ATR20 is calculated using a set of prototype algorithmic climate change functions (aCCFs³)
- Flight plan**
 Based on the pre-selected airport list, a synthetic flight plan consisting of all possible flights between spoke and hub airports was established. To have an average ATR regarding morning and afternoon flights, the 9 am for flights from hub to spoke and 5 pm for flights from spoke to hub had been used—these two times represent average morning and afternoon connecting bank at KLM hub.

³ Yin et al. (2021) in preparation

- **Aircraft and engine performance data**

Aviation Environmental Design Tool (AEDT) version 3d is used to extract the required Aircraft-type related data for the entire representative airlines' fleet

- **Meteorological data**

Selection of weather data could be quite challenging as network planning decisions are relatively long-term, and the results would be in place for at least 3-6 months. While climate-related parameter, specifically ATR20, is highly sensitive emission's weather condition and 3D profile. Based on pre-processed weather data used by AirTraf and to provide a higher level of consistency among OI in D2.3, we chose the closest possible days to the days used in the OI "flying low and slow." The dates are 01/04, 01/06, 01/08, and 20/12, which are assumed to be the representative days for quarters one to four, respectively.

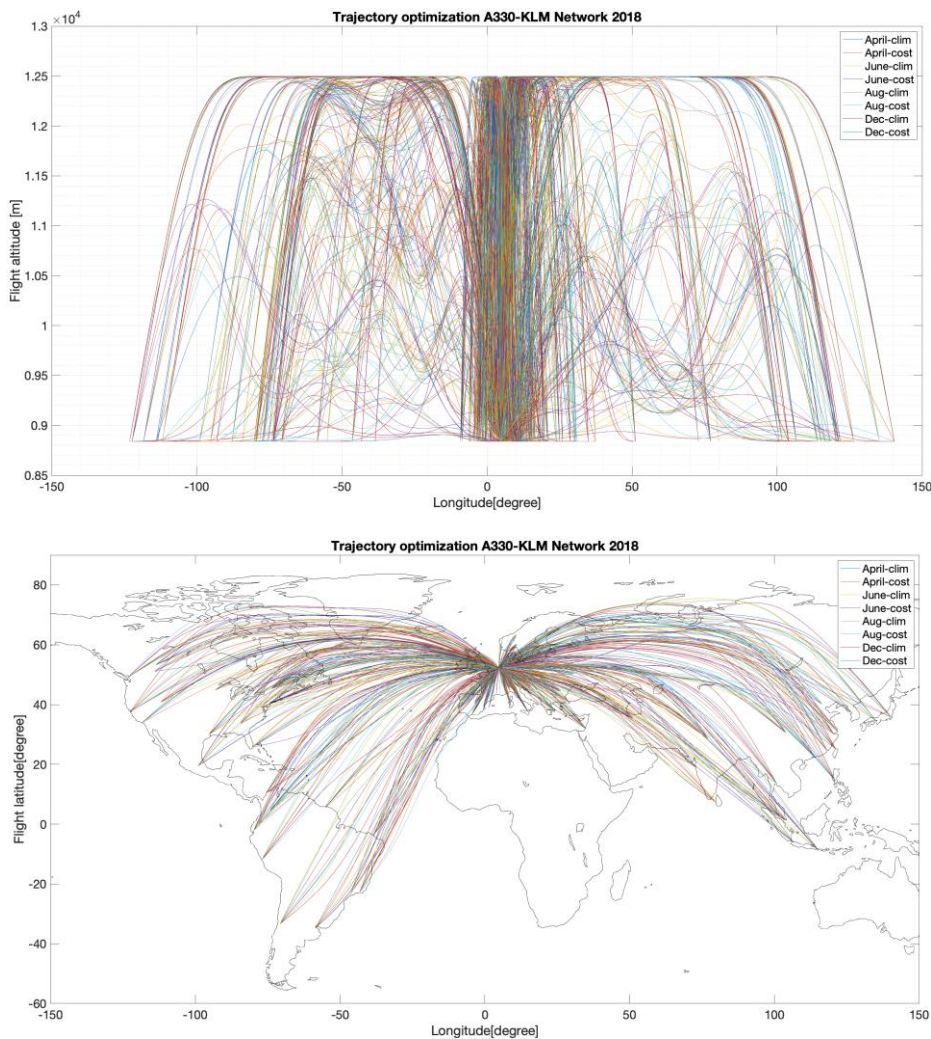


Figure 20. AirTraf result for flight trajectories using KLM network on all representative days with respect to ATR20 and cost objectives (A330)

AirTraf calculates the following parameters for all flights in the flight schedule for a given aircraft type and day.

- NO_x [g]

- H₂O [g]
- ATR20 [K]
- Fuel consumed [kg]

Note that the calculations in this model are only considering the cruise phase of the flight. To prepare the required data for D2.3, AirTraf output was aggregated for all the combinations of following input. Figure 20 shows the optimised trajectories for four representative days and two objectives using A330 for all flights in the flight plan.

- Objective: cost and ATR20
- Aircraft type: all available type in KLM fleet (9 aircraft types)
- Weather condition: four representative days in 2018

2.5.2.4 AOMAS

AOMAS is a multi-agent model aiming to solve airline network planning and flight schedule problems. In the network planning problem, the primary decision variables concern whether or not to fly in a specific route. Flight scheduling produces plausible aircraft rotation schedules that cover all target routes suggested by network planning and grantee the passenger connections in hub airports. These two problems are usually solved separately and sequentially in the literature, but AOMAS can solve them using an integrated dynamic programming approach.

AOMAS solves integrated network and scheduling at the airline level, which means the input set should be based on the target airline's operational conditions. The number of dynamic programming (DP) agents in AOMAS is equal to the number of fleet types in the target airline, as each DP agent is responsible for finding the best route and schedule for its aircraft type. For instance, in the Figure 21, the configuration with four DP agents is shown. The user can easily adjust the number of DP agents base on the use case. The idea is to divide the optimization problem into small sub-problems regarding one aircraft at a time. The subroutine finds the most profitable route and schedule by comparing the profitability of the best result for each fleet type under consideration. This iterative process is repeated until the fleet type is no longer profitable, does not respect the minimum and maximum aircraft utilization values defined by the user, or does not respect the minimum ATR20 desired by the user.

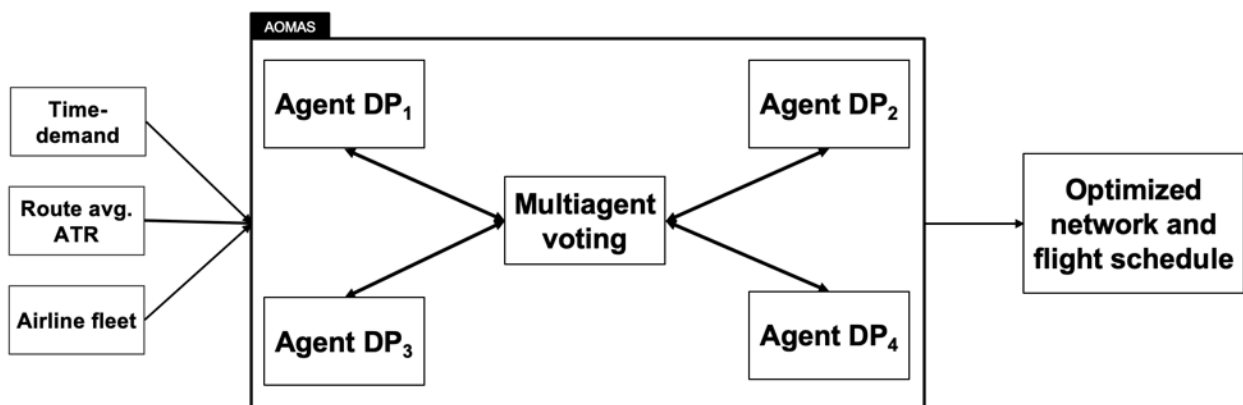


Figure 21. AOMAS input, output and structure

The Bellman-Ford algorithm is adopted to carry out the optimization [27]. A time-space graph model [29]. is used to represent the possible aircraft movements over time (Figure 22). In this time-space model, the set of nodes represent a position of the aircraft in time k (vertical axis) and space i (horizontal axis, representing airports). The edges represent either fly or the decision to keep the aircraft at the same airport for one time period.

The first step in the dynamic programming algorithm is the backwards computation of the objectives. That means that the optimization process starts at the end of the week and moves towards the start of the week when analysing the best schedule for the fleet type under analysis. The value of being at each node (time and station) is stored in a variable (Profit in Figure 22), and it represents the future profit that the aircraft can still do from that point in time until the end of the week.

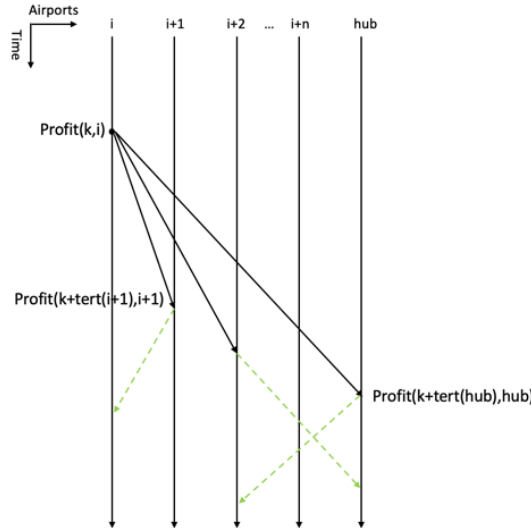


Figure 22. Visualisation of the time-space network – decision to be made at airport i at one time step k ($tert$ refers to the time of the flight; $Profit(k, i)$ refers to the potential profit from time k onward if aircraft is at airport i at time k)

The schedule optimization starts by assuming a negative penalty profit if the aircraft is not at the hub at the end of the week. No penalty is given for the equivalent node at the hub, and a value of zero is assumed. The algorithm then moves backward, checking at each airport the possibility to have a flight starting at that airport at the time under analysis. If a flight is possible, the Profit value is computed:

$$Profit(i,t) = Profit(i,t+1) + cash_{flight}(i,j,t+tert)$$

where $Profit(i,t)$ is the future profit value at airport i at time t and $cash_{flight}(i,j,t+tert)$ is the profit computed for the flight between airports i and j , starting at time t and landing at time $t+tert$, where $tert$ is the time of the flight. Hence, if $Profit(i,t)$ is higher than $Profit(i,t+1)$, the algorithm will save the flight as a possible flight for the schedule, and the departure time and destination airports are stored in memory. In Figure 22, the different flights that can be done at any time t with the origin at the hub are shown. The profit contributions of flights to each destination are compared through the relaxation method, and the destination that contributes to the highest profit is chosen (represented in green in Figure 22). The green dotted arrows indicate the flight legs that have already been chosen from a previous edge relaxation, while the black arrows indicate possible flight legs from station i at time k .

The algorithm continues this process until it reaches 0h00 on the first day of the week. At the end of the process, two $1008 \times \# \text{airports}$ matrices are computed: one with the Profit values and the other with the indication of the airport to which we should fly when staying at a specific node in the time-space network. The first matrix is a monotonically decreasing matrix (from 0h00 Monday to 23h59 Sunday) for all airports.

The next step is to define the most profitable schedule. Starting at the hub, the algorithm goes forward through both matrices and selects the flight movements that compose the total weekly

future profit value obtained for 0h00 on Monday at the hub airport. This procedure is done for all aircraft that are available in the fleet type and that flights are added to the schedule.

In order to determine the amount of demand that is served by the airline after the routing of one aircraft, the schedule produced from the dynamic programming subroutine is examined. The number of passengers on each flight in the schedule is the demand that has to be subtracted from the time-demand matrix. It is important to notice that the passengers who are onboard a flight might not all prefer the departure time due to the application of the attraction band. As such, the demand served has to be subtracted for a range of time steps within this attraction band. The time-of-day demand is reduced to zero starting from the time step of departure t and propagates out in both directions towards $t - AT$ and $t + AT$. "AT" is the "attraction band" that determines all passengers willing to compromise their preferred departure time. As soon as the summation over these time steps reaches demand served, the process stops. Figure 23(b) shows the remaining demand after the passengers served on the two first aircraft is removed.

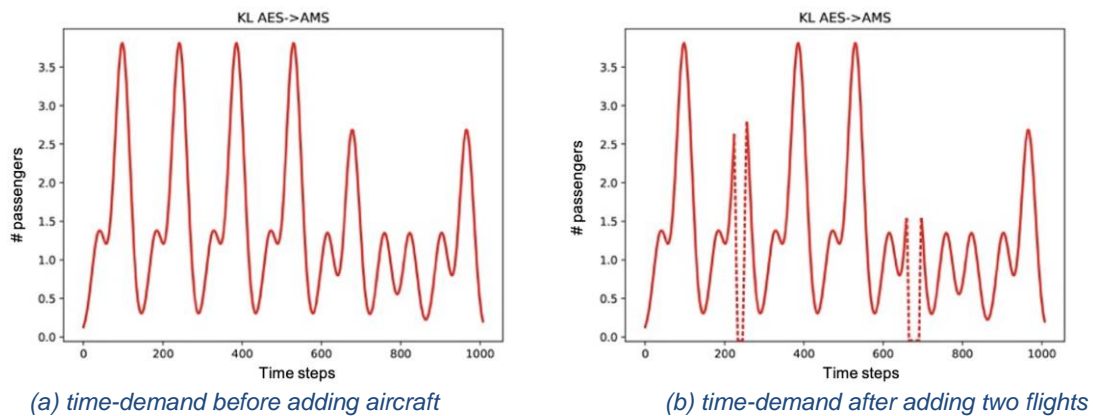


Figure 23. Visualization of updating time-demand after the addition of two aircraft

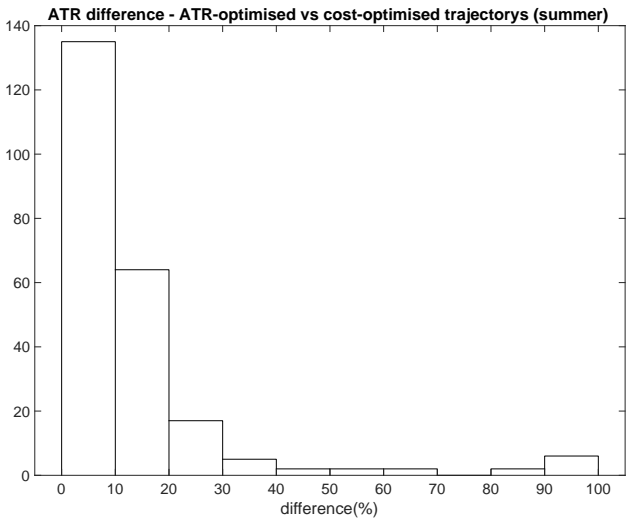
Finally, the mediator agent gathers results from all DP agents and ranks them via a heuristic adaptive search voting algorithm. The most promising ones in terms of profit and ATR20 are saved, and the rest are deleted. Accordingly, the time-demand for all OD pairs will be updated. This way time-demand only keeps the changes related to the selected solutions by mediator agents, and all other changes that took place within DP agents were replaced with their initial values. The next iteration starts with update time-demand, and DP agents follow the same procedure until they assign all their available aircraft or are no more profitable to assign aircraft. All solutions are compiled into a Pareto-frontier graph by the last iteration.

2.5.3 Results

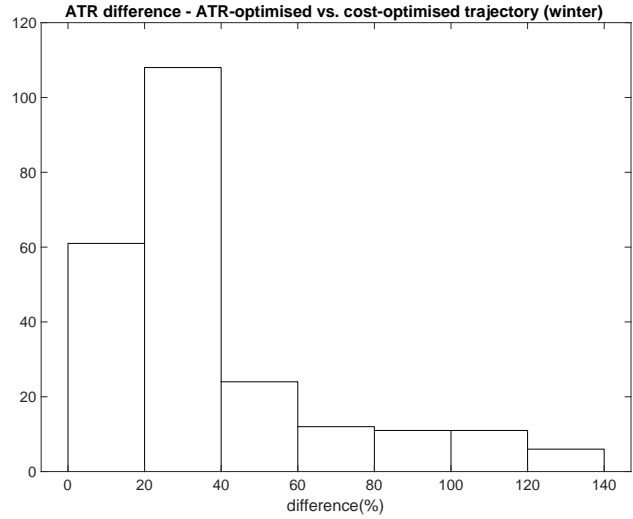
The developed workflow was used to conduct a study on KLM flights in the first quarter of 2018. Processing KLM's demand and schedule data in this period resulted in 126 spoke airports that were served during this period. A flight plan corresponding to these airports was also prepared to be used in the AirTraf. To measure the sensitivity of ATR20 to meteorological conditions, the difference of this KPI was calculated on two extreme representative summer and winter days. Figure 24 shows the relative change (in percentage) in ATR20 in two extreme weather conditions for flight to and from all spoke cities after eliminating 3% outlier data. Having up to 140% change in ATR20 in two extreme weather conditions would justify our choice to separate the calculation by quarters to have more accurate results due to providing a better meteorological representative day.

Another analysis that was carried out to find how ATR-optimised trajectories are different from cost-optimised trajectories is finding the time of flight difference in these two groups. The summer and winter representative days were used to find the maximum potential difference. The result is

depicted in two histograms in Figure 25. Results are showing in more than 98% of trajectories, the flight time difference between an ATR-optimised trajectory and a cost-optimised trajectory is less than 3% in summer. In the case of extreme weather condition in winter, this amount will increase to 4%, which is still a relatively small number to impact the network planning decisions. This difference means that if airlines want to swap their business-as-usual trajectories (considered cost-optimised trajectories in this study) with ATR-optimised trajectories, the flight time would only increase about 4% in the worst-case scenario.

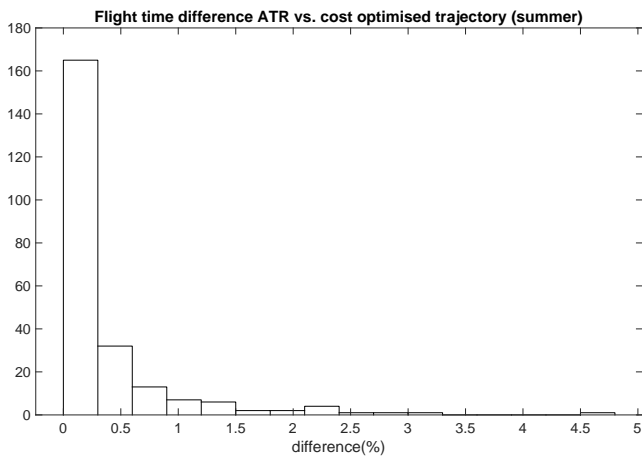


(a) Representative summer day

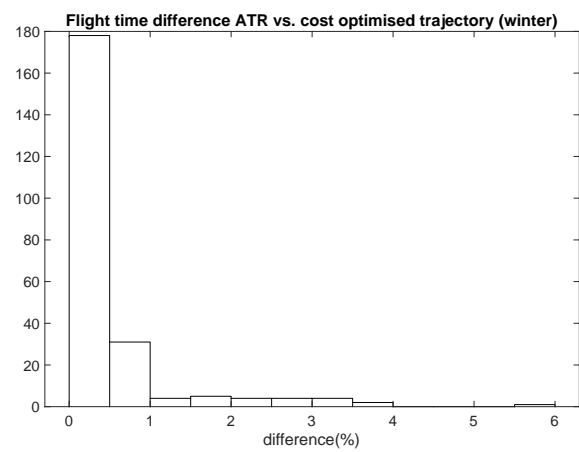


(b) Representative winter day

Figure 24. ATR20 absolute difference in two extreme summer and winter representative days (KLM-A330)



(a) Representative summer day



(b) Representative winter day

Figure 25. Flight time absolute difference in ATR-optimised vs. cost-optimised trajectories (KLM-A330)

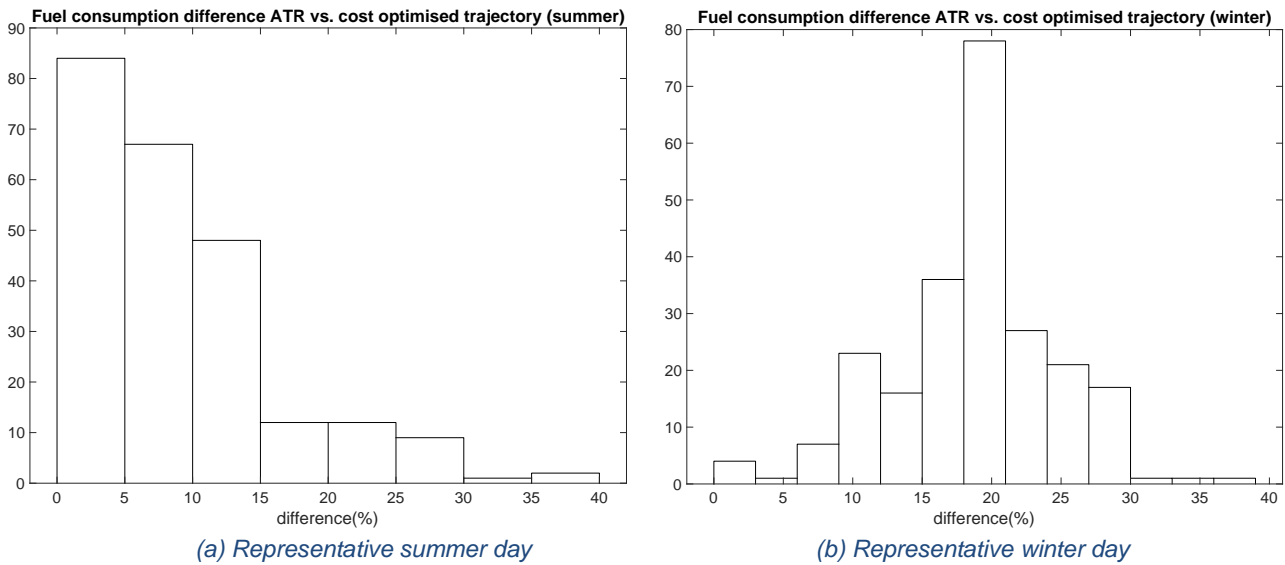


Figure 26. Absolute difference in fuel consumption for ATR-optimised vs. cost-optimised trajectories (KLM-A330)

On the other hand, airlines would face an increase in the fuel cost, which could be more significant than the flight time variation. The fuel consumption for the same simulation setup is presented in Figure 26. The results suggest that although the relative increase in consumed fuel is notable, they are all calculated under the direct operating cost of a flight which contributes a portion of the total cost of a flight. A more detailed calculation of changes in the total cost of a flight will be reported in D2.4.

The analysis of AirTraj output indicates that by burning about 12 and 20 percent more fuel in summer and winter, KLM could reach on average 16 and 39 percent reduction in ATR20 in summer and winter, respectively. This ATR20 reduction would be possible with a maximum 4% flight time deviation. To further investigate this number, we normalised the ATR20 for each trajectory by non-climate values in that trajectory, namely, flight time, distance and consumed fuel. The goal in this step was to find trajectories that have a relatively higher climate impact. In other words, we need to spot OD pairs that on average would have more ATR20 effect. The rationale behind this approach is that the flight time difference due to exchanging cost-optimised and ATR-optimised trajectories is far less than the resolution of the data that we have at hand. It is also believed to have a negligible effect on the business-as-usual operation state of airlines. So, if airlines want to reduce the ATR20 more than it is achievable by flying in a climate-optimised rather than the cost-optimised trajectory, they need to have a ranking of their operating route with respect to ATR20 and cost. Then it would be possible to balance the trade-off between their total profit and ATR20 over their network.

Figure 27 displays the expecting Pareto-frontier between the airline profit and ATR20, based on the previously mentioned analysis results. Point 1 represents the airline's business-as-usual and Point 4 shows the airline's net profit if it does not operate anymore. Obviously, at this point, the ATR20 is equal to zero, and the total profit is negative. If the airline opts to exchange the cost-optimised with climate-optimised trajectories, we would reach Point 2. If the desired ATR20 reduction was more than the amount of ATR20 at Point 2, the airline would need to change its network to reduce climate impact while maximising the profit to find a Pareto-optimal point such as Point 3.

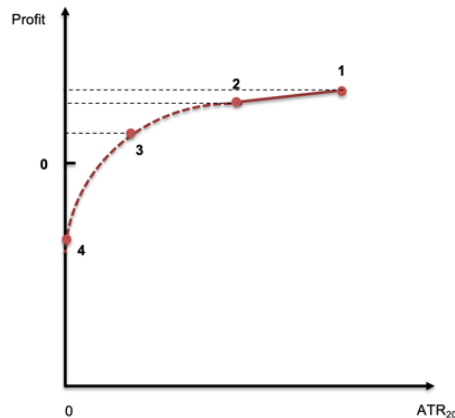
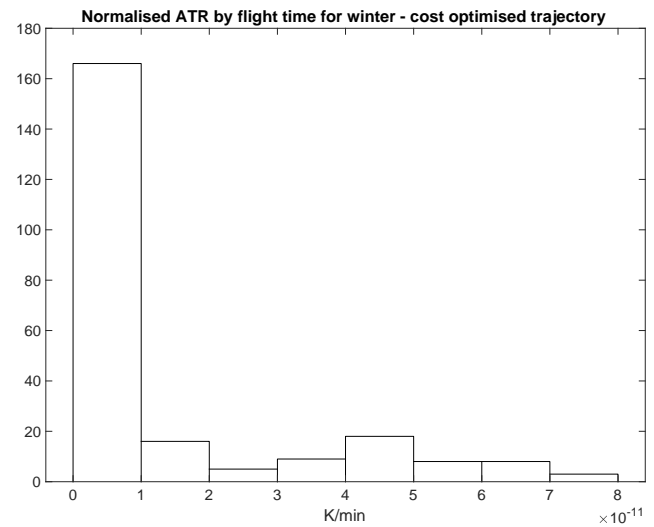
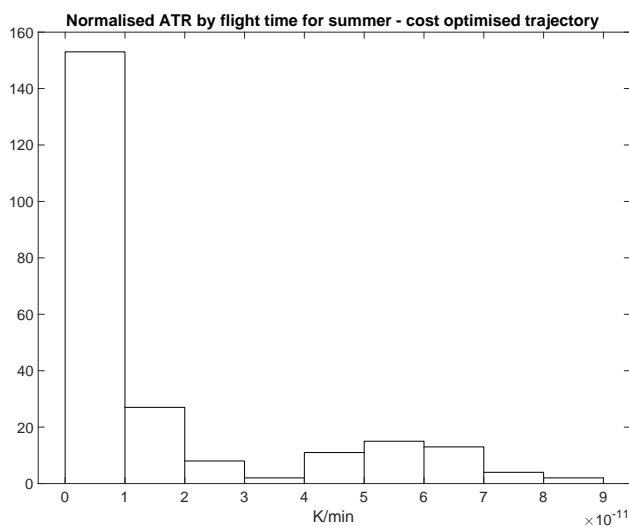
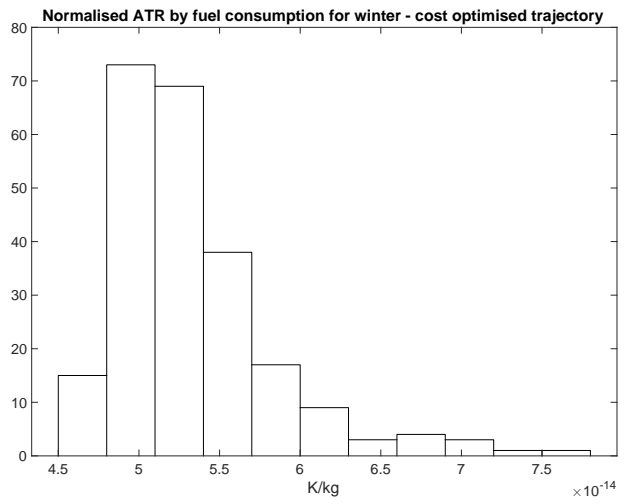
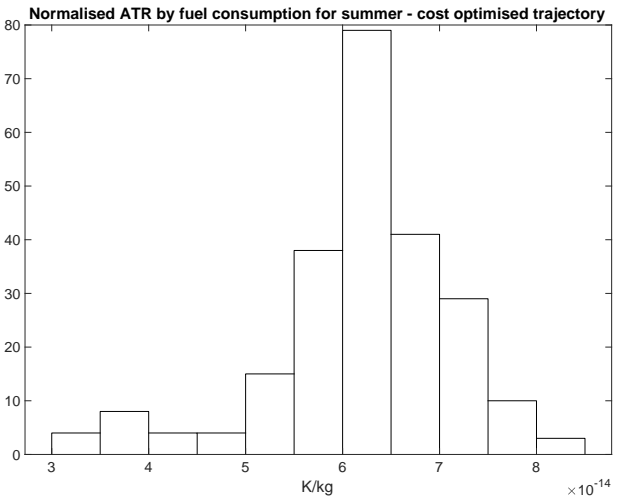
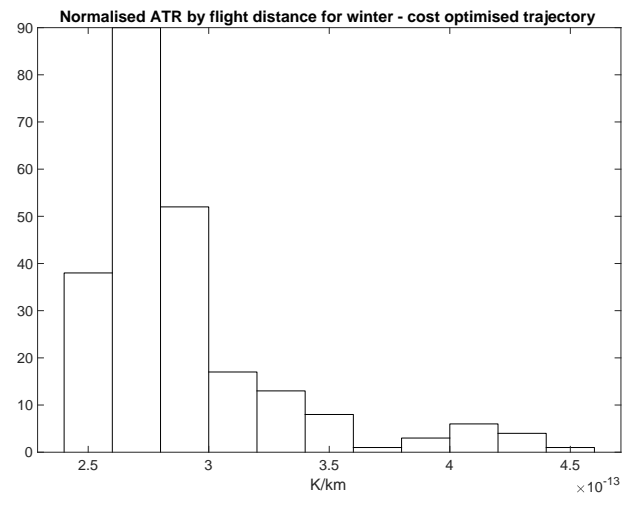
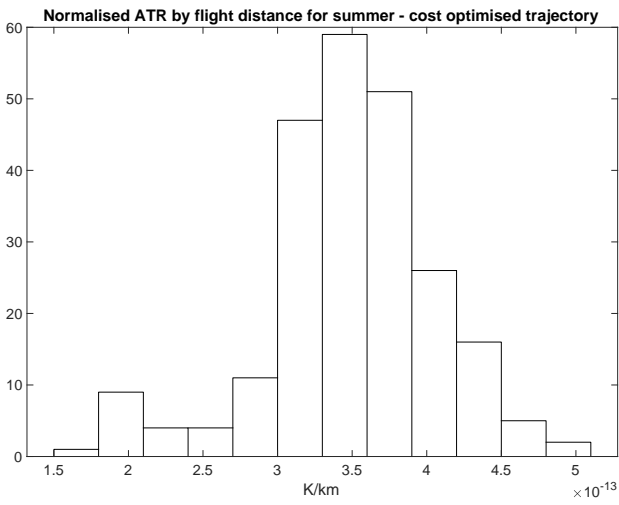


Figure 27. Expecting form of Pareto frontier for an airline

In the next step, we normalised the ATR20 for each trajectory by its flight time, flown distance, and fuel consumption for all OD pairs in the representative summer and winter days. In this way, a ranking of routes according to the ATR20 per minute, ATR20 per kilometre, and ATR20 per kg of fuel is obtained. In Figure 28 and Figure 29 the histograms of this analysis are presented.

Preliminary results from normalised ATR20 values by flight time for trajectories within the KLM network in 2018 are less than 1% of ATR20 in each trajectory. This means more than 99% of ATR20 in all routes are proportional to the flight time and not the trajectory itself. Furthermore, comparing the normalised fuel and distance results indicates a tighter correlation between flight distance, fuel consumption, and ATR20, as normalised values are less than 0.01% of total ATR20 in all trajectories.

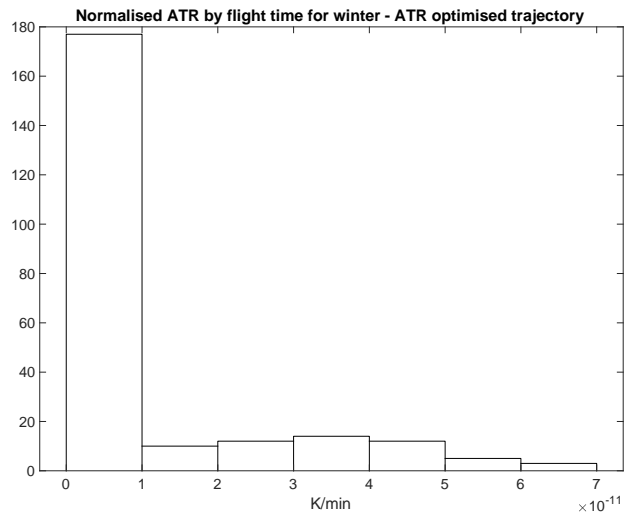
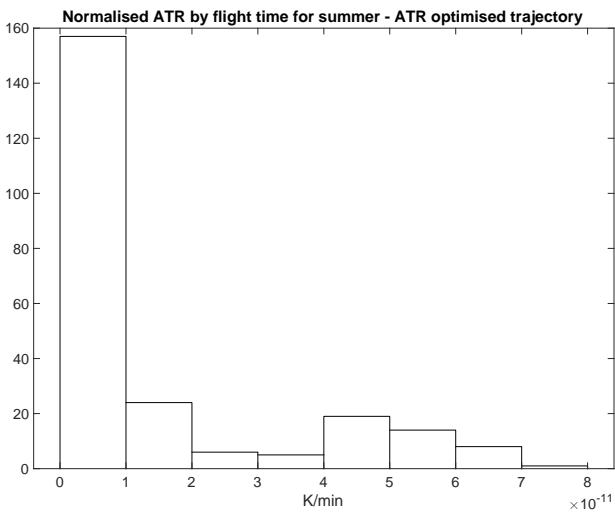


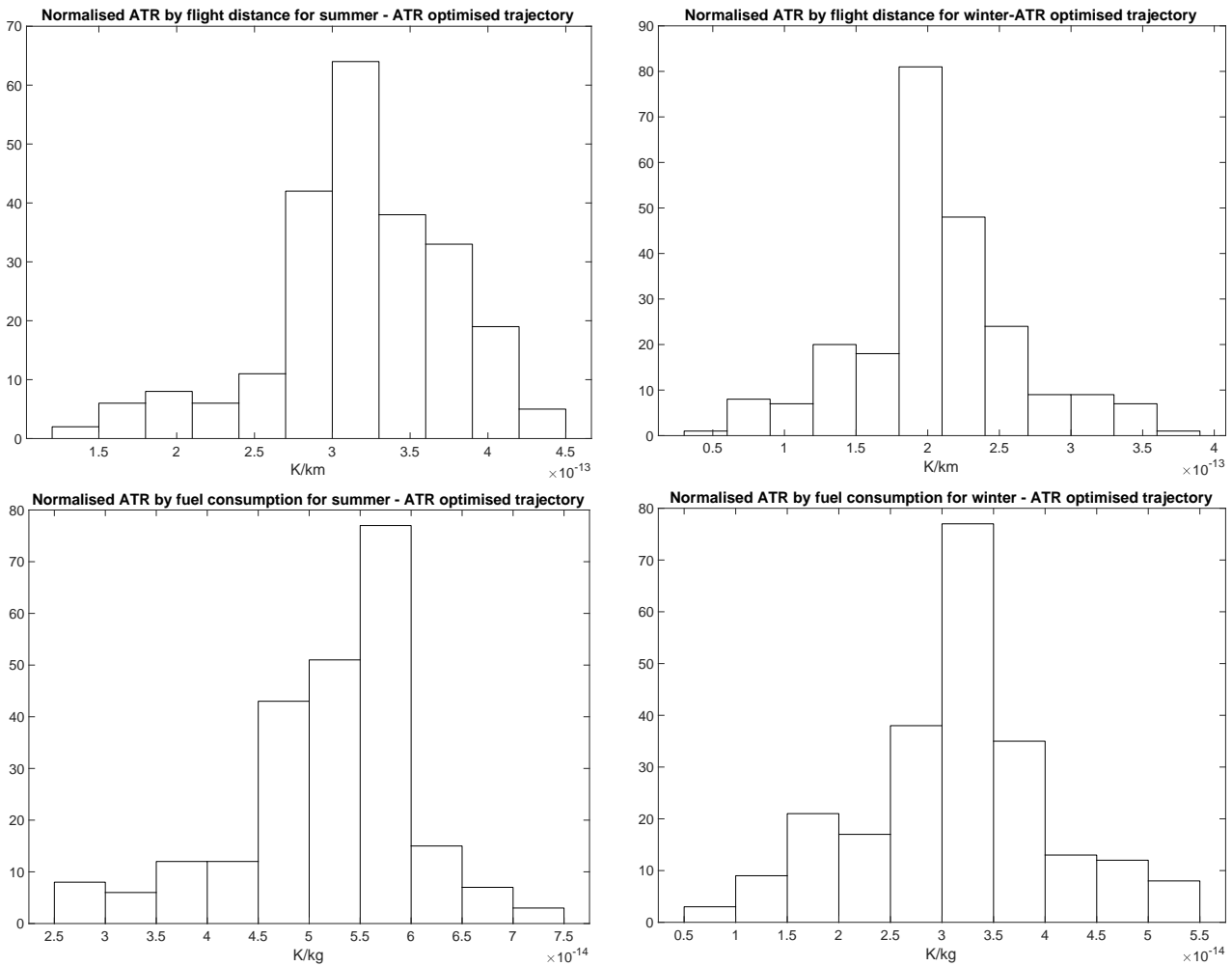


(a) Representative summer day

(b) Representative winter day

Figure 28. Comparing normalised ATR₂₀ for cost-optimised trajectories (KLM-A330). In this and in the following figure, the panels from top to bottom show ATR₂₀ per minute, ATR₂₀ per kilometre, and ATR₂₀ per kg of fuel, while left-column panels show the results for a typical summer day and right-column panel represent a typical day in the winter.





(a) Representative summer day

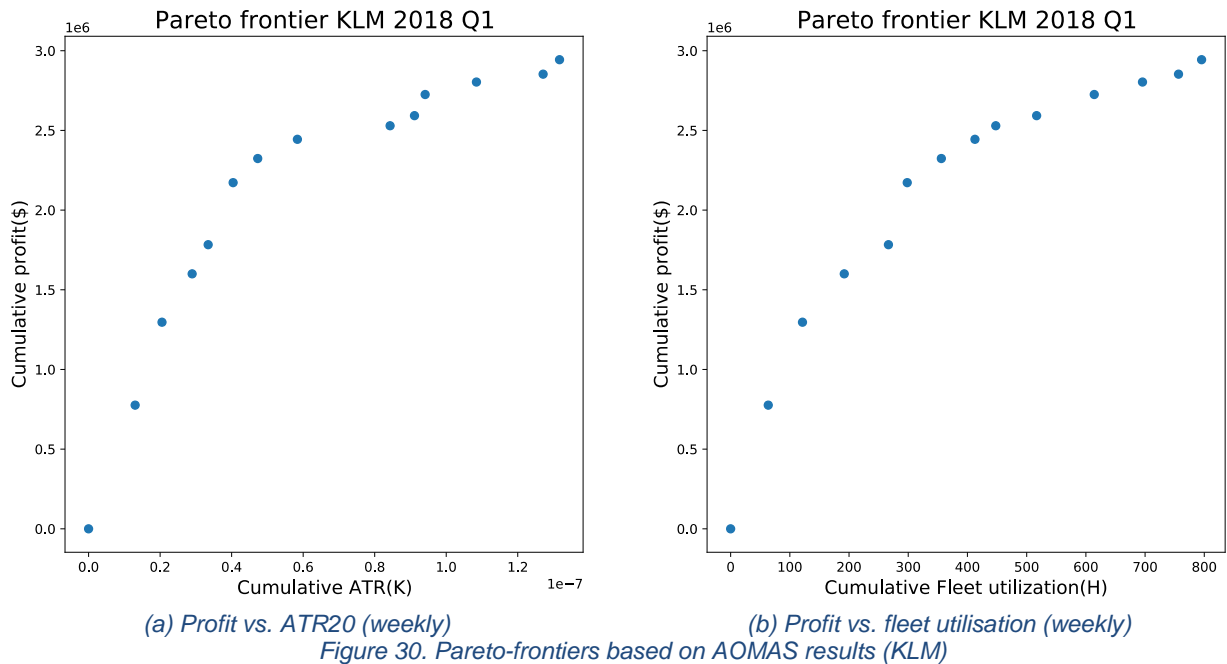
(b) Representative winter day

Figure 29. Comparing normalised ATR20 for ATR-optimised trajectories (KLM-A330)

The results suggest that there is not a meaningful difference between route's average ATR20 to be used as a metric to rank the within the KLM network. So, if an airline wants to find a point similar to Point 3 in Figure 27, it should choose one of the following options:

- Operate in route with shorter distance
- Using a smaller fleet
- Or reducing the total utilisation of the fleet

The AOMAS is being calibrated to replicate the business-as-usual state of the representative OI. In this deliverable, a preliminary result assigning three fleet types A330, B737-700, and B777-200ER (6 aircraft from each), is presented in Figure 30. In each voting iteration of AOMAS, one (or more) aircraft is chosen, saving its weekly routes and schedule into the airline plan. Then the weekly results will be multiplied by 13 to obtain the quarterly results. The final iteration establishes a Pareto-frontier indicating cumulative main KPIs values of solutions in each iteration. This diagram could also be used for cost-benefit analysis. All climate-related KPIs are gathered from AirTraf results. Non-climate KPIs are driven from the network and schedule solutions in the final iteration of AOMAS. As the calibration procedure of AOMAS is not completed yet, the rest of the KPIs will be reported in the next deliverable.



2.5.3.1 Conclusion

The workflow developed in this OI has a major difference from other OIs concerning the climate-impact measurement. In this OI, we aim to replicate the representative airlines' operation using the input data in the first place. Following that, the potential changes that may happen along with the implementation of the OI. Specifically, we are looking into the network planning and scheduling of an airline and the variations due to the climate-optimized strategic network planning in the input parameters of these two problems. In contrast, most of the other OIs in this project assume that the reference air traffic scenario would remain unchanged even after implementing all the OIs. This assumption facilitates the calculation of KPIs before and after implementing OIs.

Modelling the OI implementation at the airline level adds a set of parameters under the concept of "airline preferences." For instance, by the end of the calibration process of AOMOS, it should be able to replicate the airline's business-as-usual operation state by having only the demands and fleet of all three representative airlines. The next step is to use the calibrated model to find the airline operation after implementing the OI. Here is the point at which airline preference comes into play. A point on the Pareto-frontier (Figure 30) for each representative airline should be chosen that shows its preference to compromise profit in favour of reducing climate impact.

In conclusion, climate-optimized strategic network planning OI would report a Pareto-frontier rather than a single value of relative changes before and after implementing the OI. This approach is inevitable because we are incorporating airlines' preferences as they face the changes in cost, flight time, etc., after implementing OI. The advantage of this approach would be the application of Pareto-frontier as a quantitative cost-benefit tool in work package three.

2.5.4 Open issues

There are five main topics to be investigated in the next deliverable D2.4:

- Finalizing the model calibration in order to cover the entire representative airlines' fleet
- We are considering the demand dynamic in terms of market share. Currently, we are assuming the demand for all OD pairs is constant regardless of the airline's frequency. In

practice, this is not necessarily the case. Demand could evolve based on the frequency offered in each OD pair.

- Currently, AirTraf uses aCCFs that are calibrated only for the northern hemisphere, but it's being used for flights with an origin or destination in the southern hemisphere. For D2.4, correction and recalibration would be needed to compensate for the error in such flights.
- CO₂ emission is not one of the AirTraf outputs, but it is only taken into account in calculating the ATR20. Adding a module to AirTraf to extract the amount of CO₂ is a must for the next deliverable.
- Assessment of the relevant non-climate KPIs for this OI.

2.6 Climate-optimised intermediate stop-over

2.6.1 Executive Summary

The effort of burning fuel for carrying fuel can be reduced by intermediate stop operations (ISO). Instead of performing a direct long-haul flight, the mission is interrupted by an intermediate landing for refuelling. Less fuel has to be carried, weight and thus fuel consumption can be reduced. Previous studies [30], [31], [32] have shown a fuel-saving potential of approximately 5% on a global scale of long-range flights. Furthermore, CO₂ and non-CO₂ emissions such as NO_x, H₂O and contrail formation and their effect on the climate can be reduced. While this concept has been analysed comprehensively for fuel-optimal solutions, this OI investigates the innovative aspect of climate-optimized ISO. Thus, the goal is to minimize the climate impact and select the intermediate stop airport on climate-related criteria. To achieve additional savings, constant flight levels are assumed for ISO missions, so high flight altitudes can be avoided.

To model these effects, direct long-haul missions, their trajectories, emissions, and their climate impact, is calculated for the reference case representing the status quo. The implementation of the OI is modelled as follows: a selection of ISO airports is taken per mission and the trajectories, emissions and climate impact is simulated for all considered ISO missions. On the one hand, this enables comparisons between different ISO airports as well as identifying characteristics of climate-optimal ISO missions. On the other hand, the full potential of ISO can be derived from comparing the reference scenario to a flight plan of implemented ISO missions.

The results show a climate-mitigation potential of more than 6 % with regards to ATR20 and ATR100, which is associated with a detour of approx. 4% and an additional flight time of 11%. Fuel consumption increases by 3% compared to the non-stop reference case. Furthermore, it appears that there are differences in location for climate-optimal and fuel-optimal ISO. Further analyses will be performed in the next iterations, among other things, by considering step-climbs for fuel-optimal operations and considering aircraft optimized for shorter routes. Network and stakeholder effects will also be considered in the following deliverables.

2.6.2 Methodology

The modelling work flow and the utilized database have already been described in Deliverables D2.1 and D2.2 [7][8]. A summary of the workflow is shown in Figure 31.

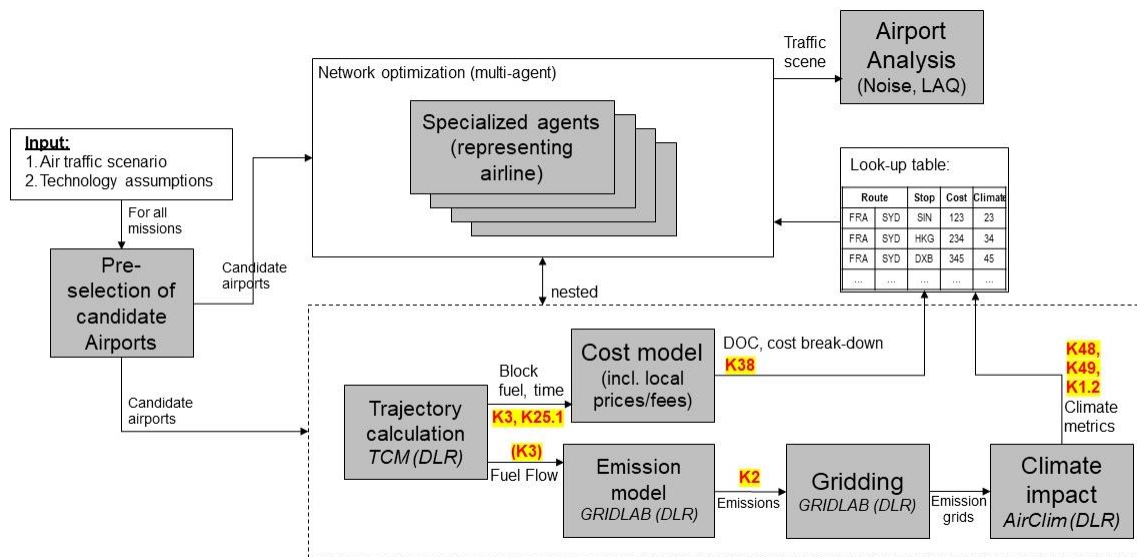


Figure 31. Model workflow for OI of ISOC

Reference scenario

The basic input for the modelling workflow is derived from Sabre Market Intelligence Data base, where a global flight plan for the year 2018 is provided. This flight plan contains information on origin and destination airports, aircraft type, seats, and frequencies of the different flights. This data is enriched with Airport location (latitude, longitude, elevation) and whether the mission starts or ends within the ECAC region. The airport-related data is provided by globalflights.org [33]. The detailed flight plan is filtered for flights with a great circle distance of more than 2,500 NM. Furthermore, the origin or destination of the mission has to be within the ECAC⁴ area. The considered aircraft are limited to types available within BADA4 and to those referred to as long-haul aircraft, i.e. A330, A340, A350, A380, B747, B767, B777, and B787. This results in approx. 2,800 different missions representing 800,000 flights that cover approx. 15% of all global ASK (see Table 14). The reference case represents the status-quo of European long-haul flights in 2018.

Table 14. Share of global ASK covered with OI of ISOC

	ASK [billion]	Share of Total ASK
Total ASK	10,055	100%
Long-range	3,528	35.1%
Long-range from/to ECAC	1,837	18.3%
Long-range from/to ECAC with selected fleet	1,794	17.8%

The scenario of implemented OI

Modelling the OIs implements the same flight plan as the reference case to ensure comparability of results. However, the direct missions of the flight plans are replaced by missions with an intermediate stop at an airport to refuel. The location of those ISO airports is derived from a database of all global airports [33]. A preselection of possible ISO airports is performed based on the detour and eccentricity metrics. That means only those airports are considered for an

⁴ ECAC member states according to European Civil Aviation Conference [34]

intermediate stop per OD pair if the detour distance resulting from an intermediate landing at this airport is below 20%. In addition, the better an airport is suitable for fuel-efficient ISO, the closer it will be located to the centre of the great circle connection between origin and destination. Thus, the eccentricity of the intermediate stop airport is limited to 75% percent: That means

$$f_{detour} = \frac{\overline{AS} + \overline{SB}}{\overline{AB}} \leq 1.2 \quad (1)$$

$$f_{offset} = \frac{\max(\overline{AS}, \overline{SB})}{\overline{AS} + \overline{SB}} \leq 0.75 \quad (2)$$

where A represents the starting point, B is the destination point, and S is the point of the examined intermediate stop airport.

To further reduce computational efforts, possible ISO airports that are geographically close to each other are clustered regarding their position (latitude and longitude) into the following grid cells⁵:

- Latitudinal: -90° to -60°, -30° to 0°, 0° to 30°, 30° to 45°, 45° to 60°, and 60° to 90°
- Longitudinal: -180° to -150°, -150° to -120°, -120° to -90°, -90° to -60°, -60° to -30°, -30 to 0°, 0° to 30°, 30° to 60°, 60° to 90°, 90° to 120°, 120° to 150°, and 150° to 180°

For each grid cell, the airport with the smallest detour is selected as representative. This results in an average of 9.5 possible ISO connections per OD pair. Figure 32 illustrates the selected ISO airports from the preselected ones according to offset and detour. A further check if the selected airports fulfil the requirements of e.g. runway length and capacity is not performed in this context.

In the first place, it is assumed that airlines use the same aircraft types for ISO as they did for non-stop operations, although it might make sense to replace those with aircraft optimized for shorter distances. In doing so, implementing the OI is possible without changes in the airline's fleet.

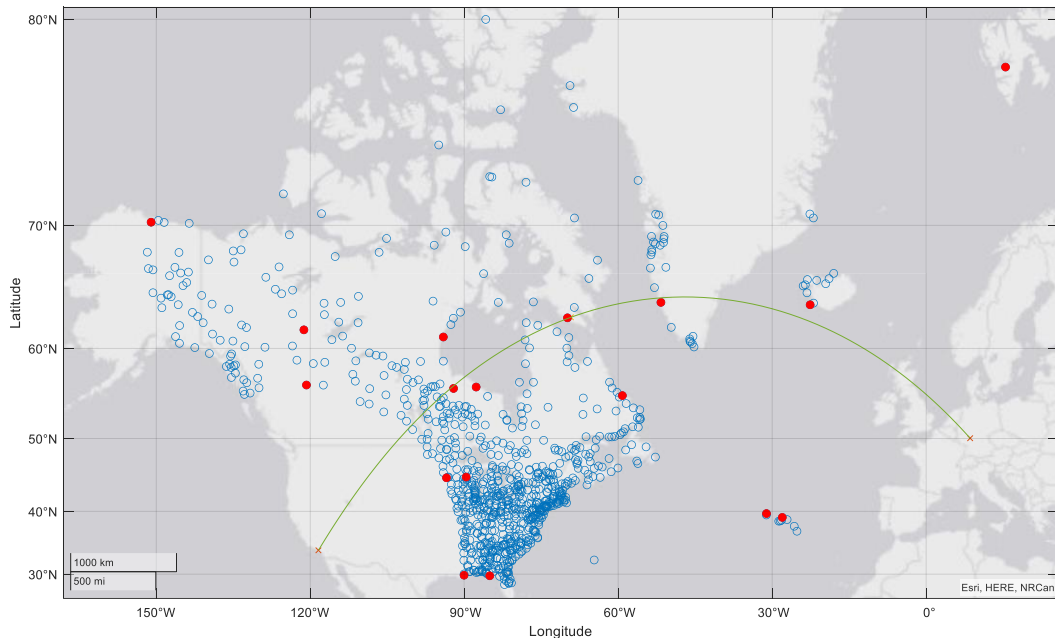


Figure 32. Possible and selected ISO airports for route connecting FRA and LAX

⁵ Grid cells are oriented towards AirClim's granularity for assessing different climate impacts [35]

Modelling the climate impact of the OI

Calculating the trajectories for every mission (direct and non-stop) is the basis for assessing emissions and climate impact metrics for this OI. To do so, DLR's Trajectory Calculation Module (TCM) is used to create reduced emission profiles. For details on this tool, please refer to D2.1. For each aircraft type, the trajectories are calculated one-dimensional and non-georeferenced for flight lengths in 100NM steps leading to the respective altitude and fuel flow profiles.

The following assumptions were made to calculate the trajectories:

- The load factor of all aircraft is set to a European average of 0.84 (according to [11]). If a connection cannot be performed due to too heavy weight, the mission is replaced with two aircraft and a load factor of 0.42. This ensures that the passenger demand is fully covered.
- The connection between airports is assumed to be a great circle.
- Atmospheric conditions are approximated with ICAO International Standard Atmosphere (ISA). Daily specific weather conditions are not covered because the annual global flight plan will be analysed as a whole.
- Cruise altitudes from 29,000ft to 39,000ft (in 2,000ft steps) are assumed. For the direct connections, a fuel optimal flight profile ('step climbs') is calculated additionally to represent the status quo as well as possible.
- BADA4 Aircraft performance metrics are deployed.

The reduced trajectories are then adjusted successively to match the respective OD pair.

The Global Air traffic emission distribution laboratory (GRIDLAB) tool from DLR is applied to generate 3D emission inventories for each flight of the described traffic sample. Based on the flight plan for each mission, the best-fitting reduced emission profile in terms of aircraft type and mission length is picked from the before-mentioned trajectory database both for the non-stop scenario and for both legs of the considered ISO missions. Afterwards, the selected trajectory is adjusted to the exact great circle distance between the two connected airports by extending or truncating the trajectory in the cruise phase. Airport elevation is also regarded by modifying the respective climb and descend profile within its phases with speed curtailments. Emissions caused by taxiing and the take-off itself are considered following the landing take-off cycle (LTO) from ICAO, assuming the reference emission indices from ICAO engine emission database [20] in both idle and take-off mode and multiply them with the respective reference fuel flow from the same database to obtain emission flows. At the beginning of the trajectory on-ground emissions of engine running in idle mode for 19 minutes are added for taxiing out, followed by 42 seconds in engine take-off mode. At the end of the trajectory, another emissions amount of 7 minutes in idle mode are attached, representing taxiing in. Finally, the emission profile is projected on the great circle between the connected airports, and the calculated emission amounts are distributed spatially on a numerical grid.

The following assumptions are made for the emission modelling and gridding:

- CO₂ & water vapour emissions are linear to fuel burn
- Nitroxide (NO_x) emissions are simulated with the fuel flow method from DLR [12] reference emission indices for engines obtained from the ICAO engine emission database [20]
- Sulphur dioxides emission index regional varies according to fuel sulphur content
- Volatile organic compounds (VOC) and carbon monoxide (CO) emissions derived with Boeing fuel flow correlation method [19], reference emission indices for engine obtained from ICAO engine emission database [20]

- Black Carbon (BC) emissions based on the ICAO smoke number using reference values from the engine emission database [20] and applying a method from DLR [21] to derive BC emission index, extrapolation of BC emissions beyond the LTO cycle to cruise phase with P3-T3 correlation [22]
- Horizontal resolution of the emission grid: $0.25^\circ \times 0.25^\circ$ and vertical resolution: 1000ft

Calculation of Climate Metrics

The GRIDLAB results for all relevant grid cells in terms of longitude, latitude, altitude in pressure unit, fuel burn, nitroxide emissions, and the aggregated distance for the derivation of contrail effects are fed into AirClim⁶ individually in the first step to simulate ATR20 and ATR100 for the different emission species as well as in total. It is assumed that an implementation of this OI starts 2025 and thus, simulations start in this year and run until 2125. Background emissions are expected to develop with ICAO FESG⁷ scenario Fa1 case of contrails, and RCP4.5 development is applied for CO₂ and CH₄ emissions. In a second step, emissions of the aggregated reference scenario and the climate-optimize ISO flight plan is fed into AirClim. In doing so, saturation effects can be considered, and the full potential of this OI can be calculated more precisely than by linearly adding temperature response values. To do this, the background emission scenario is defined as for the single mission case. A ramp-up scenario to implement this OI can be considered, e.g. starting with ISO operations in 2025 and implementing it over a 10-year time span, so that in 2025 all direct flights are replaced with their climate-optimal counterpart.

2.6.3 Results

The study's results are presented in this section. A single mission from Boston to Dublin with an A330 as a first case study is presented to display the work flow and the results on an individual flight's basis. Subsequently, an aggregation of all considered flights is performed. The location of all ISO airports is analysed and changes between fuel- and climate-optimal scenario are identified. Furthermore, the full potential of climate-optimized ISO is analysed for a constant flight level.

Case study: Boston – Dublin (A330)

Boston, United States, and Dublin, Ireland, is connected with 671 flights per year by an A330-243. The direct connection (approximated with a great circle) is 4,780km long and covers approximately 1.02 billion ASK. The flight takes approximately 6 hours and 3 minutes (21,810s). Assuming flying at a constant cruise flight level 33,000 ft, one mission requires 33.74 tonnes of fuel leading to 106.2 tonnes of CO₂ emissions. Non-CO₂ emissions consist of:

⁶ For more details on the tools used, please refer to D2.1 and D2.2.

⁷ FESG: Forecast and Economic Analysis Support Group of ICAO

- H₂O: 41.50 tonnes
- NO_x: 429.77 kg
- SO₂: 31.24 kg
- VOC: 2.26 kg
- CO: 40.98 kg
- Soot: 0.303 kg

This leads to an ATR20 of 2.027e-09 K and an ATR100 of 2.702e-09 K. Further fuel reduction can be achieved by adjusting the flight altitude continuously to its fuel-optimal level.

The direct mission can be separated in two legs of ISO. Possible ISO airports for this O-D pair according to the methodology described in 2.6.2 are displayed in Figure 33 as well as the selected ISO airports for the following evaluations. According to the defined resolution, five airports are further analysed that come along with different emission quantities and climate metrics.

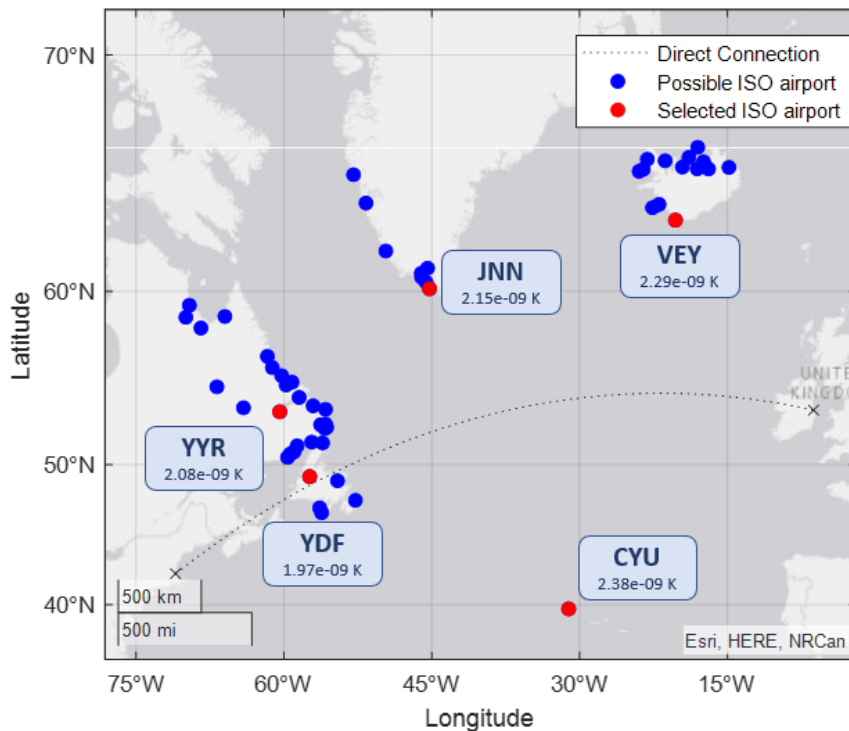


Figure 33. Location of considered ISO airports and the ATR20 of the corresponding mission

Table 15 summarizes the main KPIs for the different ISO missions. The selected airports vary widely regarding their position and the corresponding detour and eccentricity. In this context, fuel consumption and climate impact also vary a lot between the different ISO missions as well as in comparison with the direct mission. A comparison of the different missions shows the following differences:

- None of the selected ISO airports makes sense from a fuel-optimizing point of view. All ISO missions require a higher amount of fuel than the direct connection. This might change if fuel-optimal flight levels (i.e., step-climbs) are assumed.
- Although fuel consumption and thus CO₂-effects of all ISO missions is higher than for the direct connection, the average temperature response is lower for an intermediate stop at YDF. Compared with other ISO airports, this one is also the best in terms of fuel consumption and emission quantities.
- It gets obvious that large detours do not make sense in a way that additional fuel consumption and related climate effects cannot be compensated by other effects. Furthermore, this is not beneficial from an airline or passenger's point of view.

Table 15. Comparison of possible ISO airports at FL330 with climate-optimal ISO scenarios for BOS-DUB with A330

ISO Airport	CYU	YYR	YDF	JNN	VEY
Lat Lon [°]	39.7 -31.1	53.3 -60.4	49.2 -57.4	60.1 -45.2	63.4 -20.3
Detour [%]	20	3.1	0.03	5.8	11
Eccentricity [%]	58	71	73	52	74
Distance [km]	5,743	4,950	4,801	5,089	5,341
Flight Time [s]	27,879	24,627	24,024	25,159	26,266
Trip Fuel [kg]	41,739	36,579	35,621	37,320	39,226
CO ₂ [kg]	131,440	115,190	112,170	117,520	123,520
H ₂ O [kg]	51,339	44,993	43,814	45,904	48,248
NO _x ⁸ [kg]	549.85	489.32	478.20	496.76	521.35
SO ₂ [kg]	39.83	33.87	32.99	34.56	37.05
HC [kg]	4.48	4.46	4.46	4.47	4.46
CO [kg]	71.08	68.67	68.26	69.18	69.67
Soot ⁹ [kg]	0.37	0.32	0.31	0.33	0.35
ATR20 [mK]	2.38e-06	2.08e-06	1.97e-06	2.15e-06	2.29e-06
ATR100 [mK]	3.22e-06	2.74e-06	2.60e-06	2.83e-06	3.02e-06

Overall scenario: Location of ISO airports

While fuel- and climate-optimal ISO airports are identical for the mission presented above, there are missions where fuel-optimal and climate-optimal airports are different from each other. One example is a flight from Frankfurt to Los Angeles with a B747-300 (Figure 34). From a fuel-optimal perspective, an intermediate stop at YLC (detour: 0%, eccentricity: 50%) with the smallest detour and lowest eccentricity factor represents the fuel-optimal solution: 5.4% of fuel can be saved when comparing flights at constant FL330. ATR20 can be reduced by 7.5%. Choosing YMN as a climate-optimal intermediate stop (detour: 2%, eccentricity: 53%) also leads to fuel savings compared to the direct connection (- 3.9% fuel consumption) and an even higher reduction in ATR (- 8.9 % ATR compared to direct flight).

⁸ Calculated with DLR fuel flow method [12]

⁹ Calculated with DLR method [21]

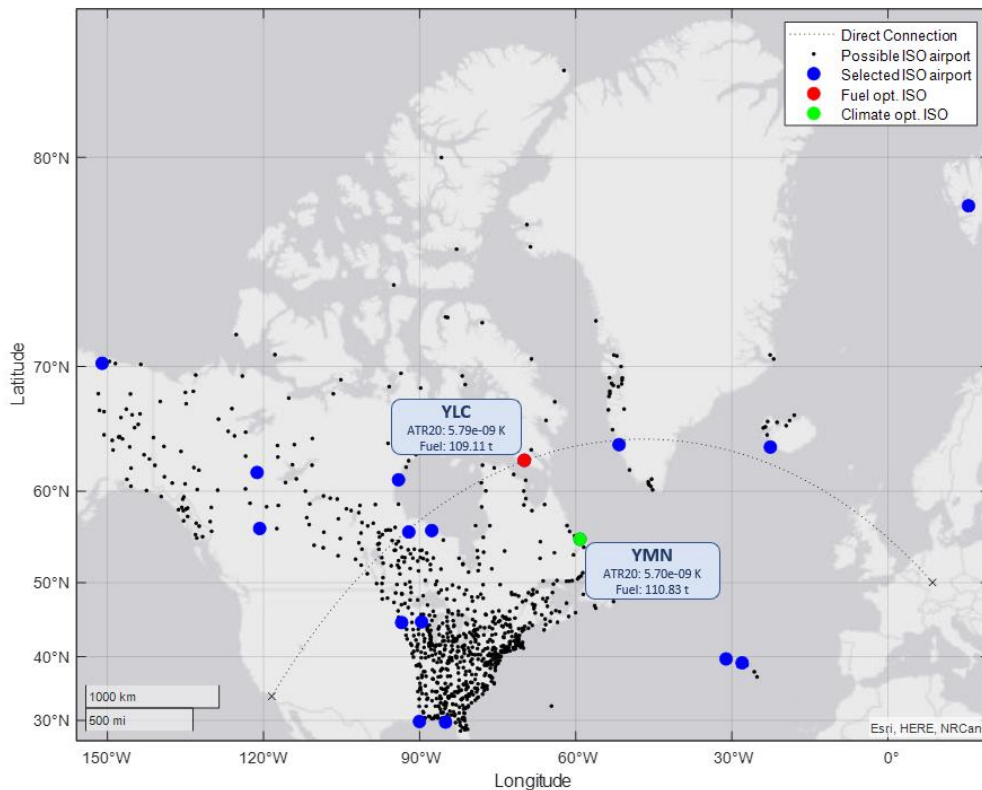


Figure 34. ISO airports for mission FRA-LAX (B747)

Comparing fuel-optimal and climate-optimal ISO missions shows that for 1914 missions, i.e. approx. 37% of all analysed flights, fuel- and climate-optimal ISO airports are identical. While eccentricity factors of climate- and fuel-optimal missions vary widely across the tolerated range (fuel-opt. mean: 60.25%; climate-opt. mean: 63.51%), detour factors of climate-optimal ISO missions are on average higher compared to their fuel-optimal counterparts. Fuel-optimal intermediate stop airports are typically the ones with the shorter detours (mean: 0.08%) as shorter distances are typically associated with less fuel-consumption. Furthermore, this leads to less CO₂ emissions and thus a lower climate impact from these emissions. However, this fuel-optimal solution is not necessarily equivalent to the climate-optimal solution as non-CO₂ emissions, and their climate impact depends not only on fuel consumption and mission length. Consequently, longer detours can still lead to improvements in average temperature response if, for example, climate-sensitive areas are avoided (climate-optimal mean for a detour: 2.23%).

Figure 35 illustrates the changes of ISO airport location from fuel-optimal to climate-optimal scenario relative to the absolute ISO airports considered in the respective grid. A positive value (red colours) represents a higher share of fuel-optimal ISO airports, whereas negative values (blue colours) represent a higher share of climate-optimal ISO airports in that cell. Although no full systematic pattern can be identified from this visualization, it is reasonable to hypothesize that more southern airports would be preferred in a climate-optimal scenario. Further investigations on this will be required in the following research work. Among other things, more detailed gridding and an analysis of the climate impact of the different emission species (CO₂ and non-CO₂) is expected to provide a clearer picture.

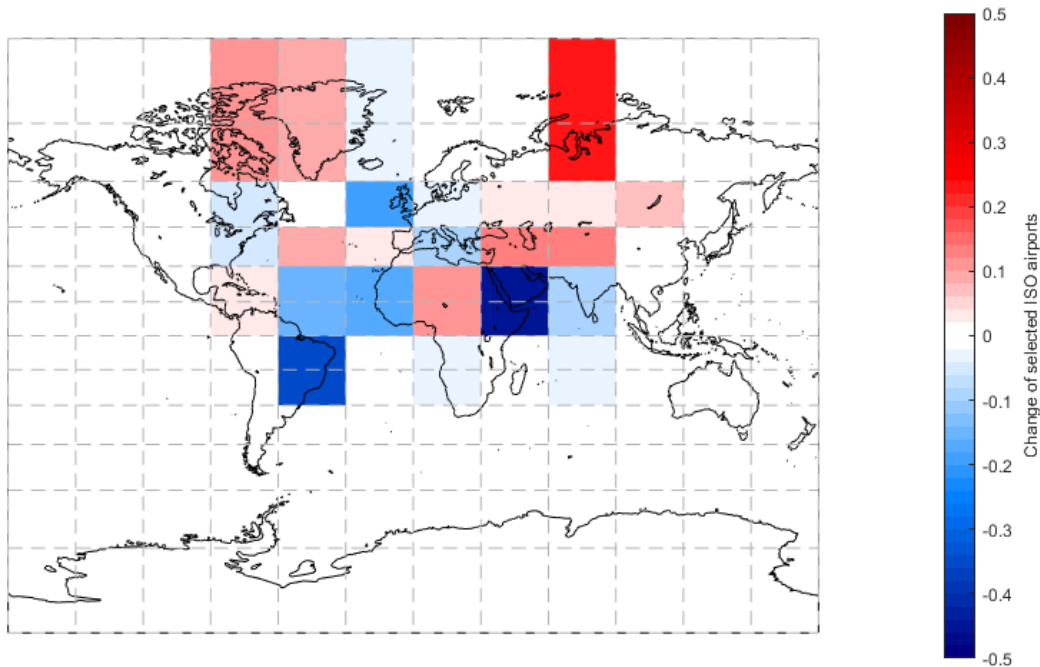


Figure 35. Change in selected ISO airports as share of total ISO airports available per grid cell (red: more fuel-optimal ISO airports, blue: more climate-optimal airports)¹⁰

In addition, it makes sense to analyse the ISO airports regarding their equipment available (e.g., runway conditions or ILS availability) as well as their capacity. A first analysis shows the following most-frequented airports from ISO operations in Table 16. A large number of additional start and landings leads to the hypothesis that not all intermediate stops could be handled at the respective airport infrastructure.

Table 16. Top Ten of climate-optimal ISO airports

		Location (Lat Lon)	Add. starts/landings in 2018
BXR	Bam Airport, Iran	29.1 58.5	72,872
YQX	Gander International Airport, Canada	48.9 -54.6	63,074
TOF	Bogashevo Airport, Russia	56.4 85.2	39,595
YYT	St. John's International Airport, Canada	47.6 -52.8	38,409
CND	Mihail Kogalniceanu International Airport, Romania	44.4 28.5	33,244
YMN	Makkovik Airport, Canada	55.1 -59.2	32,474
SPC	La Palma Airport, Spain	28.6 -17.8	26,922

¹⁰ Numbers displayed in figure are calculated by $C_i = \frac{n_{fuel,i} - n_{clim,i}}{N_i}$, with C_i is change in grid i , N_i is number of all possible ISO airports in that cell (after preselection), $n_{fuel,i}$ is number of fuel-optimal ISO airports in that cell, and $n_{clim,i}$ is the number of climate-optimal airports in that cell.

YJT	Stephenville Airport, Canada	48.5 -58.6	22,923
AJF	Al-Jawf Domestic Airport, Saudi-Arabia	29.8 40.1	13,280
FSP	St Pierre Airport, Saint-Pierre	46.8 -56.2	13,184

Overall scenario: Full potential of climate optimized ISO

The full flight plan of the considered mission contains 811,283 flights and 5,182 different missions (consisting of origin, destination, and aircraft type). Not all direct missions can be replaced by a more fuel- or more climate-optimal ISO mission. For all three aggregated scenarios, a constant flight level of 33,000 feet is assumed. Thus, the optimized scenarios consist of direct and intermediate stop flights. While for the fuel-optimal ISO selection, only 46% of the missions are split into two legs, almost all missions are replaced by ISO in the climate-optimal case. A first summary of the main KPIs is displayed in Table 17. Climate-optimized ISO leads to a potential of approximately 6% reduction in ATR20 and 6.4% in ATR100. In absolute numbers, this means a decrease in ATR100 from 3.80 mK to 3.55 mK¹¹ for the full-aggregated flight plan of 2018.

Table 17. Comparison of average KPIs per mission

	Reference scenario	Fuel-optimal ISO	Climate-optimal ISO
Flight level [100 ft]	330	330	330
Share ISO missions [%]	-	46.08	99.98
Avg. Distance	7,252 km	+ 1.59 %	+ 3.99 %
Avg. Flight Time	08:43 h	+ 4.65 %	+10.63 %
Avg. Trip Fuel	60.505 t	- 0.13 %	+ 3.21 %
CO ₂ emissions	190.53 t	- 0.13 %	+ 3.21 %
H ₂ O emissions	74.42 t	- 0.13 %	+ 3.21 %
NO _x emissions ¹²	940.40 kg	- 2.66 %	+ 1.57 %
SO ₂ emissions	52.27 kg	- 4.66 %	- 2.53 %
HC emissions	5,87 kg	+ 24.56 %	+ 53.23 %
CO emissions	79.80 kg	+ 21.93 %	+ 47.08 %
Soot emissions ¹³	1.77 kg	- 4.26 %	- 2.56 %
ATR20	3.38e-09 K	- 2.36 %	- 6.03 %
ATR100	4.68e-09 K	- 2.71 %	- 6.39 %

Interpretation of the results has to be performed with care since a constant flight level is assumed. Thus, no fuel optimization regarding flight altitude is performed, and aircraft will mainly fly below their weight-optimal altitudes, i.e. step-climbs are avoided. This is also the reason for the small difference in terms of fuel consumption between the reference case and the fuel-optimal scenario:

¹¹ Approximation by linearization of effects. More detailed analysis of full flight plan will be performed in second iteration.

¹² Calculated with DLR fuel flow method [12]

¹³ Calculated with DLR method [21]

As less fuel is required for ISO, the aircraft would typically fly at higher altitudes to save fuel, which is not considered here. Therefore, a comparison with missions at fuel-optimal flight levels will be performed in the following work.

2.6.4 Open issues

The following deliverable D2.4 will further analyse the climate effects of the aggregated climate-optimal ISO flight plan. For this purpose, the full flight plan will undergo a second iteration of modelling the climate metrics for the full flight plan instead of individual flights, among other things to include saturation effects and to also consider a ramp-up of ISO in the future. Furthermore, the effect of replacing long-haul aircraft with aircraft designed for shorter ranges will be subject to the next iteration. Non-climate KPIs such as cost and network effects will also be covered in the following work as well as a possible combination of operational improvements. Especially, a combination with flying lower indicates additional climate mitigation potential, which will be focused on in combination with modelling the fuel-optimal step climb missions.

As modelling the trajectories as well as calculating emissions and climate metrics are only approximations of the real-world case, some improvements in terms of more realistic modelling assumptions could potentially improve the results of this study. However, this would also increase computational efforts. Improvements could be made regarding:

- Instead of ISA, real atmosphere data could be applied containing realistic wind situations. This has not only effects on fuel consumption but also climate effects derived from the different emissions.
- Instead of calculating all missions with a constant load factor, actual values per flight mission could be considered to calculate required fuel and resulting emissions more precisely.
- As discussed in 2.6.3, further details could be investigated by considering more possible ISO airports per mission with more detailed grid. This could also help to analyse the geographical characteristics of ISO airport locations.
- The applied airport database does not contain detailed information about the airport runway setup and layout. A further check if the selected airports fulfil the requirements of e.g. runway length and capacity, that would be necessary for ISO missions is not part of this study.
- As the current analysis limits missions to only one intermediate stop, the impact of more than one intermediate stop cannot be analysed. From the available results, it can be hypothesized, that more than one stop would only make sense for ultra-long-haul missions (e.g., LHR – PER from this study's flight plan).
- Climate impact assessment relies on a climatological mean atmosphere and is dependent on the assumed development scenario of future climate.

These points will not be covered in the next iterations, but need to be considered when referring to the study's results.

2.7 Single engine taxiing / E-taxi and hybrid

The analysis consists of two parts: one focusing on towing at an airport that does not require any modification of the aircraft; the other where aircraft are equipped with an aircraft wheel-based system that does not require any additional airport equipment. Both of these solutions are then compared to using normal and single-engine taxiing.

2.7.1 Executive Summary

For the towing-based system, an analysis is being done looking at the largest airports globally and how many towing vehicles could be effectively used on an average day of traffic. For this study, the focus is on:

- Diesel-based vs. electric towing vehicles: A diesel-based solution will pollute more locally but could be more cost-effective as it does not require charging.
- Different sizes of vehicles, compatible with different aircraft types: Larger aircraft will require larger towing vehicles that will not be for smaller aircraft.
- Required levels of fuel saved per vehicle: A minimum amount of aircraft fuel saved per day per towing vehicle will be required. A towing vehicle will not be invested in at an airport if this is not met.

Results will focus on overall engine fuel saved vs. fuel and energy consumed by the towing vehicle and the auxiliary power unit.

Work is in progress, and the model is defined and being implemented. Results are expected in the next few months.

For the wheel-based system, the analysis is airline-based, looking at how many aircraft equipped with this system each airline could effectively deploy on their route network and flight schedules. The focus of this study is one:

- The weight the system adds to the aircraft. Additional weight adds additional fuel consumption during flight, which reduces the overall reduction in fuel consumption.
- The engine warm-up and cool-down times: Engines must be started for some time before the engines produce take-off thrust and must remain idle for some time before they can be switched off after landing.
- Required levels of fuel-saving per day per equipped aircraft: A minimum overall reduction in fuel consumption will be required before an airline will install a system on one of its aircraft.

Results will focus on overall engine fuel saved vs. fuel consumed extra during the flight and by the auxiliary power unit.

2.7.2 Methodology

For each taxi movement at each airport, the impact on fuel and environment must be calculated for normal taxiing, single-engine taxiing, e-taxiing, and towing.

Towing

For towing, an assignment model runs for each airport and assigns a number of tow trucks to tow aircraft minimizing the overall fuel consumption. The number of tow trucks starts at one and increases until the marginal savings are zero. Thus, no additional fuel is saved by adding tow trucks.

Objective function:

Minimize $Z = \sum_{j \in V} \sum_{i \in F_j} c_{ij} x_{ij} + \sum_{j \in V} c_j y_j$, where:

- V is the set of towing vehicles j . $J=0$ is not assigning a towing vehicle.
- F is the set of flight (operations) i and F_j is the set of flights compatible with towing vehicle j .
- c_{ij} is the fuel cost of vehicle j towing flight i .
- c_j is the fuel costs offset of using vehicle j .
- x_{ij} is the binary decision variable indicating if the flight i is towed by vehicle j .
- y_j is the decision variable whether vehicle j is used or not

The first constraint means every flight must be assigned to either a compatible towing vehicle or no towing vehicle ($j=0$):

$$\sum_{j \in V_i} x_{ij} = 1 \forall i \in F,$$

The second constraint allows a used vehicle ($y_j=1$) to be either assigned to a flight or fuelling (recharging) at each time interval.

$$\sum_{i \in F_{j,t}} x_{ij} + z_{j,t} - y_j \leq 0 \forall j \in V, t \in T, \text{ where:}$$

- T is a set of tie intervals t
- z_{jt} is the decision variable if vehicle j is refuelling at time interval t .

The third constraint indicates that for a time block, the fuel used must be less or equal to the energy that is refuelled.

$$\sum_{t \in T_b} \left(\sum_{i \in F_{j,t}} f_{ijt} x_{ij} + f_{jt} z_{jt} \right) \leq 0 \forall j \in V, b \in B, \text{ where}$$

- B is a set of time intervals b , which may overlap
- T_b is the set of time intervals t during block b .
- F_{ijt} is the fuel used by vehicle j towing flight i during time interval t
- F_{jt} is the fuel that can be recharged for vehicle j during time interval t .

E-taxi

For e-taxi, an analysis is done per airline over their flight schedule, and a number of aircraft is equipped with e-taxi devices and then allocated to flights to minimize fuel consumption, taking into account the extra fuel consumed during the flight sector. The number of aircraft equipped with e-taxi is increased until the marginal savings are less than zero, and thus no additional fuel is saved.

The extra fuel required during flight is calculated using the Breguet range equation:

$$R = \frac{C_L}{C_D} \frac{1}{C_T} \ln \left(1 + \frac{W_{fuel}}{W_{empty} + W_{payload}} \right)$$

$$W_{fuel} = (W_{empty} + W_{payload}) \left(e^{\left(\frac{RC_T}{\left(\frac{C_L}{C_D} \right)} \right)} - 1 \right), \text{ where:}$$

$$W_{\Delta fuel} = W_{etaxi} \left(e^{\left(\frac{RC_T}{\left(\frac{C_L}{C_D} \right)} \right)} - 1 \right)$$

- R is the range in km
- $\frac{C_L}{C_D}$ is the lift to drag ratio during cruise
- C_T is the thrust specific fuel consumption [N/Ns]
- W_{etaxi} is the weight added by the e-taxi system [N]
- $W_{\Delta fuel}$ is the extra fuel due to the weight of the e-taxi system.

Objective function:

$$Z = \sum_{i \in V} \sum_{j \in F_i} c_{ij} x_{ij}, \text{ where:}$$

- V is the set of e-taxi equipped aircraft i
- F is the set of flights j, and F_i is thus the set of flights that can be flown by aircraft i
- x_{ij} is the decision variable indicating if flight j is flown by vehicle i
- c_{ij} is the total weighed cost of operating flight j by vehicle i. The initial cost is total fuel consumption, including taxiing and flying.

Constraint one indicates that each flight can only be operated once by an e-taxi equipped aircraft

$$\sum_{i \in V_j} x_{ij} \leq 1 \forall j \in F$$

Constraint two checks for every aircraft flight combination at each airport whether the aircraft has arrived before it departs.

$$\sum_{j' \in F_{kj-}} x_{ij'} - \sum_{j' \in F_{kj+}} x_{ij'} + x_{ij} - y_{ik} \leq 0 \forall i \in V, k \in A, j \in F_{ik},$$

where:

- A is a set of airports k
- F_{ik} is a set of flights compatible with aircraft i departing airport k
- F_{kj-} is a set of all flights that have taken off before j departs at airport k
- F_{kj+} is a set of all flights that have landed and turned around before j departs at airport k
- Y_{jk} is a decision variable whether aircraft i starts at airport k

The final constraint makes sure that an aircraft cannot operate two flights at the same time.

$$\sum_{j \in F_j} x_{ij'} - x_{ij} \leq 1 \forall i \in V, j \in F,$$

where F_j is the list of operating flights overlapping in time with flight j .

Scenario

Initially, both cases will be run with a single average day of the year 2018, though more days can be added later for comparison. Optimizing the number of towing vehicles or e-taxi equipped aircraft for the entire year is currently out of scope.

Assumptions

- The taxi time remains the same for towing and e-taxi.
- Taxi time is independent of aircraft type and airline
- The impact of the weight of the e-taxi system on the maximum take of weight is neglected.
- The Breguet range equation only considers extra fuel consumption during cruise

2.7.3 Results

Unfortunately, no updated results are available, as work on the model is not finished yet.

Towing

For towing, the initial results will focus on marginal fuel savings per towing vehicle per airport, after which, a minimum marginal fuel saving per towing vehicle will be set to do a global analysis. Emissions will be calculated by multiplying the fuel consumptions with the emissions index of the ICAO emissions databank.

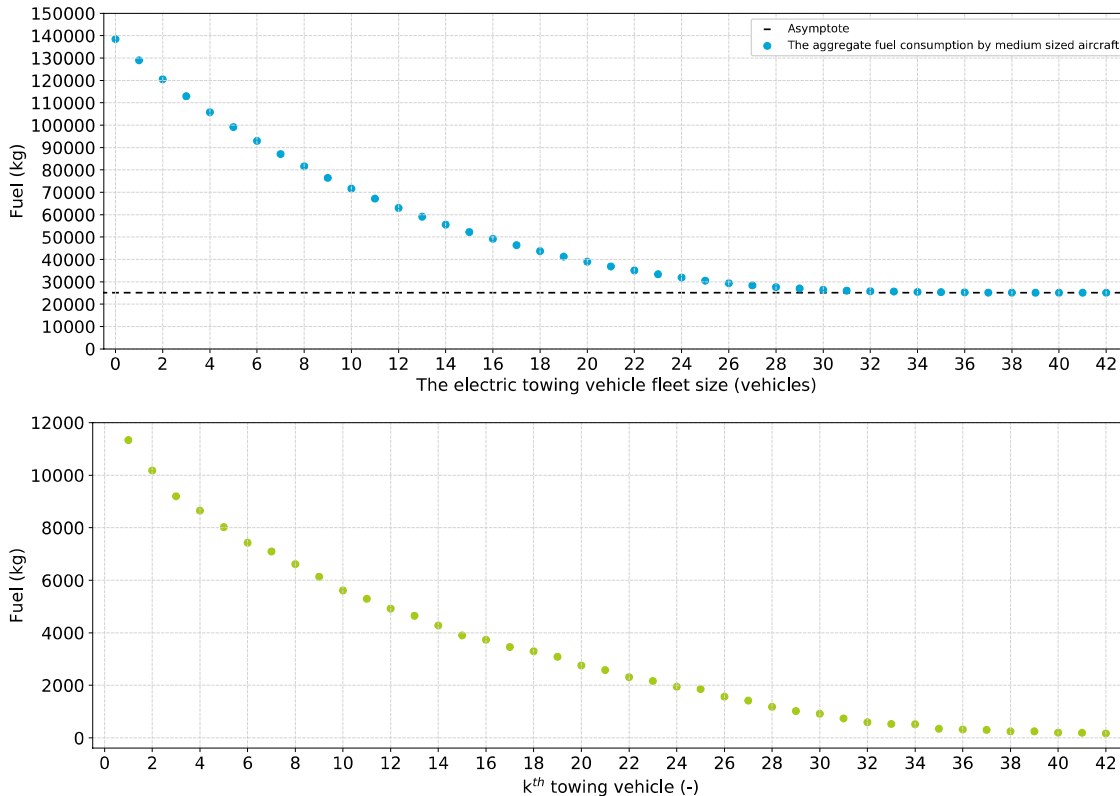


Figure 36. Total and marginal fuel consumption per towing vehicle

e-Taxi

Table 18 shows the result of an earlier study, showing the achievable fuel savings per airline.

Table 18. Initial results of maximum saving per airline

Airline	Per flight [kg]	Annual [mln kg]
KLM	107.2	17.32
Transavia	60.8	1.48
British Airways	141.9	27.66
Air France	95.8	39.29
Lufthansa	100.0	56.72
Ryanair	75.7	27.03
EasyJet	100.0	28.03
American	232.8	54.73
Delta	245.8	34.18
United	251.9	49.64

2.7.4 Open issues

Extracting a reasonable peak day schedule from the 2018 data is a bit more difficult than expected, as the data is built up in a way that creates a lot of duplicate flights. A more efficient data extraction technique will be tested in D2.4 to speed up the analysis. In addition, non-climate KPIs such as SAF and HP will be assessed.

2.8 Electrification of ground vehicles and operations

2.8.1 Executive Summary

In the context of reducing the overall emissions of the aviation industry, we want to evaluate the impact of the Ground Support Equipment and Operations. To achieve this, we model the fuel consumption of the present fossil-fuel-powered fleet and we compute the corresponding CO₂, NO_x, CO and SO₂ emissions. Subsequently, we compare this result with the emissions of a corresponding electric-vehicle-only fleet. As a first step, we developed a model which uses ground fleet data from the SEA Milan Airports MXP and LIN and we implemented a tool to visualise the results. We then propose a method to generalise our results to any airport in the EU. Section 2.8.2 briefly summarizes the main elements of the model, Section 2.8.3 shows the results. Section 2.8.4 discusses the limitations of the present analysis and further steps.

2.8.2 Methodology

The model to calculate the emission from Ground Support Equipment and Operations was described in detail in Sect. 2.8.2 of D2.2 [8]. Here, we summarise the main steps of the implementation process. The input data of the model consists of the number of ground vehicles at the airports of LIN and MXP, the vehicle category, fuel used, and average yearly distance covered. This file is pre-processed using Python.

1. The entire vehicle set is then divided into small, medium, and large, based on their model types.
2. Two reference tables are created: One table contains the average fuel consumption per vehicle size and fuel type, and another contains the average GHG emissions per vehicle size and fuel type.
3. For each size category, the number of vehicles and the number of yearly kilometres are counted. The vehicles from each of the three size categories are then cross referenced with the consumption data to obtain an annual fuel consumption value as well as a yearly GHG emissions value.
4. The synthetic fleet is then created using equivalent electric vehicles as replacements for current vehicle models found at SEA airports. In most cases the model has a direct alternative electric model. If this is not the case, a similarly sized and purposed model is used. Data about power consumption was collected for the new electric vehicles [37][38]. Their range, capacity, and use, provide a value for the yearly electrical energy required to power the electric fleet.
5. The model uses literature results [39] to calculate the GHG emission corresponding to the generation of an amount of electrical energy equal to the energy demand of the electric fleet computed at the previous step. The emissions are also broken down into the gases that compose them such as CO₂, SO₂, NO_x, and CO.
6. The tool then calculates a percentage denoting how much of last year's total global GHGs it is responsible for, using its current fleet. The same calculation is performed with the reduced emissions from the synthetic fleet using various sources of energy generation.
7. These percentages are used to calculate a series of possible reductions in global GHG emissions, due to the electrification of the ground operations fleet.
8. Using recent values for the global change in atmospheric CO₂ concentrations, a value for a resulting change in CO₂ ppm per ton of emissions is calculated.
9. Using the previously mentioned change in CO₂ concentration, the subsequent radiative forcing is calculated using the radiative forcing formula from IPCC, 2001 [40].

10. The reduction to the yearly increase of RF alongside the concentration changes are used to calculate the change in average global temperature. The formula used for this change in global temperature is available in the IPCC 2001 Climate Change Report [40].
11. The model also estimates the costs and benefits associated with replacing the current, fossil-fuel-based vehicles with a fully-electric fleet. The variables that are taken into account are purchase and maintenance costs of the current and new vehicles, and the costs of fuel and electrical energy. The model will enable the user to decide the time span for the transition of the fleet. Therefore, literature projections of the evolution of vehicles and fuels prices over the next decade are used, and possible incentives and disincentives that National and EU regulators put, or will likely put, in place to foster this transition. The cost-benefit analysis also indirectly accounts for the change in reputation of the airport among passengers and citizens as a result of the commitment to reduce the emissions. This step of the analysis will be refined in the upcoming months and documented in deliverable D2.4 of the project.
12. All the information computed by the model is stored and sent to an ad-hoc visual component for displaying to the user. The outputs are estimated values which help the user identify the emissions for their current fleet, energy requirements and emissions savings for their future fleet, and financial information for guiding the transition.

2.8.3 Results

SEA Model Fleet

The following set of results are from SEA's combined Linate and Malpensa ground operations fleets. Table 19 shows the vehicle size distribution for the combined fleets at SEA.

Table 19. Ground operations vehicle size distribution across SEA airports

Vehicle Size	Number of vehicles		
	MXP	LIN	Milan airports combined
Small	130	54	184
Medium	112	78	190
Large	306	150	456
Total	548	292	830

- Kilometres driven and fuel consumption per year

The combined number of kilometres for both SEA airport fleets is 6.55 Million kilometres across all vehicle sizes. The category with the most kilometres is the 'large' category of vehicles, mainly due to the apron buses. Values can be found in Table 20.

Table 20. Total kilometres driven each year by each size category of ground operations vehicle for SEA Malpensa and Linate.

Vehicle Size	Kilometres driven		
	MXP	LIN	Milan airports combined
Small	451.5x10 ⁵	240.6x10 ⁵	6.8x10 ⁵
Medium	799.2x10 ⁵	425.9x10 ⁵	1.2x10 ⁶

Large	3.1x10 ⁶	1.64x10 ⁶	4.6x10 ⁶
Total	4.3x10 ⁶	2.2x10 ⁶	6.5x10 ⁶

- Fuel consumption per year

Fuel consumed includes petrol and diesel. SEA ground operations consume a yearly total of 906,177.5 litres of fuel, spread 74% and 26% across Malpensa and Linate respectively.

- Theoretical Fleet

After replacing all vehicle sizes with their respective electric equivalents, a synthetic electric-vehicle-only fleet is devised. This new fleet takes into account the energy capacities and autonomies of the electric vehicles and provides a required energy value based on the kilometres driven by each vehicle size. For SEA Malpensa and Linate combined, the energy required to operate the fleet is estimated at 2.73 Million kWh. Here are the results for the energy required for each vehicle type:

Table 21. Kilowatt hours required to power each vehicle size category across both SEA airports.

Vehicle Size Category	Kilowatt hours required per year
Small	97.7K
Medium	302.6K
Large	2.33Mil

Environmental results

The main interest of this OI is to see how much less an electric airport ground operations fleet would impact the environment as opposed to the current fleet in use. For this, two metrics are used: Greenhouse gas emissions and impact on global temperature.

- Greenhouse gas emissions

Based on the current vehicle models and their emissions values the current fleet at the two SEA airports emits a yearly total of 3973.6 metric tons of greenhouse gases per year. The main contributor of the greenhouse gas composition is CO₂ at over 93% of the emissions. The remaining fraction of the emissions includes NO_x, SO₂, and CO.

To calculate the emissions of the theoretical electric fleet, the emissions of energy generation are used. The process to generate the required 2.73 million kWh will emit different amounts of greenhouse gases based on the method of energy generation. The following table shows the greenhouse gas emissions for different sources of electrical generation:

Table 22. GHG emitted per kWh for different sources of electric energy generation [39][41]

Electric Energy Generation Source	GHG emitted per kWh generated (kg)
Coal	1.199
Petroleum	0.869
Natural Gas	0.549
Average European Mix	0.231

The three sources generate energy by burning fuels and consequently they release the most emissions per kWh of energy generated. In Europe, energy is produced by a variety of sources, which include: fossil fuels, nuclear power, hydro-electric, wind and biofuels. Renewable energy sources account for approximately 35% of the total energy generated. The most popular renewable energy sources are wind turbines, hydropower plants, biofuels and solar power. The combination of these electrical energy (EE) sources drastically lowers the emissions per kWh, as shown in Figure 37:

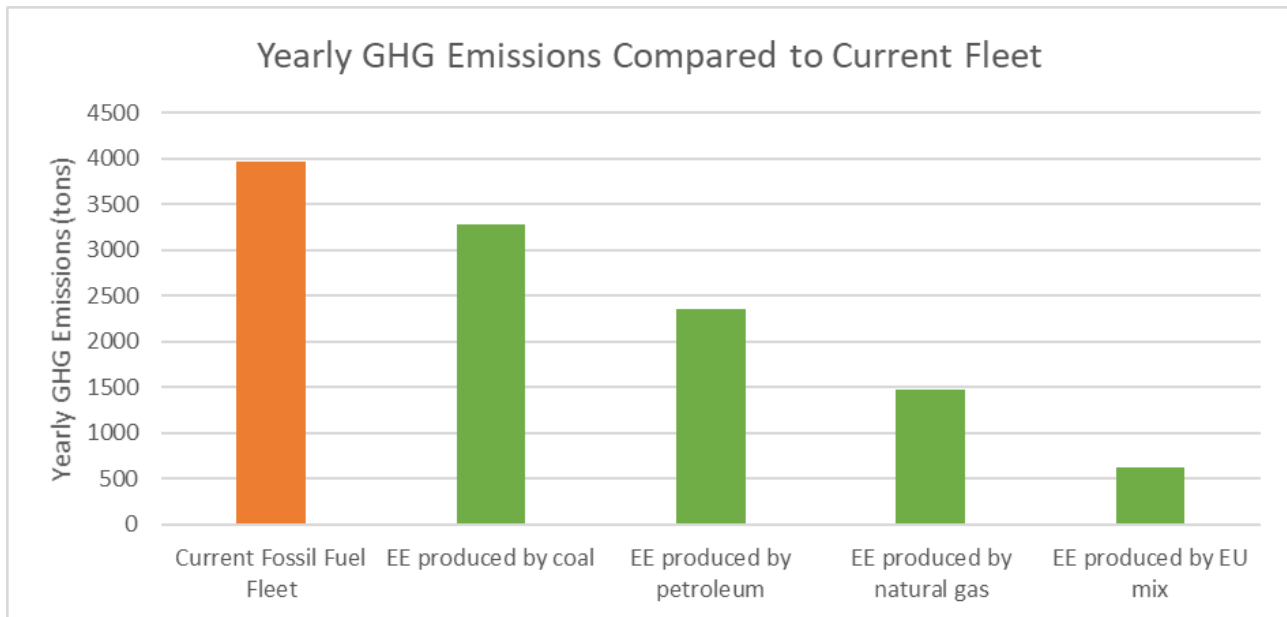


Figure 37. The current yearly greenhouse gases (GHG) emissions (orange bar) compared to GHG emissions from generating electric energy (EE) from different production sources (green bars).

Figure 37 shows the GHG emissions from the current combined fleets of Malpensa and Linate (3974 T), and the emissions from generating the required electricity from a coal source (3273 T), a petroleum source (2358 T), a natural gas source (1470 T) and the average European mix of sources (630 T).

- CO₂ concentration calculation

In order to understand the global climate impact of the OI, we need to calculate the variation in global CO₂ concentration caused by the airport emissions. Since the impact scope is of a global scale, the global CO₂ emissions are used with the subsequent global change in CO₂ concentration to obtain a change in concentration per ton of CO₂ emitted.

We need to calculate the variation in global CO₂ concentration caused by the airport emissions.

- CO₂ emissions 2018 = 36.65 Billion tons [42]
- Atmospheric CO₂ concentration increase after 2018 = 2.31 ppm [43]

We can see this yields an increase in CO₂ ppm of 6.3×10^{-11} per ton of CO₂ emitted. This simplification of calculating atmospheric concentration change does not reflect real CO₂ emission models or more sophisticated climate models. It does, however, provide a fast solution towards an estimation which deals with a comparatively small change in the concentration which, as shown later on, proves to be relatively inconsequential.

For the following calculations we will record two scenarios: Scenario 1 where the airport maintains the fleet as it is and does not integrate the OI, and scenario 2 where the OI is completely integrated and all ground operation vehicles are replaced with electric equivalents.

Using the change in concentration calculation above, the change in CO₂ can be estimated for each of the two scenarios. In scenario 1, nothing changes, so we can assume that the global emissions will pursue their course and change in CO₂ ppm will remain unaltered. In scenario 2, 3344 tons of CO₂ are no longer being released into the atmosphere, translating into a proportional reduction in change of global CO₂ ppm. The calculation shows that the OI as applied to the SEA airports would result in a 2.1x10⁻⁷ ppm reduction in the following year's CO₂ concentration increase.

- Radiative forcing

Another climate KPI being measured is radiative forcing (RF), which is the atmospheric change in energy flux caused by climate change, measured in Wm⁻². As the CO₂ concentration increases, so does the RF. It is calculated using the following formula [40]:

$$\Delta F = 5.35 \ln(C / C_0)$$

where C₀ and C are the atmospheric CO₂ concentration at time t₀ and t, respectively [40].

We previously calculated the estimated CO₂ emissions of the current fleet at SEA airports combined to be 3974 tons (reference year 2018). These emissions cause an increase in the global average CO₂ concentration of 2.5x10⁻⁷ ppm. Consequently, the global RF increases by an amount equal to 3.3x10⁻⁹ Wm⁻². By contrast, the energy generation (e.g. with a typical EU mix) to power a fully electric fleet of vehicles for SEA airports would have produced 630 tons of CO₂, which corresponds to a reduced global increase in CO₂ concentration of 4.8x10⁻⁸ ppm and to a lowered global increase in RF equal to 5.18x10⁻¹⁰ Wm⁻².

- Temperature change

The last climate KPI being measured is the change in global temperature response that occurs if the OI is implemented, measured in Kelvin (K). It is calculated using the following formula [44]:

$$\Delta T = 1.66 \ln(C / C_0)$$

where C₀ and C are the atmospheric CO₂ concentration at time t₀ and t, respectively [44].

As mentioned previously, this formula is derived from the 2001 IPCC Climate Change Report and will be replaced with that used in the TransClim model to consolidate results with other OIs. Results are subject to change with the implementation of the new formula. Preliminary results show that SEA Malpensa and Linate combined current fleets contribute a yearly RF of 1.0x10⁻⁹ Wm⁻². If the OI were implemented, the yearly global temperature contribution would drop to 1.6x10⁻¹⁰ Kelvin.

Table 23. Yearly climate KPI contributions estimation for the current and electric replacement fleet

Fleet	Yearly CO2 emissions (tons)	Yearly CO2 concentration contribution (ppm)	Yearly RF contribution (Wm ⁻²)	Yearly temperature response contribution (K)
Current	3974	2.5x10 ⁻⁷	3.3x10 ⁻⁹	1.0x10 ⁻⁹
Electric Replacement	630	4.8x10 ⁻⁸	5.18x10 ⁻¹⁰	1.6x10 ⁻¹⁰

- Most contributing vehicle types

Results show that the highest contributing vehicle type, both in economic and environmental factors, are the large vehicles. This is due not only to their dominance in number, but also their fuel/energy requirements and frequency of use. Their replacement with electric equivalents will result in the most GHG saving as well as the largest increase in purchase cost, but also long-term fuel/energy cost savings.

EGO Tool

The presented analysis can be visualised in an ad-hoc interface. A snapshot of such visualisation tool is shown in Figure 38. The tool takes an airport name or a ground fleet size from the user at the left section. It then displays all the information predicted about the current fleet in the central section and the climate KPI improvements from implementing the OI in the right-side section. An extra section highlighted in green at the bottom right shows the financial data for the OI implementation, notable purchase and maintenance costs and savings. The tool offers the ability to select what fraction of each size category to replace with electric through 3 sliders. The values are updated accordingly. The tool is still undergoing improvements and fixes to better reflect the vast advantages of the OI.

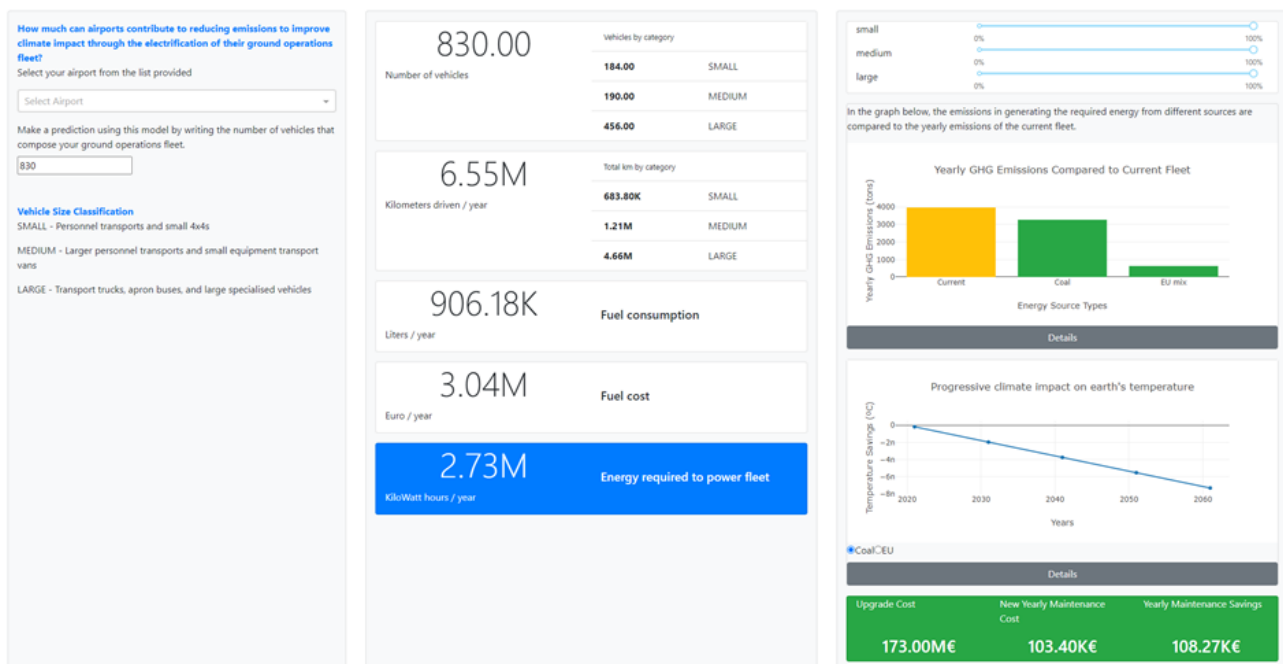


Figure 38. The EGO visualisation tool created for the OI.

Modelling other airports

All the results shown for the SEA airports can be extrapolated to other airports in Europe with an added degree of uncertainty. This is achieved using the number of annual flight operations for a distinct airport and comparing this to that of SEA Milano and SEA Malpensa separately. For this OI and until we have collected data from other airports, it is assumed that the relation between flight operations and ground vehicle numbers and size distributions is linear.

2.8.4 Open issues

The fleet considered in the model approximates a real fleet. We consider only three size categories of vehicles and we consider average consumptions and emissions for these three categories. The model assumes that every existing vehicle has an electric equivalent. This is not always true, considering that some of the large specialised airport vehicles which require large amounts of power have not yet seen electric equivalents, though some are under development. Hence, in our model we assume that one day an alternative will exist.

When we extrapolate to all airports, we are assuming that all airports have the same vehicle distribution as SEA, and that the only relevant parameter is the total number of vehicles. We assume that this number scales linearly with the number of airport operations. In our future work we will try to obtain more data about other airports to validate these assumptions.

These assumptions mean that while the results for SEA airports will be more accurate, all results for other airports will somewhat diverge from their actual status.

The next step of the model is to perform the calculations for the climate KPIs with all the larger airports in Europe, to arrive at values representative of the OI's implementation across Europe. In addition, in the next deliverable D2.4, the assessment of the relevant non-climate KPIs for this OI will be performed, which in particular include a cost-benefit analysis.

2.9 Upgrade of the airport infrastructure according to energy efficient criteria

2.9.1 Executive Summary

Airport buildings consume a significant amount of energy to maintain comfortable occupancy conditions, which require space heating and domestic hot water preparation, ventilation and air conditioning/cooling, power supply for lighting, and other airport systems (e.g., elevator). The improvements in the infrastructure according to energy-efficient criteria are expected to significantly reduce the energy consumption of airports, and hence their GHG emissions. Applying energy-efficiency measures to the airport infrastructure is immediately feasible and is effective over the long term. However, the initial investment is rather demanding, and the renovation works might cause problems for the operations, especially when they are carried out at terminals.

The assessment of this OI focuses on analysing the change in CO₂ emissions thanks to the application of a selection of energy-efficiency measures on the office buildings of European airports. The energy consumption of a conceptual office building is simulated with the open-source software of the US Department of Energy, EnergyPlus¹⁴. The considered energy-efficiency measures are implemented to calculate the reduction of energy consumption with respect to the baseline. The results are, then, generalized to assess the effect throughout Europe by considering the hypothesis that the energy demand is proportional to the aircraft movements to and from an airport. The calculation is repeated for future climate conditions to estimate the effectiveness of this OI in reducing climate change. Throughout Europe, ATR20 is 9.33e-8 K and ATR100 is 9.10e-8 K.

2.9.2 Methodology

General assumptions

¹⁴ <https://energyplus.net/>

The aim of this study is to assess the reduction in energy consumption thanks to the upgrade of the airport infrastructure all over Europe. The problem is rather complex, and needs to be tackled on different levels. On the one hand, it is necessary to have a detailed representation of the energy cycle within a selected building. On the other hand, it is fundamental to generalize this detailed analysis to assess the climate impact of the OI for all the European airports.

To ensure the applicability and scalability of the energy model results, we focus on airport office buildings. The reason for this choice is twofold. Firstly, the office buildings can be upgraded with a minimal impact on the operations compared to, for instance, airport terminals. Secondly, it is possible to define a conceptual office building that is representative of the general characteristics in terms of geometry, components and use. By contrast, other buildings in the airport area, such as the terminals, are difficult to conceptualize, and hence to draw general conclusions from.

The list of analysed energy-efficiency upgrade measures is the following.

a) *Insulation of exterior walls.*

The objective of this energy efficiency measure is to decrease the demand for thermal energy for heating the building, through the addition of an external layer of expanded polystyrene (EPS) foam insulation board on the exterior walls. The advantage of EPS is that it offers the lowest thermal conductivity per euro over other types of rigid insulation. In our study, we apply a layer with a thickness of 10 cm.

b) *Optimization of windows.*

Given the great variability of weather conditions in Europe, we consider different energy-efficiency measures related to the windows. In the case of cold climates, this measure involves the introduction of triple-glazed windows, strongly effective for keeping inside the energy generated by the heating system in winter. For the case of warm climates, we model the implementation of reflective window films, useful to reflect the solar radiation hence reducing the energy demand for the cooling system in summer.

c) *Introduction of LED lights.*

With this energy efficiency measure, we want to assess how effective it is to use LED light throughout the airport buildings. Among the many advantages provided by LED lights with respect to standard incandescent or halogen bulbs, the most relevant one for our study is their high efficiency. Indeed, an LED light typically uses 90% less energy than an equivalent incandescent or halogen bulb.

Phase 1: energy simulation of a conceptual office building

In the first step, we simulate the energy consumption of a conceptual office building. To this end, EnergyPlus simulation software is used. EnergyPlus is the open-source software developed by the US Department of Energy, and is the most widely used package for building energy simulation (BES). Figure 39 displays the conceptual building utilized for this study. The simulated building is a medium-sized office building, with three floors, covering a total area of about 5000 m², and with a window-to-wall ratio of 33%.

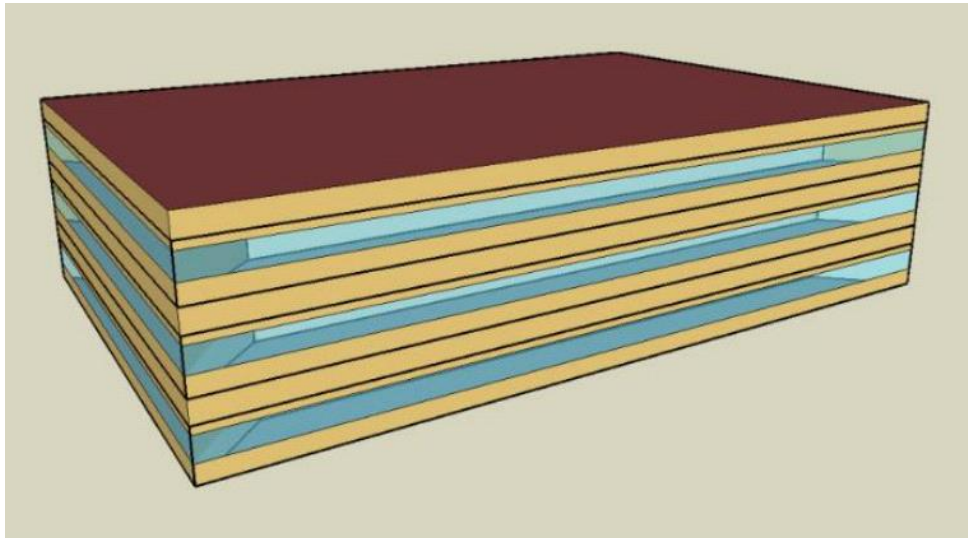


Figure 39. Characteristics of the conceptual building utilized for the energy simulations with the model EnergyPlus.

The input of the BES model are the weather data of the typical climate conditions of the region where the building is located. The most commonly used method to produce these weather input data is called *Typical Meteorological Year (TMY)*. The data is assembled by compiling the individual months, which best correspond to the long-term monthly means of different climate variables. A common praxis in energy studies is to classify the climate in categories generally called *climate zones*. As shown in Figure 40 [46], in Europe, the most widely present climate zones are four (warm humid, mixed humid, cool humid, and cold humid), covering approximately all the areas of the continent. The TMY method is then applied to each climate zone separately, leading to representative data for the different weather conditions

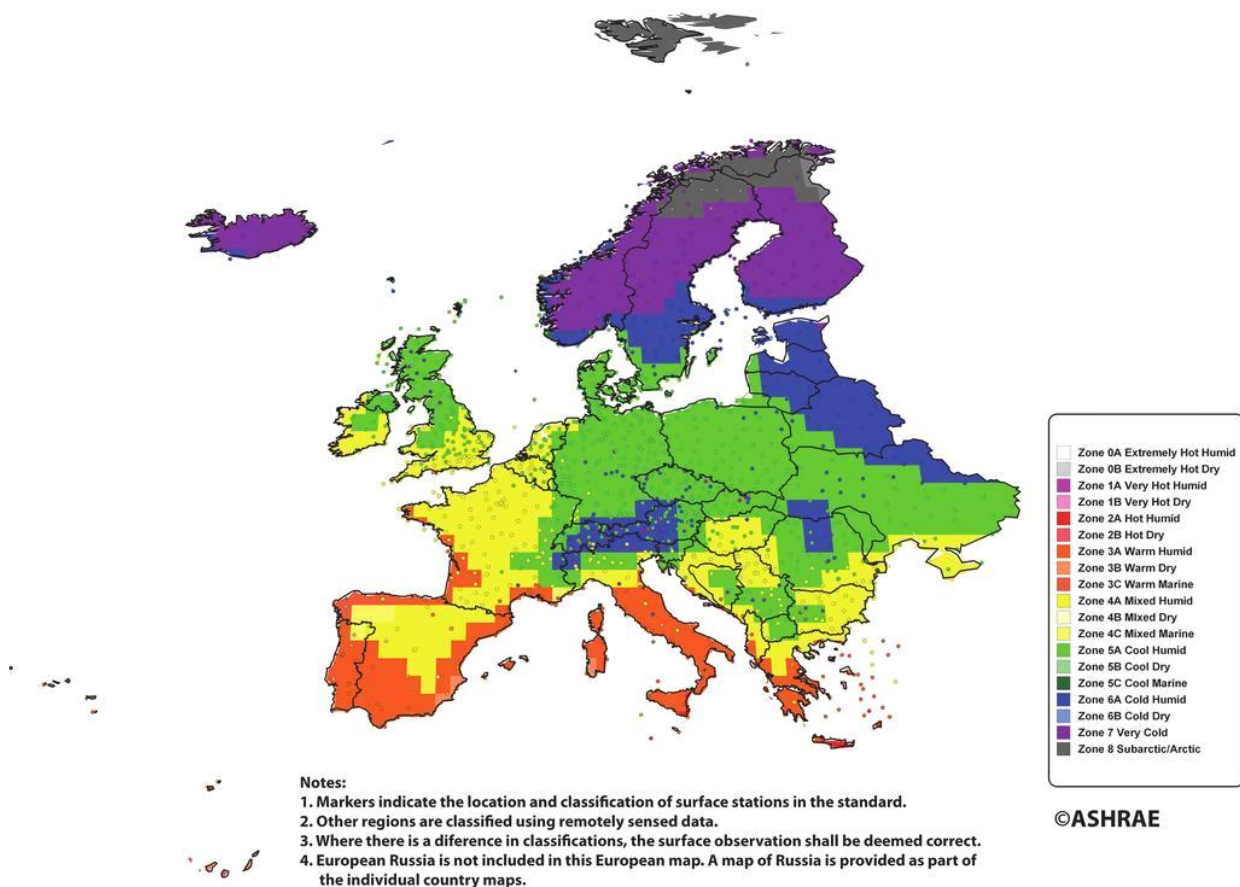


Figure 40. Climate zones distribution in Europe according to ASHREA Standards 90.1/169.

The analysis is repeated for future climate conditions. The most commonly used method to produce future climate input data for BES is called *morphing*. Such a method preserves real weather sequences, and is specific to an observed location. The algorithms use three simple operations to modify present-day weather data: (1) a shift is applied when an absolute change to a variable is required, (2) a stretch or scaling factor when the change is projected in a percentage, and (3) a combination of both shifting and scaling may be used to adjust present-day data to reflect future projections.

The future climate conditions are representative of 2050 for four emission scenarios as defined in the Special Report on Emissions Scenarios (SRES) report [47]. Assumptions about future technological development as well as future economic development are made for each scenario. The scenarios range from very rapid economic growth and technological change to high levels of environmental protection, from low-to-high global populations, and high-to-low GHG emissions. More importantly, all the scenarios describe dynamic changes and transitions in generally different directions, while do not include specific climate-change policies but make assumptions on numerous other socio-economic developments and non-climate environmental policies. As time progresses, the scenarios diverge from each other in many of their characteristic features. In this way, they span the relevant range of GHG emissions and different combinations of their main sources.

Phase 2: generalization of the simulation results

- The results of the BES model are generalized to estimate the effect of the OI if applied to all the airports in Europe. The generalization method comprises four steps. Each Country in

Europe is associated with the percentages of the area covered by the 4 climate zones (see Figure 40).

- The energy consumption of one building is scaled by using a proxy calculated for each Country as a logarithmic function of the number of aircraft movements. Such a proxy is estimated as the result of a logarithmic fit of the number of employees as a function of the number of aircraft movements for ten airports in Europe. The idea at the basis of the calculation is that the energy consumption is proportional to the number of employees. The number of employees has been found on the airports' websites, while the number of aircraft movements is from the Airport OE Dataset. We consider 2019 as the reference year for the "business as usual" to avoid including the effect of COVID-19 pandemic in the calculations
- The CO₂ emission resulting from the energy consumption is estimated by using the following conversion factors.

Table 24. Conversion factors used for the OI assessment.

Initial variable	Final variable	Conversion factor	Source
Electric energy	Primary energy	3.167	[52]
Thermal energy	Primary energy	1.084	[52]
Primary energy in GJ	Primary energy in TOE	0.024 TOE/GJ	[48]
Primary energy in TOE	Tons of CO ₂	2.683 tons CO ₂ /TOE	[48]
Tons of CO ₂	PPM of CO ₂	0.470e-9 PPM / tons CO ₂	[49]

The amount of CO₂ emitted depends on the energy source. Therefore, the results of the BES model are first converted to *primary energy*, generally estimated in Tons of Oil Equivalent (TOE). In this way, it is possible to estimate the total emissions due to different energy sources through the conversion factor.

We calculate the reduction in temperature increase thanks to the energy saving. To this end, we apply the following formula from the IPCC report 2001 [50]:

$$\Delta T = 1.66 \ln \left(\frac{C_o - \Delta C}{C_o} \right)$$

where ΔT is the temperature change corresponding to the effect of this OI alone, C_o corresponds to 407.4 ppm and is the global value of CO₂ in ppm in 2019, and ΔC is the value calculated from the previous analyses. The idea behind this formulation is to isolate the contribution of this OI to climate change from all the other human activities.

- The previous steps are repeated for future climate scenarios.

KPI calculation

The first climate assessment for this OI includes the calculation of the following KPIs:

- ATR20;
- ATR100;
- Annual electricity consumption per unit of volume;
- Annual thermal energy consumption per unit of volume;
- Tons of CO₂ emitted annually;
- CO₂ emitted annually in PPM.

It is worth clarifying that the BES model provides energy consumptions and hence CO₂ savings at present and in 2050. We use a linear fit to estimate the value of ΔT used for ATR20 and ATR100.

2.9.3 Results

Results for one office building

The first part of our analysis focuses on the results of the BES model. Our goal is to understand how effective the analysed energy-efficiency measures are in reducing the CO₂ emissions. Figure 41 compares the energy saved thanks to each energy-efficiency measure and the combination of all of them in the different climate zones. The results are presented as percentages of energy saved with respect to the simulation without energy-efficiency improvements. It is noticeable how the local climate conditions influence the effectiveness of the energy-efficiency measures. The considered measures are more effective in cold climates with respect to warm climates. This is because they enhance the heating trapping inside the building, hence reducing the energy consumption during winter. On the other hand, the use of LED lights is the most effective energy-efficiency measure in warm climates. The previously presented results are obtained considering the hypothesis that only electrical energy is used. However, airports commonly use a combination of energy sources. Therefore, we need to estimate the variability of our results due to different *energy scenarios*, where with energy scenarios we indicate different combinations of electric and thermal energy to satisfy the total energy demand. The energy sources, in the energy scenarios, are exploited as followed:

- Energy scenario 1:
75% electric energy and 25% thermal energy
- Energy scenario 2:
60% electric energy and 40% thermal energy
- Energy scenario 3:
50% electric energy and 50% thermal energy

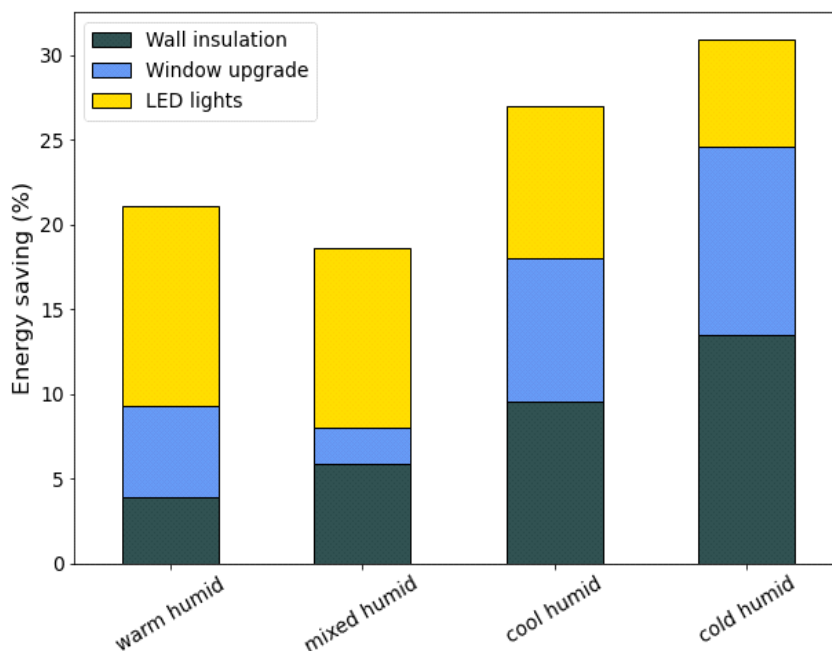


Figure 41. Percentages of energy saved by each energy-efficiency measure with respect to the simulation without energy-efficiency improvements.

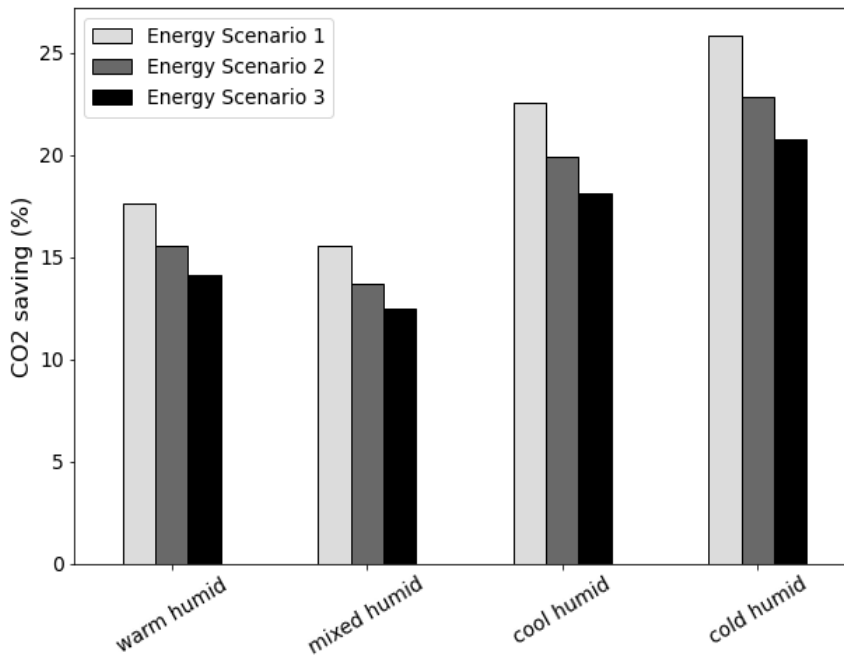


Figure 42. Percentage of CO₂ saving with respect to the simulation without improvements for the different energy scenarios and all the climate zones.

Figure 42 displays the percentage of CO₂ saving with respect to the simulation without improvements for the different energy scenarios. The more electric energy is used, the more effective the energy-efficiency measures are. However, the variability of our results due to the combination of energy sources is about 3%, while the variability of the results between climate zones is about 15% (see Figure 41). Since the variability linked to the climate zones is dominant, in the remainder of our analysis, we maintain the hypothesis stated previously, i.e. the energy demand is satisfied with electric energy alone.

Results at Country level

The method to generalise the results of the BES model is applied to estimate the impact of the OI at Country level. Figure 43 shows the total energy saving in TOE and the corresponding CO₂ saving for each Country separately. The results for one Country depend on the percentage of area covered by each climate zone and the total number of flight movements from and to its airports. As already discussed, the considered OI would be most effective in areas with cold or cool climates. For this reason, Norway is the Country with the highest energy saving. However, the OI effect is notable also in warm areas, such as Italy or Portugal.

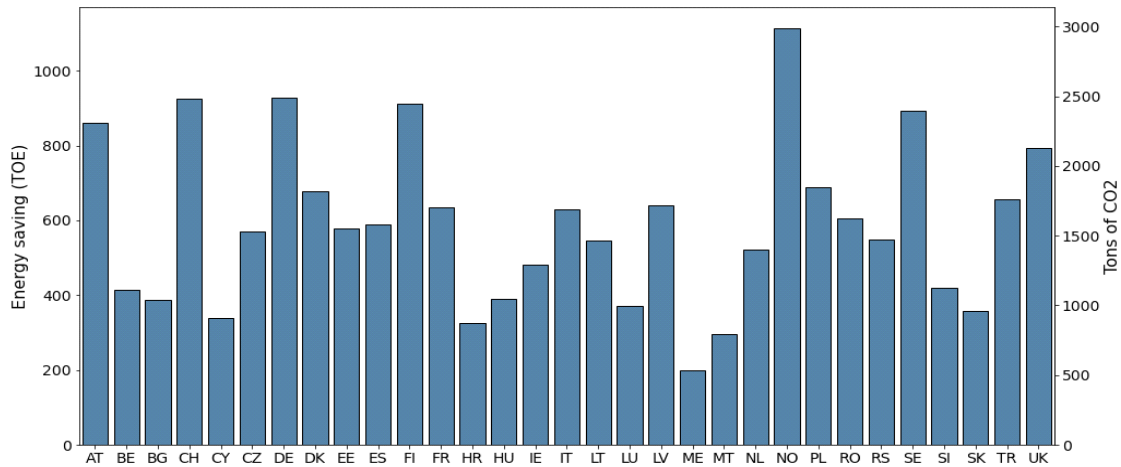


Figure 43. Total energy saving due to all the energy-efficiency measures in TOE and the corresponding CO₂ saving by country

Validation

To validate our approach, we compare the model outputs with the data of the Energy Audit 2019 of Malpensa and Linate Airports provided by the ClimOP partner SEA. This data is used as a benchmark to verify how representative our results are of any airport in Europe. The validation focuses on two aspects. On the one hand, the total electric energy consumption of the office buildings estimated by the method described in the previous section is compared to the one of Linate Airport. With our method, we estimate an energy consumption of 12,567 MWh for Linate Airport and 11,236 MWh for Malpensa Airport. The electric energy consumption of the office buildings at Linate Airport is 9,095 MWh, which is the same order of magnitude as our results. Moreover, the estimated energy consumptions correspond to 12% of the total energy demand for Linate Airport and 8% for Malpensa Airport. These results are reasonable considering that the office buildings account for around 10% of the airport energy consumption.

The second test concerns the modelling of the energy-efficiency measures. In particular, we assess how realistic the combination of measures as defined in the EnergyPlus simulations is. To this end, we use as benchmark the data provided by SEA coming from a preliminary analysis performed internally to explore the potential of energy efficiency measures for their airports. The results for the cool climate zone (corresponding to both Malpensa and Linate locations) show a total energy saving of 26% of the energy demand without improvements. The values estimated in the SEA analysis are 29% for Linate Airport and 21% for Malpensa Airport. Also, in this case, our results are in line with the benchmarks.

Results for future climate scenarios

The final part of our analysis concerns the effectiveness of this OI for future climate conditions. This is necessary because of the tight connection between the climate conditions and the energy consumption. To this end, we repeat the modelling chain for the four climate scenarios. Figure 44 displays the energy saving per unit area for present-day climate and for future climate scenarios, where the time span between the two simulations is 50 years. The results correspond to the combination of all the considered energy-efficiency measures. Interestingly, the amount of energy saved will change in the future depending on the climate zones. In the warm climates, the considered energy-efficiency measures will be more effective, whereas in the cold climates their efficacy will be reduced in the future. This can be explained by the fact that the energy-efficiency measures are more effective in cold climates. With the climate warming, the cold climates will

become milder, and the effectiveness of the energy-efficiency measures will be reduced although still notable. For the warm climates, we see the effect of including solar films in the window upgrades (not shown in Figure 42). This energy-efficiency measure is increasingly effective with climate warming.

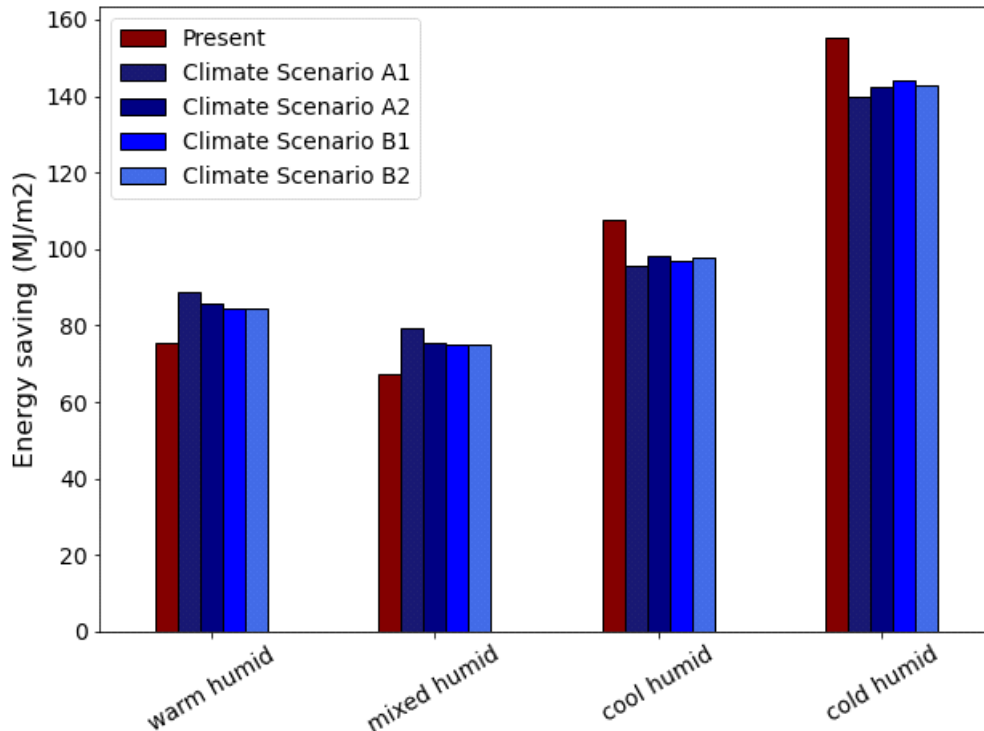


Figure 44. Energy saving per unit area for present-day climate and for future climate scenarios. The results correspond to the combination of all the considered energy-efficiency measures.

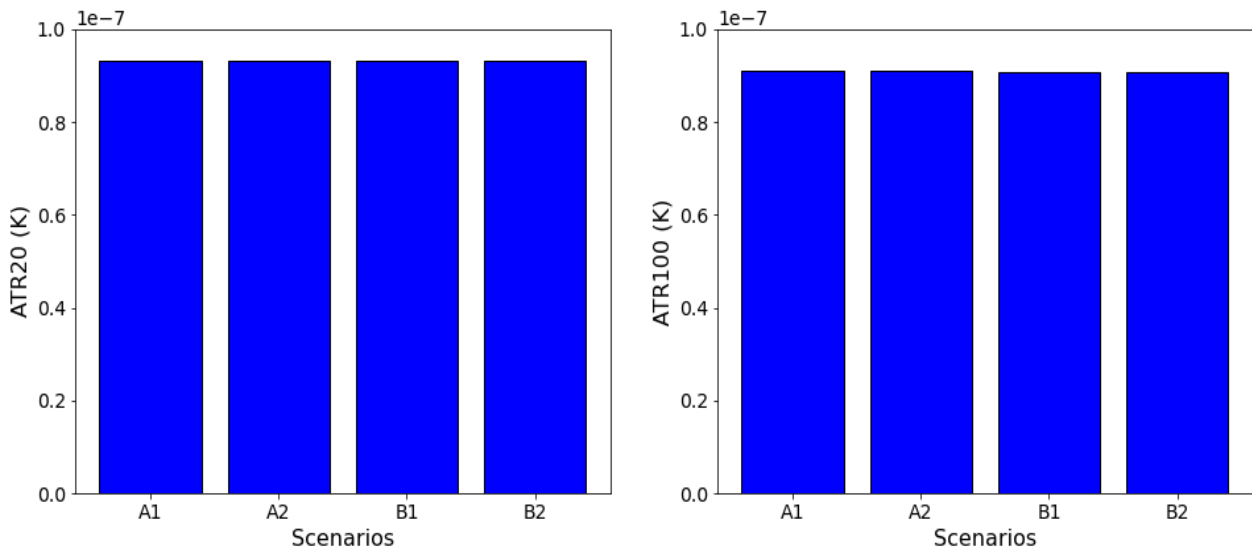


Figure 45. ATR20 and ATR100 estimated for the different climate scenarios.

Finally, we estimate ATR20 and ATR100 for the different climate scenarios as described in the methodology section. The results are gathered in Figure 45. As already appreciable in Figure 44, there is not much variability between the different scenarios. However, part of the variability might

be hidden by the lack of a prediction of how the climate zones will change in the future. Because of the lack of such information, we maintain the percentage of area covered by each climate zone constant between present-day climate and future climate simulations. Yet, it is reasonable to expect some changes in the future.

2.9.4 Open issues

Uncertainties

The uncertainties of our calculations span a wide range of sources. Firstly, the BES simulations of the conceptual office building entail the uncertainties due to the model assumptions as well as modelling of any office building. The preliminary validation indicates that the results are realistic, but a quantification of the level of uncertainties is hard to define. Similar considerations apply also to the energy-efficiency measures. It is worth mentioning, in this respect, that the energy efficiency measures depend on the regulations in each Country. Therefore, considering the same energy-efficiency measures throughout Europe is another simplification. Secondly, the methodology defined to generalize the results entails other uncertainties. The basic assumption of a relationship between the energy consumption of an airport and the number of flight movements needs to be further tested. The problem is the lack of detailed data on energy consumption of airports. For this reason, we use the number of employees as a proxy of the energy demand for office buildings. However, this assumption needs to be validated further. Finally, ATR20 and ATR100 are calculated based on the hypothesis that the percentage of area covered by the climate zones in Europe will not change in the future. Although necessary because of the absence of information in this respect, this hypothesis is questionable considering that the whole climate system is changing. However, the estimate of the uncertainty related to this simplification is impossible without the necessary information of how the climate zones coverage will change.

Next steps

For the second assessment, we plan to improve the presented results. The formulation of ATR20 and ATR100 defined in [51] will be used for consistency with the climate assessments of the other OIs. The values of ATR20 and ATR100 will be presented also as percentages. More generally, we will test our generalization method and our results by engaging with the partners in the Advisory Board and beyond. Finally, we will perform a cost benefit analysis to estimate some economic KPIs, and will assess the social, market and political acceptance of the OI through a passenger survey and interviews with selected stakeholders.

3. Overview over climate impact of operational improvements

A direct comparison of different OIs is not easily possible. Nevertheless, different categories of OIs have been defined to be able to compare effectiveness of different OIs within one group. The following section will give a first impression of a possible comparison. More detailed analyses will take place after modelling work is completed.

3.1 Trajectory-related OIs

The selected trajectory-related OIs consist of

- Flying Low & Slow (LOSL)
- Free routing (FREE)
- Climate-optimized Flight Planning (CLIM)
- Wind/weather optimal Flight Planning (WIND)

The studies are comparable in terms of their modelling process: Based on a preselected air traffic scenario (limited to certain airspaces, aircraft types and days), the respective trajectories are calculated based on available BADA3 or BADA4 performance data. Point profile data is derived from EUROCONTROL DDR2 data set or ALL_FT+ data or great circles are assumed. Emissions are estimated based on fuel flow (either proportionally or with Fuel Flow correlation methods provided by Boeing or DLR). The resulting emission quantities per species are the basis for calculating average temperature response with aCCFs. A comparison of the tools and their modelling capabilities could be interesting in a next step in a way that model results will be compared for an equal reference mission.

As ATR20 has only been calculated for Flying Low & Slow and Climate-optimised flight-planning so far, a full comparison cannot be performed yet. We are seeing a higher potential in ATR reduction for CLIM compared to LOSL (Table 25). Among other things, this can be explained by the fact that flying lower is considered in CLIM if this leads to improvement on climate impact. A comparison with FREE and WIND can be performed based on fuel consumption or emission quantities, as shown in Table 25. In this context, it also needs to be considered that the reference scenarios are not defined identically. While LOSL limits its analysis to four aircraft types (long- and short-range), it considers flights to/from the full ECAC area. CLIM focusses on specific climate-optimised routes. In contrast to this, FREE and WIND restrict the definition of the reference case to a certain airspace and focus on one short-range aircraft (B737-800), which is also part of the fleet in LOSL. Furthermore, selected days differ in a way that LOSL focusses on a day in summer (June 16, 2018) whereas CLIM, FREE and WIND selected a winter day (December 18, 2015 or December 1, 2018).

However, a relative comparison between reference case and OI implementation can still provide a first impression on the measure's effectiveness. It appears that fuel flow rises for implementation of 'Flying Low & Slow', which is not surprising per definition of the OI, where as fuel flow is reduced for implementation of 'Free Routing' and 'Wind Weather-optimal Flight Planning'. Travel time is also decreased by those OIs, whereas it obviously increases by flying slower. Climate-optimised flight planning applies a different methodology, in a way that allowed additional fuel is a restriction for the analysis. In this context, fuel consumption can be limited to additional 0.5%, what also leads to additional flight times of approx. 0.8%.

As CO₂ is proportional to fuel flow, CO₂ emissions are decreasing by 2 to 3% for 'Free Routing' and 'Wind Weather-optimal Flight Planning', while it increases by 2.8% for 'Flying Low & Slow'. NO_x emissions are reduced above average by 11% in the context of free routing, whereas it is only reduced by 1% when flying wind-weather optimal. For LOSL, NO_x emissions are increased by 35.4

%. ATR20 can still be reduced because contrail and H₂O effects are significantly reduced with this OI.

Further climate and non-climate KPIs and a full evaluation of them across the different OIs will be subject to the next iterations as well as an evaluation. Uncertainties will also be quantified and compared in the following work.

Table 25. Climate impact of operational improvements for trajectory related OIs

Trajectory-related OIs			
OI	KPI	Values	Comments/Assumptions
LOSL	Fuel Flow/ CO2 emissions	+ 2.81 %	<ul style="list-style-type: none"> - Selected scenario: 4,000 ft lower and 5% slower - 1 day (June 16, 2018) - Only North-Atlantic flights (213 on that day)
	NOx emissions	+ 35.4 %	
	ATR20	- 6.3% compared to reference case	
FREE	Fuel Flow/ CO2 emissions	- 2.2 %	<ul style="list-style-type: none"> - Focused on an upper enroute airspace (above 23500ft / EDUU) - 1 day (December 1, 2018) - Free routing is implemented by flying direct routes
	NOx emissions	- 10.9 %	
	ATR20	N/A	
CLIM	Fuel Flow/ CO2 emissions	+ 0.5/1.0%	<ul style="list-style-type: none"> - Selected scenario is to allow for 0.5% 1% of fuel increase - 1 day (Dec 18, 2018) - for approx. Top 2000 in ECAC and two single flights
	NOx emissions	N/A	
	ATR20	- 45% - 53% compared to fuel optimal case	
WIND	Fuel Flow/ CO2 emissions	- 2.62 %	<ul style="list-style-type: none"> - Focused on an upper enroute airspace (above 23500ft / EDUU) - 1 day (December 1, 2018) - Simplified wind model (that will be improved in D2.4) - Optimization based on BADA3 (that will be improved in D2.4 using BADA4)
	NOx emissions	- 1.02 %	
	ATR20	N/A	

3.2 Network-related OIs

The selected network-related OIs are:

- Strategic network planning (NETW)
- Climate-optimized Intermediate Stop Operations (ISOC)

Comparability of results is limited at this point, as NETW focusses on one selected airline and analysing specific characteristic days with respective weather situations. In contrast, ISOC analyses an annual aggregated flight-plan of long-range flights from/to the ECAC area without considering specific weather situations. A relative comparison of average temperature response between reference scenario and implementation OI can still give an impression on effectiveness of both measures (see Table 26).

Strategic network planning is expected to lead to an ATR20 reduction of 16.6% in summer and 39.9% in winter respectively. Effects for climate-optimal ISO are expected to be lower (approx.

6%). A second modelling iteration with adjustments in both studies could be performed in the following work. On this basis, non-climate KPIs such as cost will be considered additionally. Furthermore, it could make sense to also analyse network/strategic planning effects of ISO and thus to potentially combine both OIs in a common scenario.

Table 26. Climate impact of operational improvements for network-related OIs

Network-related OIs			
OI	KPI	Values	Comments/Assumptions
NETW	ATR20	- 16.57% (summer) -39.86% (winter)	Further reduction in ATR would need airline preferences as well (see section 2.5.3.1)
	ATR100	Not yet calculated	
ISOC	ATR20	- 6.0 %	- For flight plan covering approx. 18% of global ASK - Comparison based for constant FL (33,000 ft)
	ATR100	- 6.4 %	

3.3 Ground-related OIs

Analysed ground-related OIs are:

- “Green Taxiing” (i.e. Single-engine or electric taxiing, hybrid models)
- Electrification of ground vehicles
- Upgrade of the airport infrastructure

Comparability of results is difficult for this set of OIs at this point as all of them focus on different sections at the airport. A first overview of the current status is provided in Table 27.

Table 27. Climate impact of operational improvements for ground-related OIs

Ground-related OIs			
OI	KPI	Values	Comments/Assumptions
SETX	ATR20	N/A	- Updates will be provided in D2.4
	ATR100	N/A	
ELEC	ATR20	- 84% compared to reference case	- Uncertainty propagation in the process of calculation. - For OI implementation at SEA Malpensa and Linate combined.
	ATR100	- 84% compared to reference case	
INFR	ATR20	9.33e-8 K	Valid for: - Upgrade of the office buildings - Geographic scope: Europe
	ATR100	9.10e-8 K	

4. Conclusion and future work

This deliverable presents the result on the climate impact of the first modelling set of operational improvements. Inputs from the previous deliverables were required to perform the assessment and methodology and assumptions were verified and also adjusted. This document adds a comprehensive overview of methodology, modelling assumptions and details of their implementation. The outcomes from the first modelling iteration are presented. These results build the basis for evaluating the OIs effectiveness with regards to climate mitigation measures as well as for the analysis of the impact on the different stakeholders.

The wide diversification of the OIs in terms of their goal and their application area as well as their modelling and simulation processes leads to a large variability of the results. This does not only relate to their format and actual numbers but also to the prerequisites and assumptions that need to be considered when interpreting and comparing them. Further work on this aspect will be performed in the following deliverable D2.4.

As described by the working groups for every OI, some further modelling activities can be performed in the second iteration to additionally refine the presented results. On the one hand, some more detailed modelling can be performed. A more detailed consideration of actual cruise altitudes is expected to improve results for LOSL and ISOC. More advanced models can be used for simulating aircraft performance, e.g. by using BADA4 performance data instead of BADA3 for WIND. Furthermore, integration of real-weather data can be improved among others by improved wind field modelling in WIND or considering more characteristic weather days in LOSL to isolate seasonal effects. In some studies, it will also make sense to expand calculations to cover an extended fleet (e.g. NETW). Adjustment to more current data from 2018 is planned for SETX and CLIM. More detailed airport data and an evaluation of relations between airport size and other KPIs will be evaluated for ELEC and INFR. Some OIs, such as NETW, LOSL and ISOC, will use more detailed models to assess the climate metrics, e.g. by adjusting AirTraf to CO₂ emissions (NETW), by incorporating aCCFs, that have been calibrated also for southern hemispheres in greater detail (LOSL, CLIM, and NETW), or by calculating an aggregated flight-plan including a ramp-up scenario within AirClim for ISOC to also include saturation effects. On the other hand, some working groups have not yet completed calculating all climate-related KPIs in general and average temperature response in particular. ATR20 will be calculated in the following work for FREE and WIND and calculation of relative changes will be provided by INFR.

For the OIs LOSL & ISOC, not only a precision adjustment is intended for the next modelling iterations, but also further modelling is planned with regards to adjusted questions of the study: The impact of different weather situations in 2018 as well as the effects resulting from long-term climatological changes will be investigated in the next iteration of LOSL. Moreover, the ISOC study will additionally take fleet adjustments into consideration and evaluate the climate impact of performing climate-optimized ISO with aircrafts designed for shorter distances.

Due to the assumptions taken in course of the modelling process, interpretation and comparability of results is naturally limited. To keep computational efforts realizable and to be able to provide results in realistic time frame, it was necessary to take some assumptions, that will not be changed in the following iterations, but could be further investigated to improve accuracy of results. One example is the use of a constant load factor for all European flights as it is utilized by LOSL and ISOC. A more differentiated approach could obviously lead to even more realistic results. In this context, it is important to evaluate uncertainties and possible errors and their propagation especially when looking out to a comparability of results. Thus, a reliability assessment and uncertainties will be in focus for the following work. As part of this, a comparison of different modelling tools will be performed, i.e. all trajectory modelling tools for instance will calculate trajectories for an OD pair and deviations in terms of fuel flow, speeds or emissions will be

analysed and compared. Additional limitations might derive from limiting analyses to certain aircraft types or geographic areas. By taking the covered ASK of the traffic scenario into consideration when interpreting the results, findings can also be transferred to other scenarios.

The second iteration of simulating the operational improvements, which will be presented in D2.4, will also consider scenarios that represent combinations of several OIs. For instance, it makes sense to combine ISOC with flying lower to additionally avoid higher and thus more climate-sensitive areas so that climate metrics would improve. Further combinations might be possible. D1.5 as the “Report on the second iteration for the identification, assessment and selection of operational improvements” will analyse these options and provide an overview for the second iteration.

Deliverable 2.4. will not only report the climate impact of the second iteration, but also include results on non-climate KPIs, for example regarding social, market and political acceptance of the OIs. In this context, cost for implementing the different OIs will be calculated so that cost-benefit analyses can be performed. For some OIs, impact on safety and human performance will be examined. In the context of FREE and LOSL for instance, impact on accident rates and changes in workload for pilots and air traffic controllers could be in focus. Further non-climate metrics defined in work package 1 will be calculated and analysed.

References

- [1] D. S. Lee et al., *Transport impacts on atmosphere and climate: Aviation*, Atmos. Environ., vol. 44, no. 37, pp. 4678–4734, Dec. 2010, doi: 10.1016/j.atmosenv.2009.06.005.
- [2] EUROCONTROL, *Five-Year Forecast 2020-2024 European Flight Movements and Service Units Three Scenarios for Recovery from COVID-19*, 2020. Accessed: Nov. 18, 2020. [Online]. Available: <https://www.eurocontrol.int/sites/default/files/2020-11/eurocontrolfive-year-forecast-europe-2020-2024.pdf>.
- [3] ATAG, *Climate change*, 2020. Accessed: Apr. 29, 2020. [Online]. Available: <https://www.atag.org/our-activities/climate-change.html>.
- [4] ATAG, *Green recovery of air transport a priority for industry leaders*, Press release, 2020. Accessed: Nov. 18, 2020. [Online]. Available: <https://www.atag.org/component/news/?view=pressrelease&id=121>.
- [5] ClimOp Consortium, *D1.3 – Report on the assessment of operational improvements against identified KPIs*, 2020
- [6] ClimOp Consortium, *D1.4 – Report on the selection and review of operational improvements to be investigated*, 2020.
- [7] ClimOp Consortium, *D2.1 – Definition of reference scenario including technological and operational boundary conditions and air traffic sample*, 2021
- [8] ClimOp Consortium, *D2.2 – Documentation of adaptation of the combined air traffic and climate impact simulation and modelling of operational improvements*, 2021
- [9] Deutscher Wetterdienst, *Description of the method and the weather types*, Accessed: Dec. 9, 2021. [Online]. Available: <https://www.dwd.de/EN/ourservices/wetterlagenklassifikation/beschreibung.html;jsessionid=740C7588959176ECBF14C2FA04490146.live21072?nn=495490&lsblId=520444>.
- [10] wetter3.de weather maps of GFS model output, available: <http://www.wetter3.de>
- [11] ICAO, *Annual Report 2018 – Presentation of 2018 Air Transport Statistical Results*, Accessed: Dec 9, 2021 [Online]. Available: <https://www.icao.int/annual-report-2018/Pages/the-world-of-air-transport-in-2018-statistical-results.aspx>
- [12] M. Schaefer & S. Bartosch, *Overview on fuel flow correlation methods for the calculation of NOx, CO and HC emissions and their implementation into aircraft performance software*, Technical Report IB321-11-13, DLR Institute of Propulsion Technology. Cologne, Germany. July, 2013.
- [13] H. Yamashita et al., *Newly developed aircraft routing options for air traffic simulation in the chemistry climate model EMAC 2.53: AirTraf 2.0*, Gesci. Mode Devl., vol. 13, no. 10, pp. 4869 – 4890, Oct. 2020, <https://doi.org/10.5194/gmd-13-4869-2020>.
- [14] EUROCONTROL & FAA, *2017 Comparison of Air Traffic Management-Related Operational Performance: US/Europe*, 2019.
- [15] EUROCONTROL, *DDR2 Reference Manual For General Users*, 2018
- [16] Baspinar, B. et al., *A 4D trajectory generation infrastructure tool for controller working position*. In 2017 IEEE/AIAA 36th Digital Avionics Systems Conference (DASC), 2017.
- [17] Baspinar, B., Balakrishnan, H., & Koyuncu, E., *Optimization-Based Autonomous Air Traffic Control for Airspace Capacity Improvement*. IEEE Transactions on Aerospace and Electronic Systems, 2020.

- [18] Jelinik, F., Carlier, S., and Smith, J., Advanced Emission Model (AEM3) v1.5. Technical Report EEC/SEE/2004/004. Eurocontrol 2004, 306, 1–3.
- [19] DuBois, D. and Paynter, G.C, *Fuel Flow Method2 for Estimating Aircraft Emissions*. SAE Int. 2006, doi:10.4271/2006-01-1987.
- [20] ICAO. *ICAO Engine Exhaust Emissions Data*; Databank, Doc 9646-AN/943, Issue 18; ICAO: Montreal, QC, Canada, 2012. Available online: <http://www.easa.europa.eu/document-library/icao-aircraft-engine-emissions-databank>
- [21] Döpelheuer, A.: *Anwendungsorientierte Verfahren zur Bestimmung von CO₂, HC und Russ aus Luffahrttriebwerken*, Forschungsbericht 2002-10, Deutsches Zentrum für Luft- und Raumfahrt e.V., Institut für Antriebstechnik, Köln, Germany, 2002.
- [22] Döpelheuer, A.: *Quantities, Characteristics and Reduction Potentials of Aircraft Engine Emissions*, German Aerospace Center, Paper No. 2001-02-3008, Germany, 2001
- [23] S. Matthes, B. Lührs, K. Dahlmann, V. Grewe, F. Linke, F. Yin, E. Klingaman, and K. Shine *Climate-Optimized Trajectories and Robust Mitigation Potential: Flying ATM4E*, Aerospace 2020, vol 7, 256, 2020.
- [24] B. Lührs, F. Linke, S. Matthes, V. Grewe, and F. Yin, *Climate Impact Mitigation Potential of European Air Traffic in a Weather Situation with Strong Contrail Formation*. Aerospace, 8 (50). Multidisciplinary Digital Publishing Institute (MDPI), 2021). doi: 10.3390/aerospace8020050.
- [25] J. van Manen & V. Grewe, *Algorithmic climate change functions for the use in eco-efficient flight planning*. Transp. Res. Part D, 67, pp. 388–405, 2019.
- [26] C. Fröming, V. Grewe, S. Brinkop, P. Jöckel, A. Haslerud, S. Rosanka, J. von Manen, and S. Matthes, *Influence of weather situation on non-CO₂ aviation climate effects: the REACT4C climate change functions*. Atmos. Chem. Phys., vol. 21(11), pp. 9151-9172, <https://doi.org/10.5194/acp-21-9151-2021>, 2021.
- [27] Petzold, A., Neis, P., Rütimann, M., Rohs, S., Berkes, F., Smit, H. G., Wahner, A., *Ice-supersaturated air masses in the northern mid-latitudes from regular in situ observations by passenger aircraft: vertical distribution, seasonality and tropospheric fingerprint*. Atmos. Chem. Phys. (20), 8157-8179, 2020. doi: <https://doi.org/10.5194/acp-20-8157-2020>
- [28] W. B. Powell, *Approximate Dynamic Programming: Solving the Curses of Dimensionality*. Wiley – Series in Probability and Statistics, 2 edition (2011).
- [29] P. Belobaba, C. Barnhart, and A. Odoni, *The global airline industry*. John Wiley and Sons, (2009).
- [30] F. Linke, *Environmental Analysis of Operational Air Transportation Concepts*, Hamburg University of Technology, 2016.
- [31] F. Linke, V. Grewe, and V. Gollnick, *The implications of Intermediate Stop Operations on aviation emissions and climate*, Meteorol. Zeitschrift, vol. 26, no. 6, pp. 697–709, 2017.
- [32] F. Linke, *The global fuel saving potential of intermediate stop operations considering meteorological and operational influences*, 31st Congress of the International Council of the Aeronautical Sciences, Belo Horizonte Brazil, September 09-14, 2018.
- [33] openflights.org, *Airport database*, Accessed: Aug. 11, 2021. [Online] <https://openflights.org/data.html>

- [34] European Civil Aviation Conference, *Member States*. Accessed: September 17, 2021. [Online] <https://www.ecac-ceac.org/about-ecac/member-states>
- [35] V. Grewe & A. Stenke (2008), *AirClim: an efficient tool for climate evaluation of aircraft technology*, *Atmos. Chem. Phys.* 8, pp. 4621-4639.
- [36] M. Biasiol et al., *Documentation of adaptation of the combined air traffic and climate impact simulation and modelling of operational improvements*, CLIMOP, no. D2.2, pp. 25-26, 2021. [Accessed 30 September 2021].
- [37] J. Martins, F. P. Brito, D. Pedrosa, V. Monteiro, and J. L. Alfonso, *Real-life comparison between diesel and electric car energy consumption*, *Grid Electrified Vehicles: Performance, Design and Environmental Impacts*, pp. 209-232, 2013.
- [38] B. A. Davis and M. A. Figliozzi, *A methodology to evaluate the competitiveness of electric delivery trucks*, *Transportation Research Part E*, vol. 49, pp. 8-23, Jan. 2013, doi: <https://doi.org/10.1016/j.tre.2012.07.003>.
- [39] T. Mahlia, *Emissions from electricity generation in Malaysia*, *Renewable Energy*, vol. 27, no. 2, pp. 293-300, 2002.
- [40] IPCC, 2001: *Climate Change 2001: The Scientific Basis. Contribution of Working Group I to the Third Assessment Report of the Intergovernmental Panel on Climate Change* [Houghton, J.T., Y. Ding, D.J. Griggs, M. Noguer, P.J. van der Linden, X. Dai, K. Maskell, and C.A. Johnson (eds.)]. Cambridge University Press, Cambridge, United Kingdom and New York, NY, USA, 881pp.
- [41] European Environment Agency. 2021. *Greenhouse gas emission intensity of electricity generation in Europe*. [online] Available at: <<https://www.eea.europa.eu/ims/greenhouse-gas-emission-intensity-of-1>> [Accessed: Nov 18, 2021].
- [42] H. Ritchie and M. Roser, *CO₂ and Greenhouse Gas Emissions*, *Our World in Data*, 2021. [Online]. Available: <https://ourworldindata.org/co2-and-other-greenhouse-gas-emissions>. [Accessed: Dec 3, 2021].
- [43] N. Change, *Carbon Dioxide Concentration | NASA Global Climate Change*, *Climate Change: Vital Signs of the Planet*, 2021. [Online]. Available: <https://climate.nasa.gov/vital-signs/carbon-dioxide/>. [Accessed: Dec 3, 2021].
- [44] R. Ellis, *Global warming equation - derivation and application to climate change*, 'globalwarmingequation.info', 2013. [Online]. Available: <http://www.globalwarmingequation.info/>. [Accessed: Dec 3, 2021].
- [45] M. Bertolini, C. D'Alpaos and M. Moretto, *Electricity prices in Italy: Data registered during photovoltaic activity interval*, *Data in Brief*, vol. 19, pp. 1428-1431, 2018. Available: 10.1016/j.dib.2018.06.018 [Accessed: Dec 3, 2021].
- [46] ASHRAE, Standards 90.1/169
- [47] Intergovernmental Panel on Climate Change, *Special Reports on Emission Scenarios* [online]. Available: <https://www.grida.no/climate/ipcc/emission/index.htm> [Accessed: Oct 06, 2021].
- [48] Cordinamente Ambientalista Rifiuti Piemonte, *Studio sulle fonti energetiche rinnovabili in provinciale di Pavia* [online]. Available: <https://www.carp-ambiente-rifiuti.org/sites/default/files/CO2%20-%20tep%20conversione%20equivalenze%20GHG%20del%20punto%20ENERGIA.pdf> [Accessed: Dec 13, 2021].

- [49] Carbon Dioxide Information Analysis Center (U.S. Department of Energy, Office of Science), *Carbon Dioxide Information Analysis Center - Conversion Tables*, 2012. [Online]. Available: <https://cdiac.ess-dive.lbl.gov/pns/convert.html> [Accessed: Dec 13, 2021]
- [50] J.T. Houghton et al., "Climate Change 2001: The Scientific Basis", Contribution of Working Group I to the Third Assessment Report of the Intergovernmental Panel on Climate Change, 2001. [Online]. Available: https://www.ipcc.ch/site/assets/uploads/2018/03/WGI_TAR_full_report.pdf [Accessed Dec 13, 2021]
- [51] Sausen, Robert and Ulrich Schumann. *Estimates of the Climate Response to Aircraft CO₂ and NO_x Emissions Scenarios*. *Climatic Change* 44 (2000): 27-58.
- [52] EnergyPlus v. 9.6.0, available at <https://energyplus.net/> [Accessed Dec 21, 2021]

Annex A

Table 28. ATR from different emission species for flight JFK - ZRH

	ATR20 _{CO2}	ATR20 _{NOx_O3}	ATR20 _{NOx_CH4}	ATR20 _{H2O}	ATR20 _{Contrail}
Reference case 1	0.25e-09 K	1.04e-09 K	- 0.65e-09 K	0.03e-09 K	2.70e-09 K
Reference case 2	0.25e-09 K	1.09e-09 K	- 0.65e-09 K	0.03e-09 K	1.37e-09 K
Scenario 1.1	0.26e-09 K	1.27e-09 K	- 0.70e-09 K	0.03e-09 K	2.26e-09 K
Scenario 2.2	0.26e-09 K	1.44e-09 K	- 0.69e-09 K	0.02e-09 K	1.35e-09 K
Scenario 3.3	0.26e-09 K	1.65e-09 K	- 0.69e-09 K	0.02e-09 K	0.23e-09 K

Table 29. Changes in major KPIs compared to reference scenario for selected flight DOH - MAD

	CFL [100 ft]	CMa [-]	Fuel Flow [t]	Flight Time [h]	ATR20
Reference case 1	320 (Step climbs/descents)	0.84	52.25 t	06:41h	2.61-09 K
Reference case 2	320 (const. FL)	0.84	+ 1.64 %	- 0.52 %	+ 13.3 %
Scenario 1.1	300	0.84	+ 3.12 %	+ 1.44 %	+ 26.7 %
Scenario 1.2	300	0.84	+ 2.75 %	+ 6.00 %	+ 24.4 %
Scenario 1.3	300	0.84	+ 3.54 %	+ 11.1 %	+ 23.5 %
Scenario 2.1	290	0.80	+ 5.51 %	+ 4.04 %	+ 47.4 %
Scenario 2.2	290	0.80	+ 4.97 %	+ 8.80 %	+ 43.6 %
Scenario 2.3	290	0.80	+ 5.51 %	+ 14.12 %	+ 41.5 %
Scenario 3.1	270	0.76	+ 7.79 %	+ 6.66 %	+ 69.3 %
Scenario 3.2	270	0.76	+ 7.09 %	+ 11.61 %	+ 63.9 %
Scenario 3.3	270	0.76	+ 7.55 %	+ 17.13 %	+ 60.8 %

Table 30. Changes in Emissions reference scenario for all considered long-range flights

	CO2	H2O	NOx	HC	CO	Soot
Reference case A	124,730 t	49,891 t	686.7 t	8.35 t	63.68 t	629 kg
Reference case B	+ 0.85 %	+ 0.85 %	+ 1.79 %	- 3.14 %	- 2.47 %	+ 1.20 %
Scenario 1.1	+ 0.87 %	+ 0.87 %	+ 0.02 %	- 8.39 %	- 3.95 %	+ 1.07 %
Scenario 1.2	+ 0.29 %	+ 0.29 %	- 5.36 %	- 7.68 %	+ 3.76 %	+ 2.11 %
Scenario 1.3	+ 1.40 %	+ 1.40 %	- 6.86 %	- 6.89 %	+ 10.3%	+ 5.80 %
Scenario 2.1	+ 2.96 %	+ 2.96 %	+ 1.69 %	- 11.9 %	- 3.97 %	+ 4.64 %

Scenario 2.2	+ 1.67 %	+ 1.67 %	- 4.91 %	- 12.9 %	+ 2.48 %	+ 3.60 %
Scenario 2.3	+ 3.21 %	+ 3.21 %	- 6.62 %	- 11.1 %	+ 11.6 %	+ 7.64 %
Scenario 3.1	+ 2.91 %	+ 2.91 %	+ 1.06 %	- 18.0 %	- 6.42 %	+ 5.08 %
Scenario 3.2	+ 2.82 %	+ 2.82 %	- 4.13 %	- 18.0 %	+ 1.33 %	+ 5.70
Scenario 3.3	+ 3.99 %	+ 4.00 %	- 6.89 %	-16 .2 %	+ 11.4 %	+ 8.52 %

Table 31. Changes in major KPIs compared to reference scenario intra-ECAC flights (June 16th, 9926 flights)

		Fuel Flow [t]	Flight Time [h]	ATR20 [K]
Reference case A	Step climbs/descents No speed change	41,442	17,130	3.014e-06
Reference case B	Constant FL, no speed change	- 0.04 %	+ 0.01 %	- 0.12 %
Scenario 1.1	- 2000ft CFL, no speed change	+ 1.93 %	- 0.30 %	+ 13.3 %
Scenario 1.2	- 2000ft CFL, - 5 % speed	+ 0.12 %	+ 3.27 %	+ 13.5 %
Scenario 1.3	- 2000ft CFL, - 5 % speed	- 0.01 %	+ 7.25 %	+ 13.8 %
Scenario 2.1	- 4000ft CFL, no speed change	+ 4.95 %	- 0.71 %	+ 15.2 %
Scenario 2.2	- 4000ft CFL, - 5 % speed	+ 2.48 %	+ 2.92 %	+ 14.9 %
Scenario 2.3	- 4000ft CFL, - 10 % speed	+ 1.41 %	+ 6.99 %	+ 14.9 %
Scenario 3.1	- 6000ft CFL, no speed change	+ 8.57 %	- 0.93 %	+ 11.2 %
Scenario 3.2	- 6000ft CFL, - 5 % speed	+ 5.48 %	+ 2.75 %	+ 9.96 %
Scenario 3.3	- 6000ft CFL, - 10 % speed	+ 3.69 %	+ 6.88 %	+ 9.39 %